Title
Organization of central visual pathways of the ferret

Author
Zahs, Kathleen Rose

Publication Date
1987

Peer reviewed|Thesis/dissertation

Organization of Central Visual Pathways
of the Ferret

by

Kathleen Rose Zahs

DISSERTATION

Submitted in partial satisfaction of the requirements for the degree of

DOCTOR OF PHILOSOPHY

in

Neuroscience

in the

GRADUATE DIVISION

of the

UNIVERSITY OF CALIFORNIA

San Francisco

This dissertation is dedicated to my parents,

Jerome and Irma Zahs

Acknowledgements

I am, of course, indebted to my advisor, Michael Stryker, for his guidance and participation in all phases of this work. I have to thank Michael for sharing more than his knowledge and his skills. Through his rigorous, thorough approach to a problem, his faithful attendance at seminars and journal clubs, and his serious regard for teaching responsibilities, Michael provides his students with an example of what it means to be a scientist.

There are several other people who have made it possible to complete this dissertation:

Sheri Strickland, expert technician, teacher, boater, without whom the lab could not function. Her help and her friendship have been, and will continue to be, greatly appreciated.

My lab-mates, Barbara Chapman, Ken Miller, Holger Reiter, and Dave Waitzman who have shared their ideas, provided company during long days and nights in the lab, and insisted that I not give up.

Steve Lisberger, who has been patient and understanding (and will always be appreciated as the creator of Phyplot).

Allan Basbaum, who gave me the opportunity to learn in his lab and who remained a friend, despite my choosing to study the visual system.

The thesis paste-up crew: Barbara Chapman, Aline McKenzie, Ken Miller, Dave Perkel, Dave Reichling, and Lee Stone.

Finally, I am grateful to my thesis committee, Michael Merzenich, Henry J. (Peter) Ralston, and Richard Van Sluyters for their interest, encouragement, and much-valued advice.

ABSTRACT

Organization of Central Visual Pathways of the Ferret
by
Kathleen Rose Zahs

The mammalian visual system has been used extensively for studying the development of specific synaptic connections in the central nervous system. Ferrets are born when the visual system is relatively immature, making them attractive animal models for developmental studies. Before beginning work in developing animals, it is necessary to characterize some aspects of the organization of the adult visual system. Such studies are the subject of this thesis. The retinotopic organization of the ferrets's lateral geniculate nucleus (LGN) and primary visual cortex are described. In addition, the current experiments demonstrate the existence of anatomically separate channels within the ferret's retinogeniculocortical pathway arising from on-center and off-center retinal ganglion cells, providing another segregated system in which to test hypotheses about developmental mechanisms.

Within the ferret LGN, axons of the retinal ganglion cells of the two eyes terminate in separate laminae. These eye-specific layers are further divided into sublaminae, termed "leaflets." Electrophysiological recordings demonstrated that these leaflets represent the segregation of on-center and off-center cells in the LGN. The eye-specific geniculate laminae segregate their projections to primary visual cortex in ferrets, as well as in several other species, suggesting that the center-type leaflets could also segregate their projections to cortex. The distribution of ON and OFF geniculate afferents within layer IV of primary visual cortex was mapped by recording from the terminals of geniculocortical axons after silencing the cortical neurons with kainic acid, an excitatory neurotoxin that kills cells while sparing terminals and fibers of passage. The results of these experiments demonstrate that ON and

OFF geniculate afferents terminate in separate patches, similar to ocular dominance patches, in the plane of layer IV.

These experiments represent the initial steps in addressing two questions of major interest: 1) What is the functional significance of maintaining anatomically separate channels that convey information about particular aspects of the visual world? 2) How does such segregation arise during development?

Table of Contents

List of Tables

List of Figures

Chapter I

Introduction

The experiments to be described demonstrate the existence of separate channels arising from on-center and off-center retinal ganglion cells within the retinogeniculocortical pathway of the ferret. They represent the initial steps in addressing two questions of major interest: 1) What is the functional significance of maintaining anatomically separate channels that convey information about particular aspects of the visual world? and 2) How does such segregation arise during development?

The mammalian visual system has been used extensively for studying the development of specific synaptic connections in the central nervous system. Of particular interest has been the development of the segregated pathways for carrying information from each eye to primary visual cortex. In many species, the axons from the retinal ganglion cells of the two eyes terminate in separate eye-specific layers of the lateral geniculate nucleus (LGN), the principal visual thalamic relay nucleus. In some species, the geniculocortical axons serving each eye in turn terminate in separate patches, termed ocular dominance patches, within layer IV of primary visual cortex (cat, LeVay and Gilbert, 1976, Shatz et al., 1977; macaque, Hubel and Wiesel, 1974, Wiesel et al., 1974). During early development, the retinal afferents serving the two eyes overlap at least to some degree within the LGN. In cats and macaques, the most-extensively studied species, the segregation of the input from the two eyes into the appropriate geniculate laminae occurs prenatally. The geniculocortical axons serving each eye also initially overlap within visual cortex; ocular dominance patches begin to form prenatally in macaques (Rakic, 1976), and during the first few postnatal weeks in cats (LeVay et al., 1978). An understanding of the mechanisms that give rise to this segregation will contribute to our understanding of the mechanisms through which the brain achieves its amazing specificity of synaptic connections.

This work began in 1981, when Guillery and his colleagues drew attention to the ferret as a particularly useful experimental animal for studies of the visual system: born before the retinal afferents have segregated into the appropriate geniculate laminae, ferrets are attractive animals for use in developmental studies. We hoped to use ferrets in our own studies of the mechanisms underlying the development of laminae within the LGN and ocular dominance columns in the cortex. Before beginning the work in developing animals, it was necessary to characterize some aspects of the organization of the adult visual system. These studies in the adult ferret are the subject of this dissertation.

The topographic organization of both the lateral geniculate nucleus and area 17 were studied in order to provide information needed for this and future work on the development and organization of the ferret's primary visual system. In particular, we wanted to know the location of the monocular segment, extent of the visual field represented, and the orientation of the retinotopic maps within area 17 and the LGN.

The major portion of the work to be reported here is concerned with the function and patterns of projection of the geniculate sublaminae, termed "leaflets" (Guillery, 1971). The ferret's lateral geniculate nucleus shows the typical carnivore pattern of lamination: the nucleus contains six layers, two parvocellular A laminae and four C laminae distinguishable by their retinal inputs. Laminae A, C, and C2 receive a projection from the contralateral eye, and laminae A1 and C1 receive an ipsilateral projection (Guillery, 1971; Sanderson, 1974; Linden et al., 1981). However, the ferret's LGN differs from that of the most widely-studied carnivore, the cat, in that the A laminae are divided into two sublaminae (Guillery, 1971; Sanderson , 1974; Linden et al., 1981). Two tiers of label are visible within each A lamina of LGNs labelled by an intraocular injection of an anterograde tracer (either ^{3}H-proline or wheat germ agglutinin conjugated to horseradish peroxidase). This sublamination is sometimes visible in sections stained by a Nissl method, especially in the ventral parts of the nucleus. At the time of

birth, there is almost complete overlap among the retinal afferents serving the two eyes within the LGN; the retinogeniculate afferents sort themselves into the appropriate eye-specific laminae during the first two postnatal weeks (Linden et al., 1981). The leaflets are first visible using anatomical methods during the third postnatal week (Linden et al., 1981), giving us hope that they would provide another example of lamination that would be amenable to study in postnatal animals.

Electrophysiological recordings of multi-unit activity in the LGN were used to determine whether the leaflets represented the segregation of geniculate cells with different functional properties. In the macaque LGN, there are two parvocellular laminae serving each eye in the region of the nucleus representing the central visual field; Schiller and Malpeli (1978) had shown that each of these laminae contain either on-center or off-center cells. This work demonstrates that, in the ferret, the leaflets represent a segregation of on-center cells and off-center cells in the LGN: within each lamina, the outer (nearer the optic tract) leaflet contains off-center cells, while the inner leaflet contains on-center cells.

The eye-specific geniculate laminae segregate their projections to primary visual cortex (area 17) in ferrets, resulting in the ocular dominance patches seen in cortices transneuronally-labelled after an intraocular injection of ^{3}H-proline (Law et al., in preparation). It therefore seemed possible that the center-type leaflets would also segregate their projections to cortex. We mapped the distribution of ON and OFF geniculate afferents within layer IV of area 17 by recording from the terminals of geniculate cell axons after silencing the cortical neurons with kainic acid, an excitatory neurotoxin that kills cells while sparing terminals and fibers of passage (McGeer et al., 1978). The results of these experiments demonstrate that ON and OFF geniculate afferents terminate in separate patches, similar to ocular dominance patches, in the plane of layer IV.

Chapter II

The projection of the visual field onto the lateral geniculate nucleus of the ferret

Introduction

This chapter describes the retinotopic organization of the ferret's lateral geniculate nucleus (LGN). Before attempting electrophysiological studies of geniculostriate connectivity, it is useful to have available retinotopic maps for both the LGN and primary visual cortex. In particular, we wanted to know the orientation of the retinotopic map in the LGN, the extent of the ferret's visual field and the metric properties of the map. Electrophysiological mapping experiments were undertaken to address these questions. These experiments were conducted at the same time as the investigation of the sublaminar structure of the LGN reported in Chapter 4. Some of these results have been reported previously (Zahs and Stryker, 1985).

Methods

Animals.

Thirteen normally-pigmented adult ferrets, obtained from Marshall Farms, New Rose, New York, were used in these experiments. Ten of the animals were adult females (700-900 g) and three were adult males (1100 g). Six of these animals were used in anatomical studies to locate the LGN and label the retinal afferents, five were used in the electrophysiological mapping studies, and two ferrets were used in retrograde transport studies. Data from three of these animals on the stratification of ON and OFF responses in the LGN are included in Chapter 4.

Electrophysiological recording.

Five ferrets were prepared for physiological recording using techniques that are conventional for the cat visual system (Shatz and Stryker, 1978). The ferrets were initially anesthetized with a mixture of acepromezine (0.04 mg/kg) and ketamine (40 mg/kg) injected intramuscularly. The femoral vein and the trachea were cannulated, and surgical anesthesia was subsequently maintained with thiopental sodium (20 mg/kg i.v.).

Animals were then placed in a modified kitten stereotaxic apparatus and the scalp, skull, and dura overlying the LGN were opened. Because of variability in the location of the LGN among animals, the exposures were large relative to the cross-sectional area of the LGN in the horizontal plane: In four ferrets, the skull was opened from Horsley-Clarke anterior-posterior coordinates -3.5 mm to +3.5 mm and lateral-medial coordinates 2.5 mm to 8.0 mm. In

one ferret, electrode penetrations were made in the parasagittal plane, on an angle inclined 40-45 degrees pointing anterior from vertical. In this animal, the skull was opened for 7 mm anterior to the tentorium, the medial and lateral edges of the opening being at Horsley-Clarke coordinates 2.0 and 8.0, respectively.

Following surgery, barbiturate infusion was discontinued, and anesthesia was maintained by ventilating the ferret with 75% nitrous oxide, 25% oxygen at a rate and volume that maintained peak inspiratory pressure at 1.5 kPa and end-tidal carbon dioxide at 3.8-4.3%. Neuromuscular blockade was then induced using pancuronium bromide (0.1 mg/kg-hr) or gallamine triethiodide (10 mg/kg-hr). Atropine sulfate (0.08 mg i.m.) was administered every 12 hours during the course of the experiment in order to reduce the ferret's mucous discharge.

The nictitating membranes were retracted with phenylephrine hydrochloride, and atropine was used to paralyze accomodation and dilate the pupils. Plastic contact lenses (2.7-2.9 mm base curve, plano) were fitted to focus the eyes on a tangent screen subtending 80 degrees at a distance of 57 cm. The center of the screen was placed either directly in front of the ferret or at approximately 60 degrees eccentricity. Focus was checked by retinoscopy and the most appropriate contact lenses selected. The projections of the two optic discs were plotted on the tangent screen using a reversing beam ophthalmoscope.

Lacquered tungsten microelectrodes (Hubel, 1957) were used to record multi-unit activity in the LGN. These electrodes had conical exposed tips tapering from 8 to 15 μm in diameter to a sharp point over 20-45 μm and impedances of 1.5-3.5 MOhm at 120 Hz. The electrodes were advanced rapidly for the first 3 mm after entering the brain, and in 100-μm steps thereafter. A Zeiss handlamp was used to plot receptive fields on the tangent screen, while neuronal responses were assessed with an audio monitor. One or more electrolytic lesions were made along the course of each electrode penetration by passing -4 to -6 μA current for 4 to 6 seconds.

At the end of the recording sessions, the ferrets were deeply anesthetized with an intravenous injection of thiopental sodium and perfused through the heart with 0.9% saline followed by 10% formol saline. The heads were placed in the fixative overnight and blocks of brain containing the LGN were removed the next day. The blocks of tissue were sunk in 30% sucrose formalin before being embedded in a mixture of albumin and gelatin. Forty-micron sections were cut on a freezing microtome, and sections containing the LGN were stained with cresyl violet. Three of the brains were cut coronally; the remaining two brains were cut sagitally. Camera lucida drawings were made of sections containing electrode tracks, and recording sites were assigned by referring to microdrive readings at the lesions and the entry point into the LGN. The brain of an additional ferret, not used for electrophysiological studies, was cut horizontally and stained with cresyl violet.

The receptive field position at each recording site was noted on the drawing. The location of each receptive field was expressed as two angles, azimuth and elevation, using a system of spherical polar coordinates (Bishop, Kozak, and Vakkur, 1962). In order to calculate these angles, it was necessary to determine the fixation point (the projection of the area centralis onto the tangent screen) for each eye. When retrograde transport studies (see below) failed to precisely locate the fixation point in relation to other retinal landmarks, the fixation point was estimated: The fixation-point elevation (i.e., the zero horizontal) was assumed to be the position of the smallest central receptive fields. The fixation-point azimuth (the position of the vertical meridian at zero elevation) for each eye was calculated using the method of Sanderson and Sherman (1971). The horizontal distance (Y) from the optic disc to the vertical line passing through the fixation point is given by the expression

$$Y = \frac{A - F}{2},$$

where A is equal to the separation of the optic discs' projections on the tangent screen. F, the mean receptive field separation on the tangent screen, was found by recording sites in the C laminae near the representation of the zero elevation where there was a response to stimulation of both eyes. The horizontal distances between the fields recorded for each eye at the same site in the LGN were averaged to give F.

Microinjections of horseradish peroxidase into the lgn.

Microinjections of horseradish peroxidase (HRP) were made into the LGNs of two ferrets in an attempt to relate locations in the visual field to locations in the retina, allowing a more direct determination of the fixation point. Two ferrets were prepared for electrophysiological recording as described above. The projections of the optic discs were plotted on the tangent screen using a reversing beam ophthalmoscope.

A tungsten microelectrode was used to locate a site in lamina A of the left LGN having a central receptive field. After locating an appropriate site, the tungsten electrode was replaced with a micropipette containing a solution of 20% HRP (Sigma, P8375) in Tris buffer (pH 8.6). The receptive field of the multi-unit cluster at the injection site was confirmed by recording with a tungsten microelectrode inserted into the injection pipette, and 35 - 45 nl solution was pressure-injected into the LGN.

The same procedure was repeated in the right LGN, except that the enzyme was injected iontophoretically through a micropipette (tip 10 μm inner diameter) that did not contain a tungsten electrode. It was still possible to confirm the location of the injection site by recording through the pipette. We intended to inject the enzyme over 8 - 12 hours using iontophoretic currents of +4 μA (1.5 sec on, 0.5 sec off). However, the actual current decreased over time as the pipette tip apparently became clogged, so that no current passed through the micropipette after 4 hours.

The animals were maintained in an anesthetized, paralyzed condition for 16 - 22 hours after the start of the iontophoretic injection, during which time heart rate, respiration rate, end-tidal carbon dioxide, peak inspiratory pressure, temperature, and electroencephalogram (eeg) were monitored. Intravenous thiopental sodium was administered at the first sign of desynchronization of the eeg. The animals were then sacrificed with an overdose of sodium pentobarbital, administered intravenously. The ferrets were perfused through the heart with lactated Ringer's solution, containing 5% dextrose and 0.1% Heparin, followed by 1% paraformaldehyde, 2.5% gluteraldehyde in 0.1 M phosphate buffer (pH 7.4), and, finally, lactated Ringer's solution with 5% dextrose. All solutions were at 35 deg C. The eyes were then removed and stored in ice-cold Tris buffer, and the brain was blocked. Blocks containing the LGNs were stored in ice-cold phosphate buffer while the retinas were dissected (Stone, 1981) and reacted for the presence of HRP. Three retinas were processed using a cobalt-intensified diaminobenzidene (DAB) method, and the fourth was processed with phenylenediamine dihydrochloride and pyrocatechol (Vitek et al., 1985). The retinas were then mounted onto gelatinized slides, placed in a chamber containing formaldehyde vapor for 3 hours, dehydrated, and counterstained with cresyl violet.

The blocks containing the LGNs were sectioned on a freezing microtome at 40 microns in the parasagittal plane. The sections were reacted to show the presence of HRP using either the cobalt-intensified DAB method or a tetramethylbenzidene (TMB) method (Mesulam, 1978). The sections were mounted on gelatinized slides and dried overnight. Alternate sections were counterstained with neutral red (TMB) or cresyl violet (DAB).

In order to locate the area centralis, retinal ganglion cell density was mapped across a 4.5 - 5.1 mm^2 region of central retina. The retinas were viewed at a final magnification of 250 X through a Zeiss compound microscope equipped with an eyepiece graticle. The graticle was divided into a 10 X 10 grid that covered 0.14 mm^2, and the number of presumed retinal

ganglion cells was counted in alternate grid squares. Relatively large cells in the uppermost cell layer were considered to be retinal ganglion cells. This identity was confirmed by the presence of HRP retrogradely-transported from the LGN for those cells in the region of the retina projecting to the injection site; it is likely that some amacrine cells were counted as retinal ganglion cells among the population of unlabelled cells. The counts for all of the grid squares were averaged to give the mean density of ganglion cells for the region of retina covered by the graticle. This value was then recorded on a camera lucida drawing of the retina on which the region containing HRP-labelled cells had been noted. The position of the slide holding the retina was then adjusted until an adjacent patch of retina came into view, and the procedure was repeated until we could define the region of greatest retinal ganglion cell density, the location of the area centralis.

Labelling the retinal afferents to the LGN.

In three ferrets, retinal afferents to the LGN were labelled autoradiographically by intravitreal injections of 200-2000 μCi ^{3}H-proline (Amersham TRK.439, specific activity 40 Ci/mmol). The brains of two of these animals were sectioned in the coronal plane, the third brain was cut sagitally. Another LGN, cut in the sagittal plane, was labelled via an intravitreal injection of 0.25 mg wheat-germ agglutinin conjugated to horseradish peroxidase (WGA-HRP) (Sigma L-9008). One additional animal received a proline injection into one eye and an injection of WGA-HRP into the other eye. One series of parasagittal sections from this animal was reacted for HRP using the TMB method (Mesulam, 1978) and then stained with neutral red; a second series was exposed for autoradiography; and a third series was stained with cresyl violet.

Measurements of the volume of the LGN.

Both labelled and Nissl-stained sections, taken at 120-μm intervals from two brains cut in the sagittal plane, were traced at a magnification of 60X in the camera lucida. The innervation volumes contralateral and ipsilateral to each of 3 labelled eyes were measured planimetrically, as was the total volume of the LGN (layers A, A1, C, and C1). A correction for shrinkage was applied to the sections reacted for HRP based on their size as compared to the adjacent Nissl-stained sections. No correction was applied to the measurements on Nissl-stained or autoradiographically-labelled sections to relate them to the size *in vivo*.

Results

Anatomy.

Laminar Structure. The pattern of geniculate lamination that has been described for several species of carnivores (Sanderson, 1971, cat; Sanderson, 1974, mustelids, raccoon, fox) is also found in the ferret (Sanderson, 1974; Linden et al., 1981). Progressing from the outside (nearest the optic tract) to the inside of the LGN, one first encounters the C laminae: lamina C3, which does not receive a retinal input, is outermost, followed by contralaterally-innervated C2, ipsilaterally-innervated C1, and contralaterally-innervated lamina C. Lamina A1, which receives the majority of the uncrossed retinal input to the LGN, is found just inside lamina C in the medial part of the nucleus. Contralaterally-innervated lamina A is the innermost layer, found adjacent to lamina A1 in the binocular portion of the nucleus and just inside lamina C in the more laterally-placed monocular segment.

This laminar organization is easily seen in parasagittal and horizontal sections through the nucleus. The coronal plane is parallel to the plane of the laminae over much of the nucleus, making the arrangement of the laminae obscure in coronal section. However, as this plane is useful for viewing the topographic organization of the nucleus, the pattern of innervation seen in coronal section will be described (Fig. 1).

The projections of the two eyes, as revealed by the antrerograde transport of ^{3}H-proline, are shown in Figure 1. The anterior part of the LGN is shaped like the capital letter "C" when viewed in coronal section (Fig. 1A). Here the nucleus receives afferents mainly from the contralateral eye, with only a small patch at the dorsomedial edge of the LGN receiving

Figure 1. Autoradiographs shown in brightfield of a series of coronal sections through the LGN. Upper row (A-D): sections contralateral to an eye in which the vitreous humor had been injected with ^{3}H-proline. Lower row (E-H): sections ipsilateral to the injected eye. The sections have been lightly stained with cresyl violet. A_i, inner leaflet of lamina A; A_O, outer leaflet of lamina A; *C*, C laminae; *M*, medial interlaminar nucleus. *Scale bar* = 200 microns. The orientation of the sections A-D is shown in (A); orientation of E-H is shown in (E).

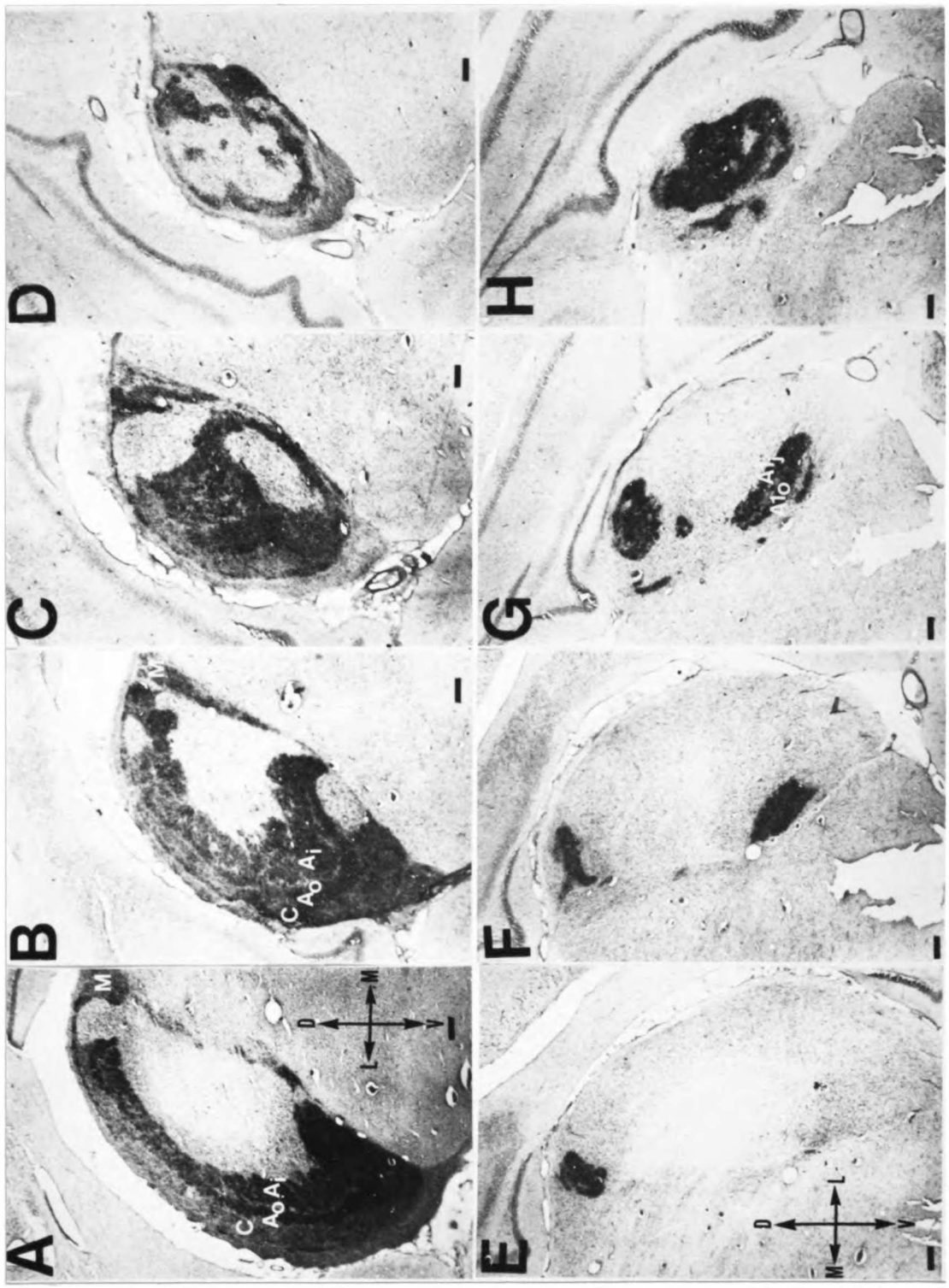
A
B
C
D
E
F
G
H
M
L
C
Ao
Ai
To
D
V

Figure 2. Autoradiographs of a series of parasagittal sections through the LGN. Upper row (A-E): sections contalateral to an eye which had been injected with ^{3}H-proline. Lower row (F-J): sections ipsilateral to the injected eye. A_O, outer leaflet of lamina A; A_i, inner leaflet of lamina A; $A1_O$, outer leaflet of lamina A1; $A1_i$, inner leaflet of lamina A1; *C*, C laminae; *OT*, optic tract; *P*, perigeniculate nucleus. *Scale bar* = 200 microns. The orientation of sections A-E is shown in (A), that of F-J is shown in (F). The arrow in (D) points to one of the bridges of label between lamina A and lamina C.


A
B
C
D
E
F
G
H
J

ipsilateral input (Fig. 1F). The laminar structure of the LGN is clear only in the most rostral sections when the nucleus is cut coronally. As seen in Figure 1A, the outer rim of the nucleus is made up of the C laminae (Linden et. al., 1981). A sublamination of the A laminae, termed "leaflets" by Guillery (1971), is visible over much of the nucleus in this section. In more caudal sections, the ipsilateral projection can be seen to expand from the medial edge of the nucleus. At its posterior pole, the LGN appears as an oval-shaped sheet in coronal section. The majority of the ipsilateral input to the LGN is found here. Lamina A1, which receives this ipsilateral input, may also be divided into leaflets, although the boundaries between the leaflets are obscure in coronal section.

The laminar structure of the LGN is most easily seen in parasagittal views of the nucleus (Fig. 2). In autoradiographically-labelled sections, the subdivision of the laminae into leaflets is apparent, especially in the ventral half of the nucleus. In some labelled sections, it is possible to resolve the C laminae into components (Fig. 2D). Label in the perigeniculate nucleus (PGN) contralateral to the injected eye (Figs. 2C and 2D) has been previously noted (Linden et. al., 1981). These authors believe this label represents fibres of passage entering lamina A rostrally or traversing the PGN on their way to other diencephalic or mesencephalic nuclei. In the case illustrated here, however, much of the perigeniculate labelling may be transneuronal because the animal survived longer than one week after the injection.

Contralateral to the injected eye, narrow bridges of label can be seen to connect lamina A with lamina C (Fig. 2D). Several such bridges were also observed in the doubly-labelled animal; they passed through thick parts of lamina A1 and were not merely features of its ragged edge. Ipsilateral-eye afferents are excluded from lamina A1 within these contralateral-eye bridges, as shown in Figure 3. Thus the retinal afferents serving the two eyes remain complementary rather than overlapping, even in the presence of such disruptions of the ordinary geniculate laminar structure. Ipsilateral-eye bridges through lamina C connecting laminae A1

Figure 3. "Bridges" in serial parasagittal sections through double-labelled LGN. Serial parasagittal sections through the LGN of the double-labelled ferret in which the contralateral eye had been injected with WGA-HRP and the ipsilateral eye with ^{3}H-proline. A) Section reacted with TMB method to make WGA-HRP label visible, then stained with neutral red, and photographed in dark-field. Note bridge of label through lamina A1 connecting laminae A and C. B) Section exposed for autoradiography and photographed in dark-field. Note that the terminal field of the proline-labelled eye excludes the bridge across lamina A1 visible in A. *Scale bar* = 200 microns. Other conventions as in Figure 2.

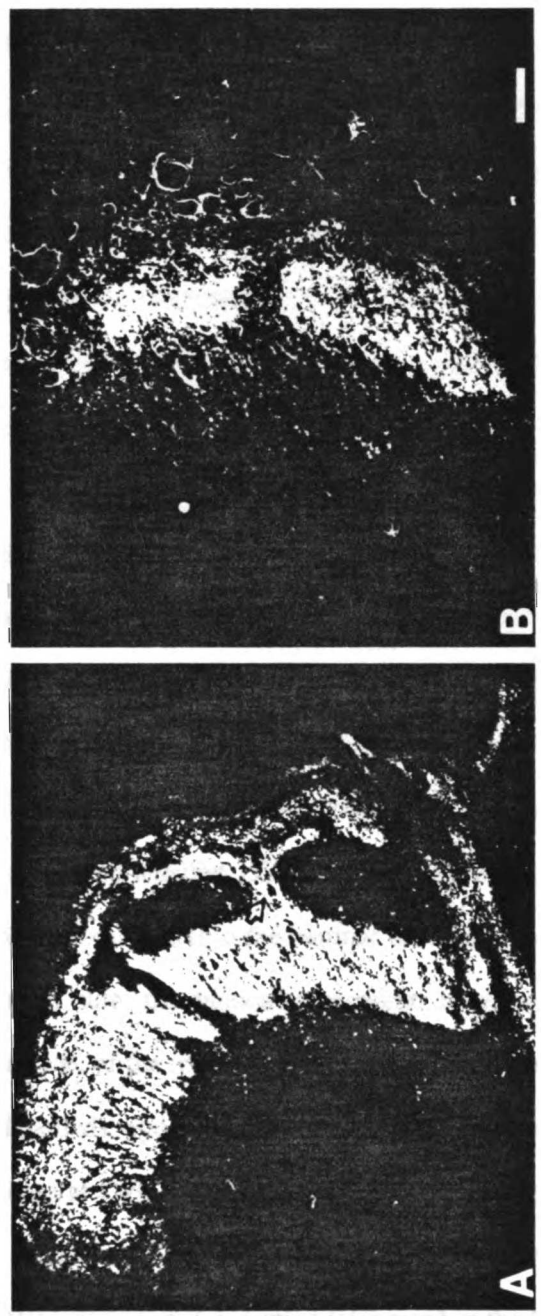
B
A

and C1 were also observed complementary to gaps in the contralateral terminal field (not illustrated).

Volume of the LGN. The total volumes occupied by the laminar LGN (including the interlaminar plexuses), measured on both sides of two animals in Nissl-stained parasagittal sections taken at 120-micron intervals, were 2.87 and 3.15 mm^3 in one 795 g female and 4.14 and 4.80 mm^3 in another 796 g female. In the animal in which one eye was labelled with WGA-HRP, the ipsilateral projection occupied 11% of this volume; the contralateral projection occupied 76%; and the balance (13%) appeared not to be innervated by either eye (interlaminar plexus, lamina C3, blood vessels, etc.). In the doubly labelled animal, the projection from the WGA-HRP labelled eye occupied 7% of the geniculate volume ipsilaterally and 70% contralaterally; while the projection from the autoradiographically labelled eye occupied 12% of the LGN ipsilaterally and 76% contralaterally. Thus, 82% and 83% of the two sides of the LGN were occupied by labelled terminal fields. The ipsilateral eye's terminal field appears to occupy only a fifth or less of the volume occupied by that of the contralateral eye.

Measurements of the volumes innervated by the two eyes in the binocular segment were also obtained from the double-labelled LGNs. The binocular portion of each section was defined by drawing lines perpendicular to the laminar borders at the dorsal and ventral edges of lamina A1. On the right side, the binocular segment, measured on Nissl-stained sections, occupied 1.96 mm^3, or 41%, of the total volume of the LGN. Terminals from the contralateral (autoradiographically-labelled) eye occupied 1.26 mm^3 in the binocular segment, while terminals from the ipsilateral (WGA-HRP-labelled) eye occupied 0.34 mm^3. On the left side, the binocular segment comprised 1.67 mm^3, or 40%, of the LGN. The terminal field of the contralateral (WGA-HRP-labelled) eye occupied 0.93 mm^3 in the binocular segment, while that of the ipsilateral (autoradiographically-labelled) eye occupied 0.49 mm^3.

Retrograde transport of HRP from LGN to retina.

The retrograde labelling experiments were undertaken to determine the location of the fixation point, which can be defined as the projection of the area centralis onto the tangent screen. We reasoned that the optic disc, area centralis, and labelled retinal ganglion cells could be located on the retinal wholemounts, and the relative positions of these landmarks determined. The fixation point could then be inferred from its location relative to the projections onto the tangent screen of the optic disc and the labelled retinal ganglion cells (the receptive field of the injection site).

A region of densely-labelled retinal ganglion cells 0.7 to 1.3 mm in radius was found in each of the three retinas processed with DAB; the fourth retina was destroyed during the processing with phenylenediamine and pyrocatechol. For each retina, the area centralis was defined as the 1-mm-diameter area in which retinal ganglion cell density was greatest. The optic disc head was easily seen in these wholemounts.

The occurrence of labelled cells over such a large area of retina, as well as the imprecision in locating the area centralis, resulted in a broad range of estimates of the location of the fixation point. Other evidence (see below) indicates that the horizontal separation between the optic-disc projection and the fixation point is approximately 30 deg. When the range of estimates of the fixation point was restricted to locations where this horizontal separation was in the range of 25 to 34 deg, the fixation point elevations ranged from 0.2 to 42 deg below the optic-disc projection in one retina, from 3 to 21 deg below the optic-disc projection in the second retina, and from 9 to 19 deg below the optic-disc projection in the third retina. These experiments therefore failed to provide a more precise estimate of the fixation-point elevation than did a consideration of receptive field sizes (see *"Fixation-point elevation and optic-disc projection"* below).

Electrophysiological Mapping.

The following sequence of events was often encountered in a vertical penetration. Upon entering the LGN, the electrode first passed through an area of high spontaneous activity. Histology later showed this region to be the C laminae. The multi-unit clusters here could frequently be driven by both eyes, depending on the eccentricity of the receptive field, and were usually responsive to both the onset and offset of a spot flashed in the center of the receptive field. The electrode would remain in this region for a variable distance, typically 200-400 microns. As the electrode was advanced out of the C laminae, the quality of the response would change, becoming extremely tonic, from one eye only, and of one center-type. The center-type could change during the course of the penetration. Penetrations in the rostromedial part of the LGN often passed through the perigeniculate nucleus (PGN). When the electrode was in the PGN, responses sounded less vigorous and unit clusters were binocularly driven. In the most rostral penetrations, the electrode never reentered the LGN. More caudally, the electrode would travel through the PGN for 800-1000 microns and then return to the LGN. Finally, as the lower border of the LGN was reached, the receptive fields might be in either eye, and the boundaries of the fields were less distinct.

In the most medial penetrations, our electrode sometimes entered the medial interlaminar nucleus (MIN). Recording sites in the MIN were characterized by large receptive fields, the borders of which were difficult to define with flashing or moving spots of light. No attempt was made to study the topographic organization of the MIN.

The fixation-point elevation and optic-disc projection. As noted in *Methods*, we estimated the elevation of the fixation point from the position of the smallest receptive fields. Figure 4A shows the entire complement of contralateral eye receptive fields plotted in the

Figure 4. Receptive-field size versus elevation. A) All receptive fields within the central 30 deg of azimuth recorded through the contralateral eye of one animal. Ellipses indicate the relative sizes of the receptive field centers. The projection of the right optic disc is marked by the *asterisk*. These data were obtained from the same experiment illustrated in Figs. 7 and 8. B) Receptive field area (deg^2) versus elevation (deg) for the fields shown in (A). Each open circle represents a receptive field from (A). Closed circles represent the average area of the receptive fields found at the elevation indicated $\pm$ 5 deg.

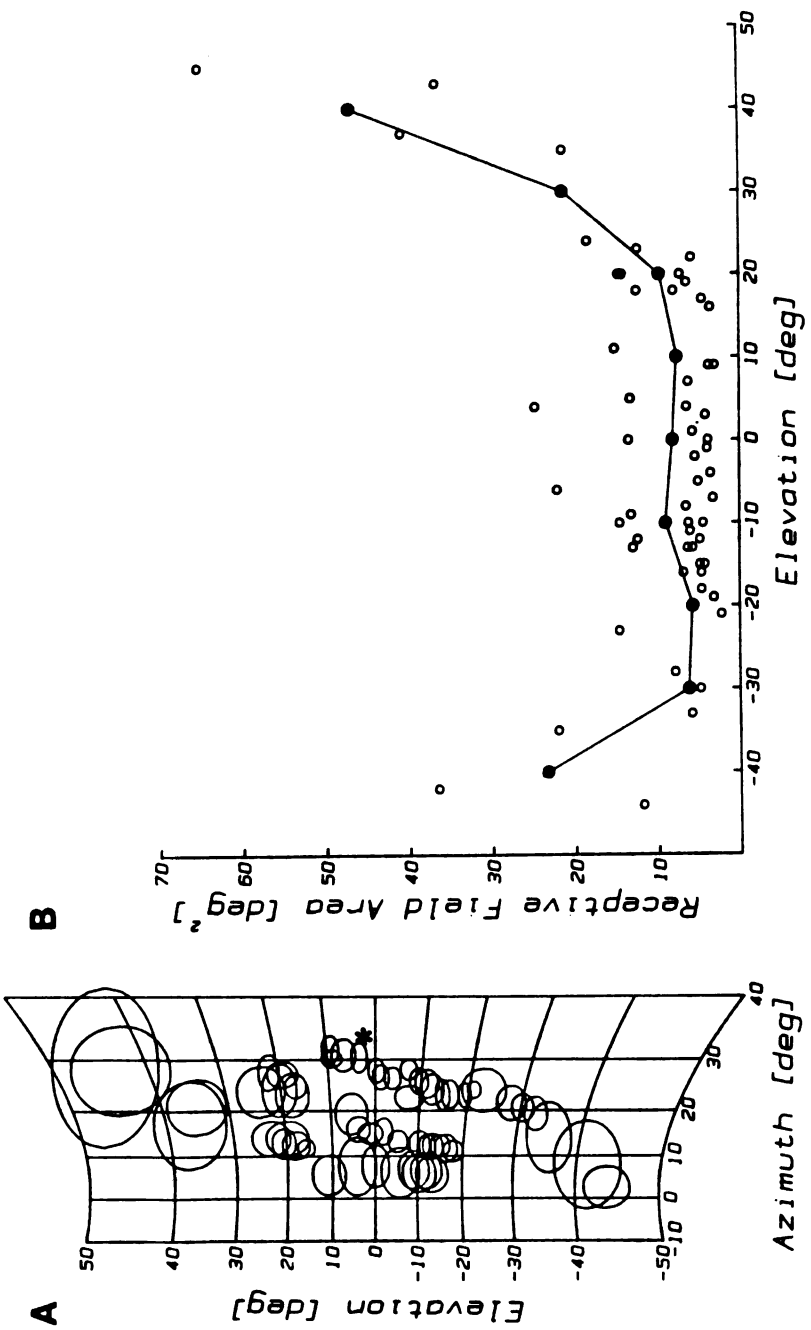
A
Elevation [deg]
50
40
30
20
10
0
-10
-20
-30
-40
-50
-10
0
10
20
30
40
Azimuth [deg]
B
Receptive Field Area [deg²]
70
60
50
40
30
20
10
-40
-30
-20
-10
0
10
20
30
40
50
Elevation [deg]

central 30 deg of azimuth in one experiment. The projection of the right optic disc, plotted with a reversing beam ophthalmoscope, is also shown in this figure. In this experiment, receptive-field size did not differ appreciably between elevations -30 deg and +20 deg. Very small receptive fields were found at the fixation-point elevation illustrated (3 deg below the optic-disc projection), consistent with the observation that the smallest fields were centered 3 deg, 4 deg, and 4 deg below the optic-disc projection in other mapping experiments. The horizontal separation between the projection of the optic disc and the fixation point was 33 deg in the case illustrated. This distance was found to be 32 deg, 33 deg, and 28 deg in the three additional experiments mentioned above.

This figure also illustrates a finding consistent in other experiments that the most medial receptive fields recorded within the LGN were located farther from a vertical line passing through the fixation point in the upper visual field than in the lower visual field. Penetrations medial to those containing the receptive fields illustrated were found to be outside the LGN. A line connecting the most medial receptive fields within the LGN formed an angle of between 10 and 20 deg with the vertical in different experiments.

Coronal plane findings. Results of a typical experiment are shown in Figure 5. Five penetrations can be seen in this coronal section from the posterior LGN. Lesions mark the lower boundary of the LGN in all but the most medial penetration. Here the upper lesion was made 100 microns below the border of the nucleus. The two most medial tracks are each marked with two lesions. The responses recorded along the two lateral tracks were elicited through the contralateral eye. The three more medial tracks are in ipsilaterally-innervated lamina A1. As the electrode travelled downward in the LGN, receptive field elevations decreased and the fields progressed toward the vertical meridian. More peripheral receptive fields mapped more laterally in the LGN, while more central fields were recorded at more medial sites in the nucleus.

The results from the three ferrets in which the penetrations were viewed in the coronal plane are summarized in the projection maps of Figure 6. The data from 306 receptive fields in 4 animals have been superimposed on five representative sections across the antero-posterior extent of the LGN. The maps from the different animals were made as consistent with each other as possible. Isoazimuths and isoelevations were drawn by connecting recording sites with receptive fields having the same azimuths or elevations, respectively. Following the method of Sanderson (1971), scatter in azimuth values along a penetration was ignored if there was no net change in azimuth. In drawing isoelevation lines, interpolations were sometimes made. (For example, a 10 degree line might be drawn between recording sites with receptive field elevations of 9 degrees and 11 degrees.) The Horsley-Clarke coordinates have been assigned relative to those obtained in the animal (an 830 g female) from which we obtained the largest number of recordings.

The isoazimuth lines, seen in coronal section, are curved, so that as a vertical electrode penetration advanced downward, receptive fields progressed toward the vertical meridian. Isoelevation lines are also curved in the coronal plane, beginning at the medial edge of the nucleus and arcing ventrolaterally. In general, peripheral fields are represented in the rostrolateral part of the LGN, while central fields are represented in the caudal and medial parts of the nucleus. There is an expanded representation of the central visual field in the caudal LGN.

The vertical meridian is represented near the medial border of the LGN. In the most caudal coronal sections, receptive fields with small negative azimuths were found in the lower visual field at the medial border of the nucleus. The representation of the vertical meridian is slightly lateral to the medial border in these sections. The horizontal meridian is found in the more dorsal part of the LGN. While superior receptive fields were recorded in the rostral LGN, most of the nucleus is devoted to the inferior half of the visual field.

Figure 5. Results of a typical mapping experiment. A) Five penetrations through a single coronal plane in the LGN seen in a Nissl stained section. A lesion (marked by *arrows*) marks the end of each penetration. The two most medial penetrations are each marked by two lesions. B) Locations of the receptive fields recorded along the penetrations through the section shown in (A). Open symbols mark sites where fields were recorded from the contralateral eye; filled symbols mark sites where fields were recorded from the ipsilateral eye. As the electrode moved downward in the LGN, the receptive fields moved down. The symbols correspond to those marking the LGN site at which the field was mapped (inset).

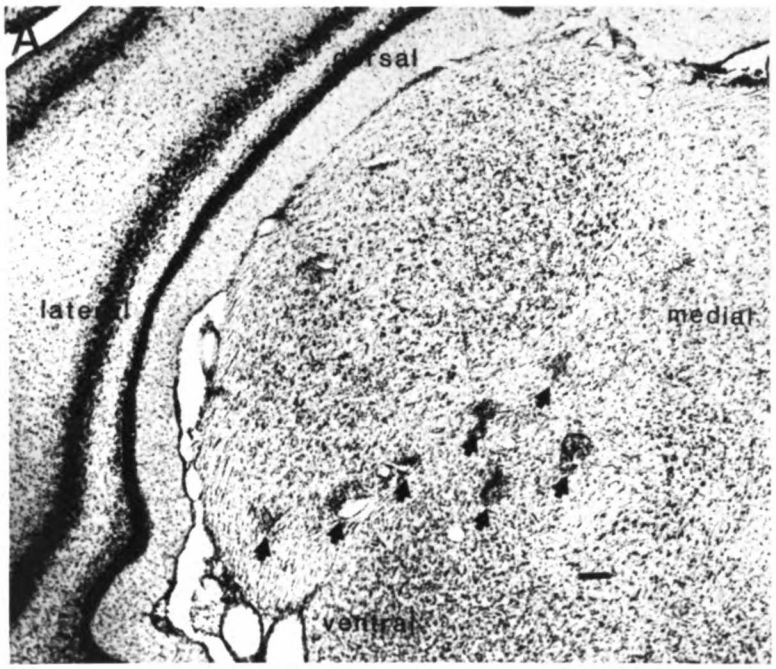
A
dorsal
lateral
medial
ventral

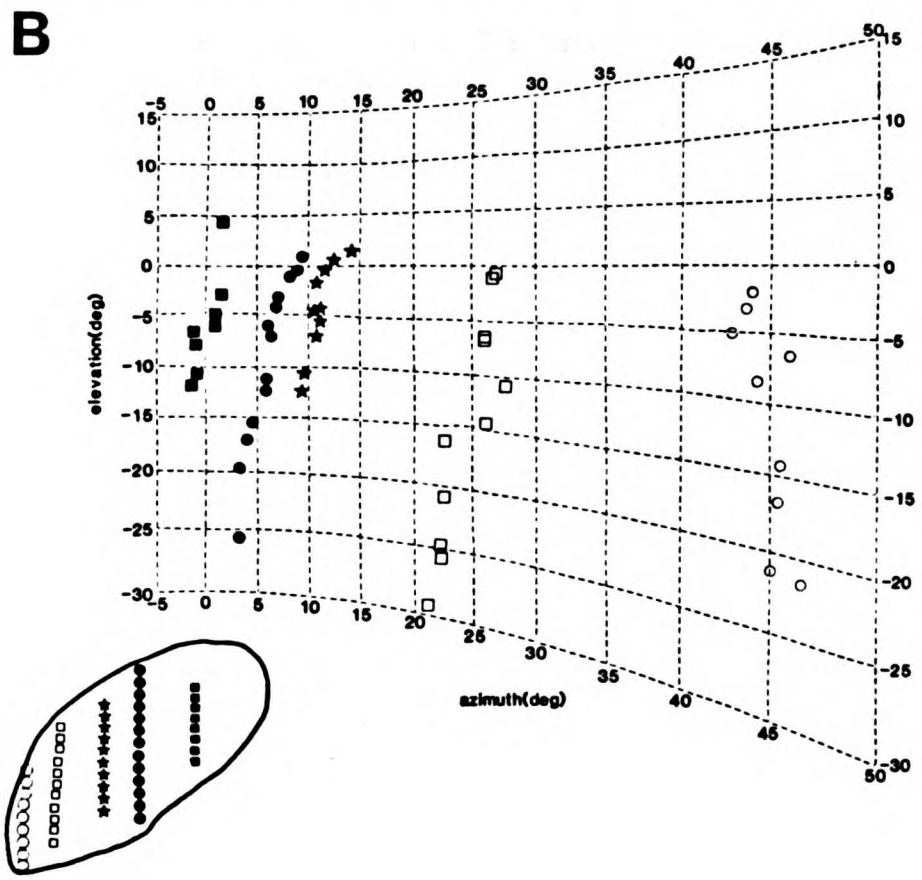
B
elevation(deg)
azimuth(deg)

Figure 6. Projection of the visual field onto coronal sections of the LGN. Data from 306 receptive fields recorded in four animals have been superimposed on five representative sections across the antero-posterior extent of the LGN. *Solid lines*, isoazimuths; *dashed lines*, isoelevations; *shaded areas*, fields recorded in the ipsilateral eye. The number above each section gives the Horsley-Clarke A-P coordinate of the section.

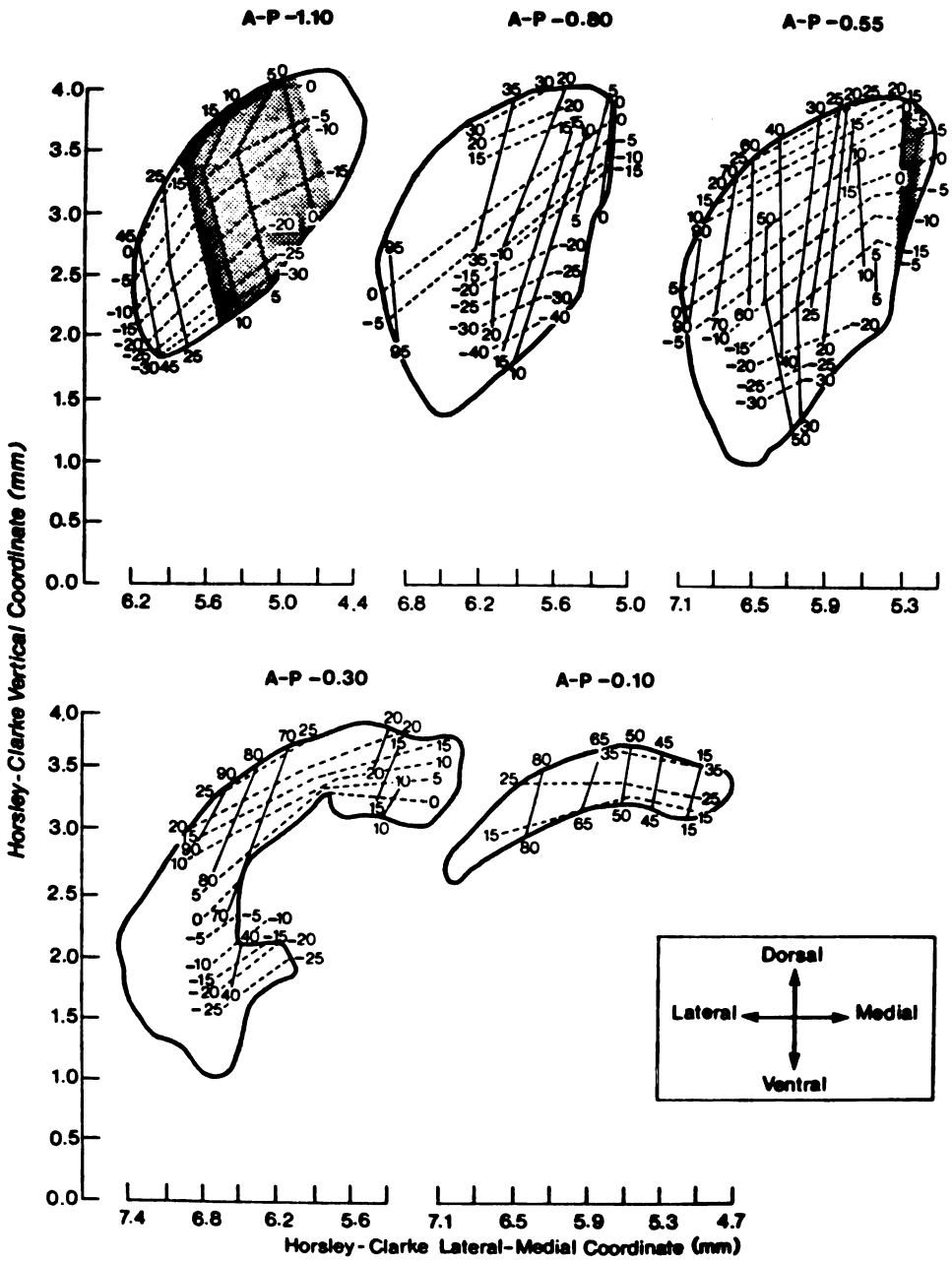
A-P -1.10
A-P -0.80
A-P -0.55
A-P -0.30
A-P -0.10
Horsley-Clarke Vertical Coordinate (mm)
Horsley-Clarke Lateral-Medial Coordinate (mm)
Dorsal
Lateral
Medial
Ventral

Sagittal plane findings. In an additional experiment, the LGN was sectioned parasagitally after electrophysiological mapping. Figure 7 shows these sections, tracings from which are aligned with the mapping data in Figure 8. Receptive fields recorded in the PGN are included. Although the quality of the responses changed when the electrode passed from LGN to PGN, progress in the receptive field locations was continuous between the two nuclei.

Isoelevations appear as lines oriented normal to the geniculate laminae when viewed in parasagittal section. Higher elevations are represented dorsally in the nucleus. The parasagittal plane is inconvenient for viewing isoazimuths; it is not possible to follow an isoazimuth from superior to inferior visual world within a single parasagittal section. Fields with the same azimuth values are found in a series of parasagittal sections, occurring higher in the nucleus in more medial planes. This observation is consistent with the outward bowing of the isoazimuth lines seen in coronal section. Within a single parasagittal plane, receptive fields with higher azimuth values are found rostrally.

The relationship of the isoelevation lines to the geniculate laminae is easily seen in the parasagittal sections of Figure 8. Isoazimuth lines are also expected to be oriented normal to the laminar borders, but this relationship would be clear only when the nucleus is viewed in horizontal section. Figure 9A shows a horizontal section from another animal taken approximately midway from top to bottom of the nucleus. The laminar structure of the LGN is apparent in this Nissl-stained section. Data from the animal illustrated in Figure 8 are superimposed on an appropriately-scaled drawing of this section in Figure 9B. The numbers shown on this figure represent the azimuth values recorded at the zero isoelevation line in each of 10 vertical penetrations. Isoazimuth lines (drawn as dashed lines) can be seen to run normal to the geniculate laminae. Only fields recorded in lamina A are shown; it is presumed that the isoazimuth lines are continuous between laminae. The expanded representation of the central visual field is also apparent in this figure. It should be stressed that this figure is a composite of

Figure 7. Electrode tracks in parasagittal sections of the LGN used in the construction of the projection maps. Parasagittal sections from the LGN of a single animal, containing the penetrations from which the maps in Figure 7 were obtained. The sections have been stained by a Nissl method. The numbers in the upper right corner give the lateral-medial coordinate of the section. The figure is arranged to reflect the relative vertical position of the sections. *Scale bar* = 500 microns.

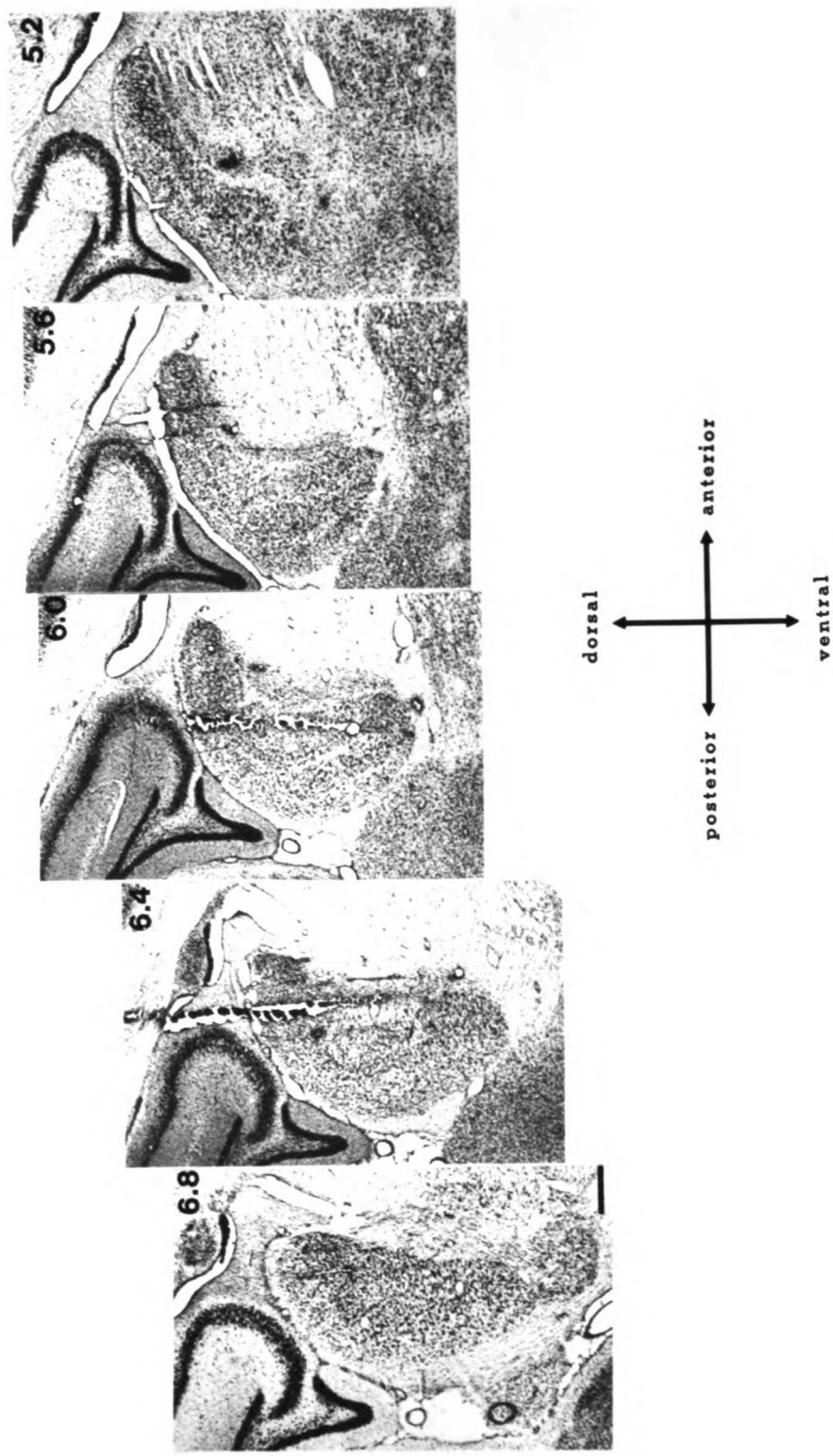
5.2
5.6
6.0
6.4
6.8
dorsal
anterior
posterior
ventral

Figure 8. Projection of the visual field onto parasagittal sections of the LGN. Five rows of penetrations in the parasagittal plane yielded 247 receptive fields in the LGN and PGN. Data were obtained from a single animal. Isoazimuths, *solid lines* whose values are postcripted with "A"; isoelevations, *dashed lines*; *shaded areas*, fields recorded in the ipsilateral eye; *A*, LGN lamina A; *A1*, LGN lamina A1; *C*, C laminae; *P*, perigeniculate nucleus. The number above each section gives the Horsely-Clarke lateral-medial coordinate of the section.

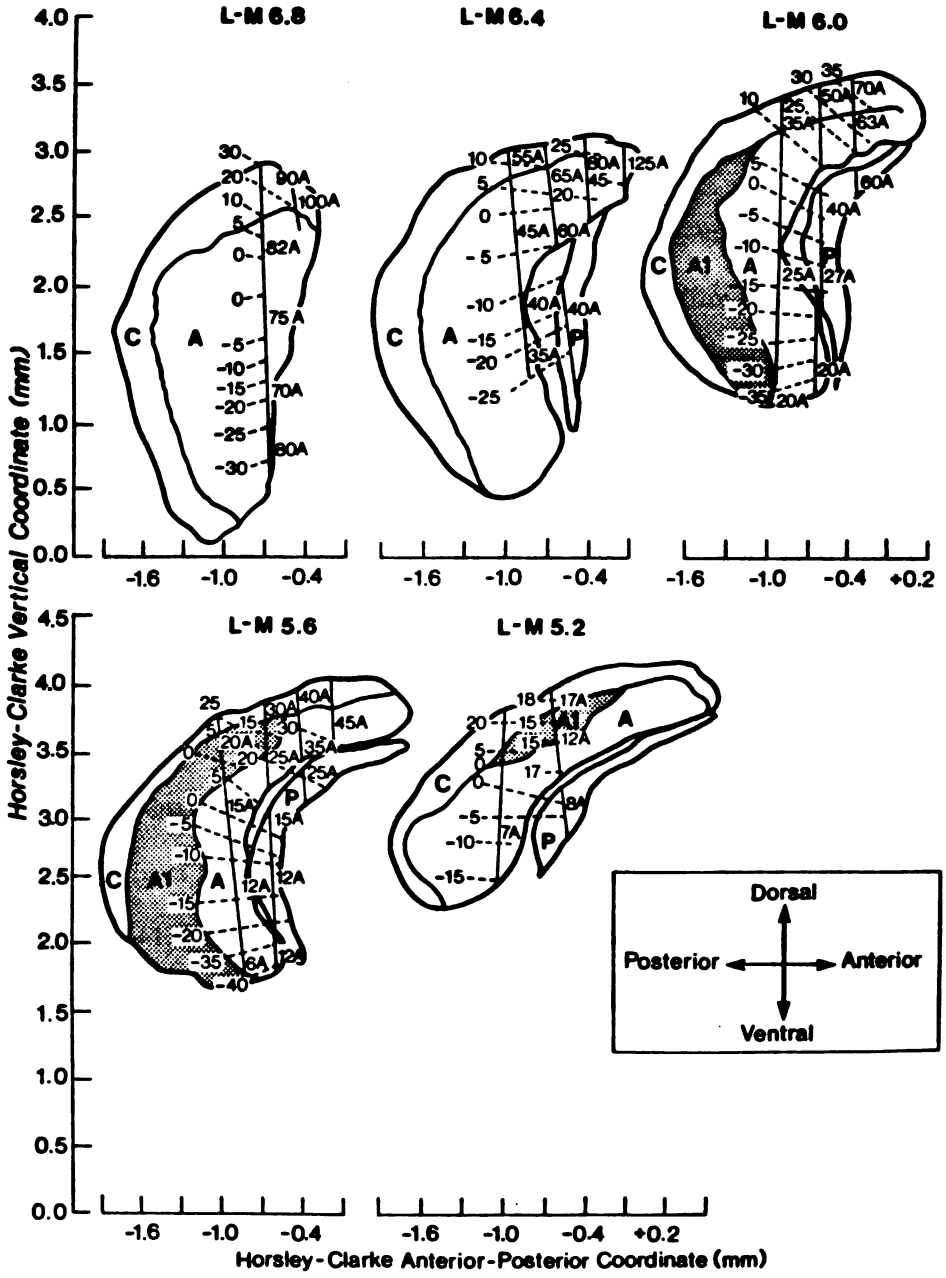
L-M 6.8
L-M 6.4
L-M 6.0
L-M 5.6
L-M 5.2
C
A
A1
P
Dorsal
Posterior
Anterior
Ventral
Horsley-Clarke Vertical Coordinate (mm)
Horsley-Clarke Anterior-Posterior Coordinate (mm)
4.0
3.5
3.0
2.5
2.0
1.5
1.0
0.5
0.0
4.5
-1.6
-1.0
-0.4
+0.2

the electrophysiological data from one animal and a section through the LGN of a second ferret, intended only to illustrate the angle the isoazimuth lines make with the laminar borders. In the drawing (Fig. 9B), lamina A1 appears to lie opposite lamina A as far laterally as the 45 deg isoazimuth. In fact, receptive fields in lamina A1 have not been found beyond the 30 deg azimuth.

Lines of projection. The maps indicate that a point in the visual world projects to a line running perpendicular to the geniculate laminae. In order to confirm this, penetrations inclined approximately 40 degrees from the vertical in the sagittal plane were made in two ferrets. Two of these oblique penetrations are shown in Figure 10. The upper penetration is nearly perpendicular to the geniculate laminae and is approximately along a line of projection. The receptive field positions change relatively little along this penetration, as compared with the progress in receptive fields encountered in the lower penetration. The 10-degree jump in elevation recorded when the electrode passed from lamina A1 to lamina A does not reflect an error in correcting for misalignment of the eyes; no such discontinuity is observed in crossing from contralaterally-innervated lamina C to lamina A1.

Extent of visual field. The range of azimuths encountered for the contralateral eye was from -2 degrees to +125 degrees, while elevations ranged from -45 degrees to +45 degrees. It is likely that more inferior fields are represented in the ferret LGN. We were unable to map the most ventral portion of the LGN, as our stereotaxic apparatus obscured the most inferior visual field. Fields of the ipsilateral eye had azimuths ranging from -5 degrees to +30 degrees. Elevations of receptive fields of sites in lamina A1 ranged from +15 degrees to -25 degrees.

Figure 9. Lines of projection are normal to laminar borders (horizontal section). A: Horizontal section approximately midway from top to bottom in the LGN. This section has been stained by a Nissl method. A_i, inner leaflet of lamina A; A_O, outer leaflet of lamina A; *A1*, lamina A1; *C*, C laminae. *Scale bar* = 100 microns. B: Azimuth values recorded along the zero elevation in the experiment illustrated in Figure 6 have been superimposed on a drawing of the section in (A). *Dashed lines*, isoazimuths; other conventions as in (A).

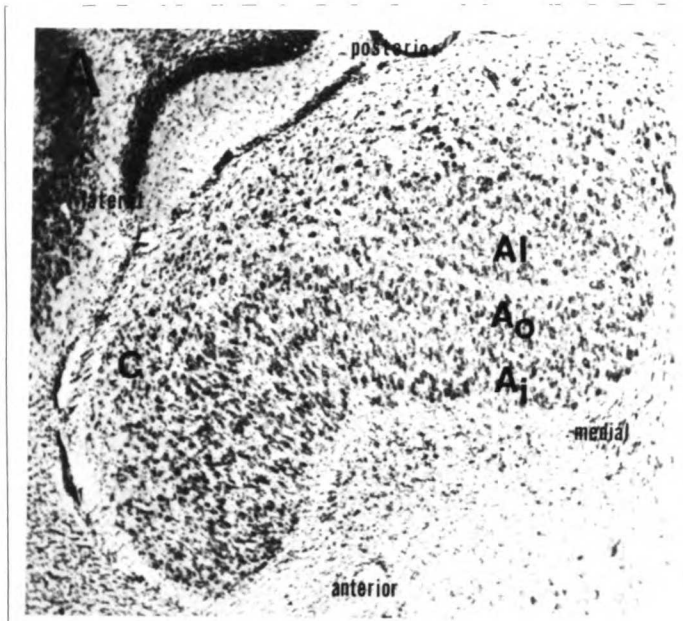
posterior
lateral
A
C
Al
Ao
Ai
medial
anterior

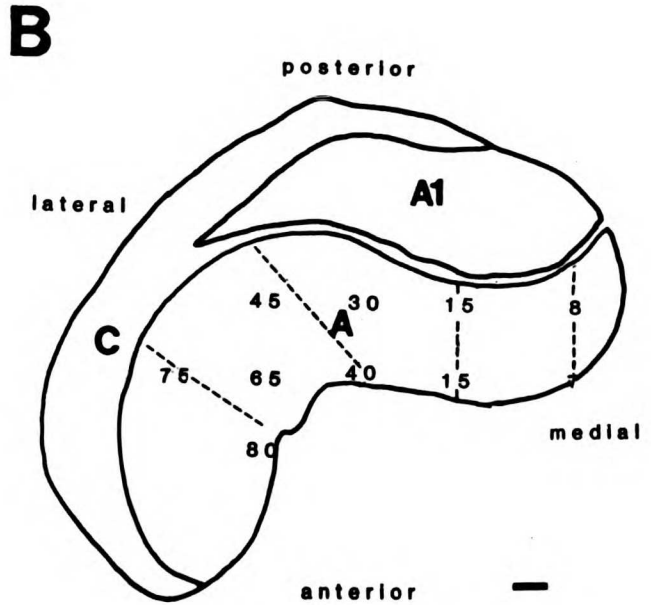
B
posterior
lateral
A1
45
30
15
8
C
A
75
65
40
15
80
medial
anterior

Figure 10. Lines of projection are normal to laminar borders (parasagittal section). A) A parasagittal section containing two penetrations angled approximately 40 degrees from the vertical. The upper penetration falls approximately along a line of projection. *Arrow* shows electrolytic marking lesion. B) Camera lucida drawing of the section shown in (A). Numbers indicate the sites from which the fields shown in (C) were recorded; *arrow* shows the location of the lesion shown in (A). C) receptive field positions recorded at the sites marked on the drawing in (B). *Scale bar* = 300 microns.

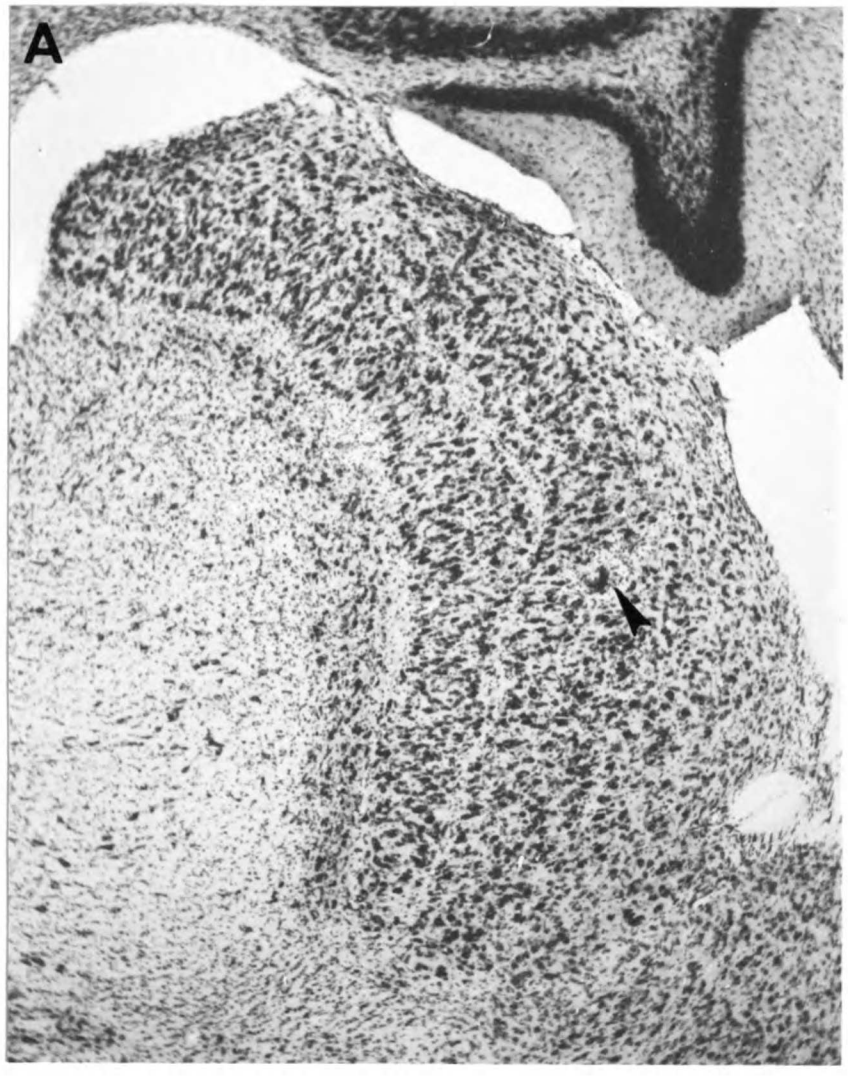
A

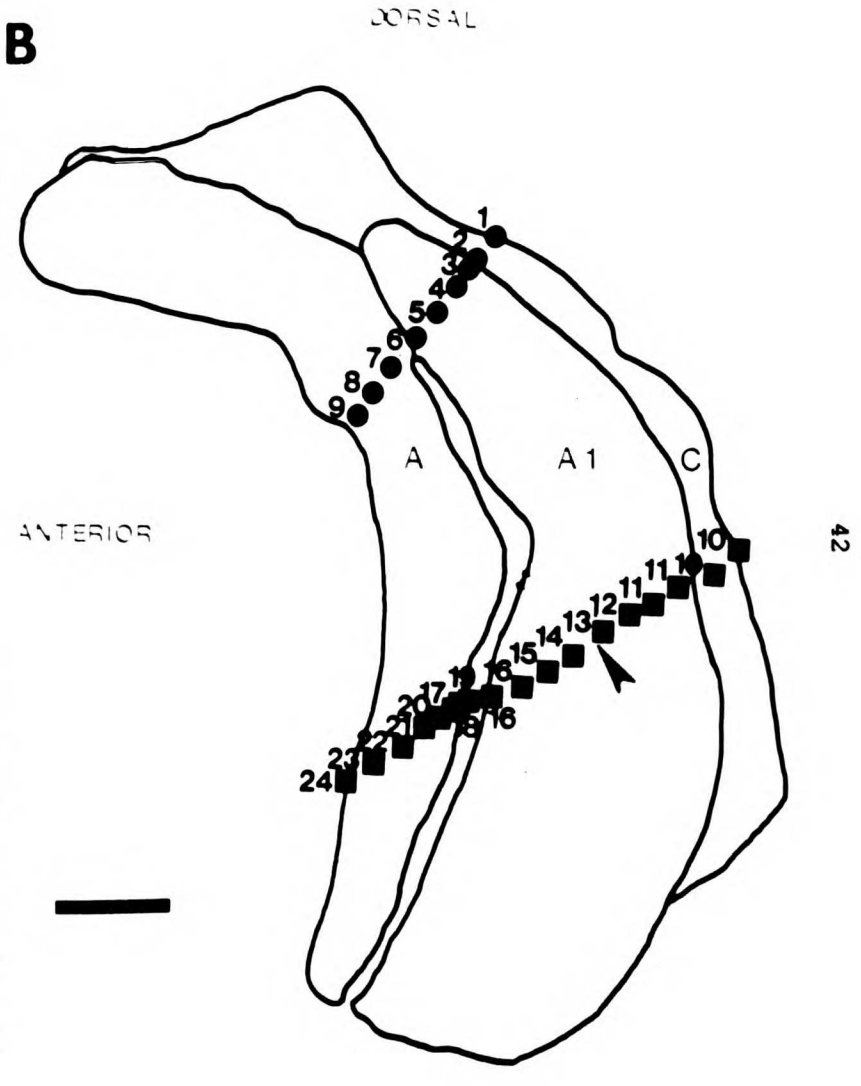
B
DORSAL
ANTERIOR
A
A 1
C
1
2
3
4
5
6
7
8
9
10
11
12
13
14
15
16
17
18
19
20
21
22
23
24

C

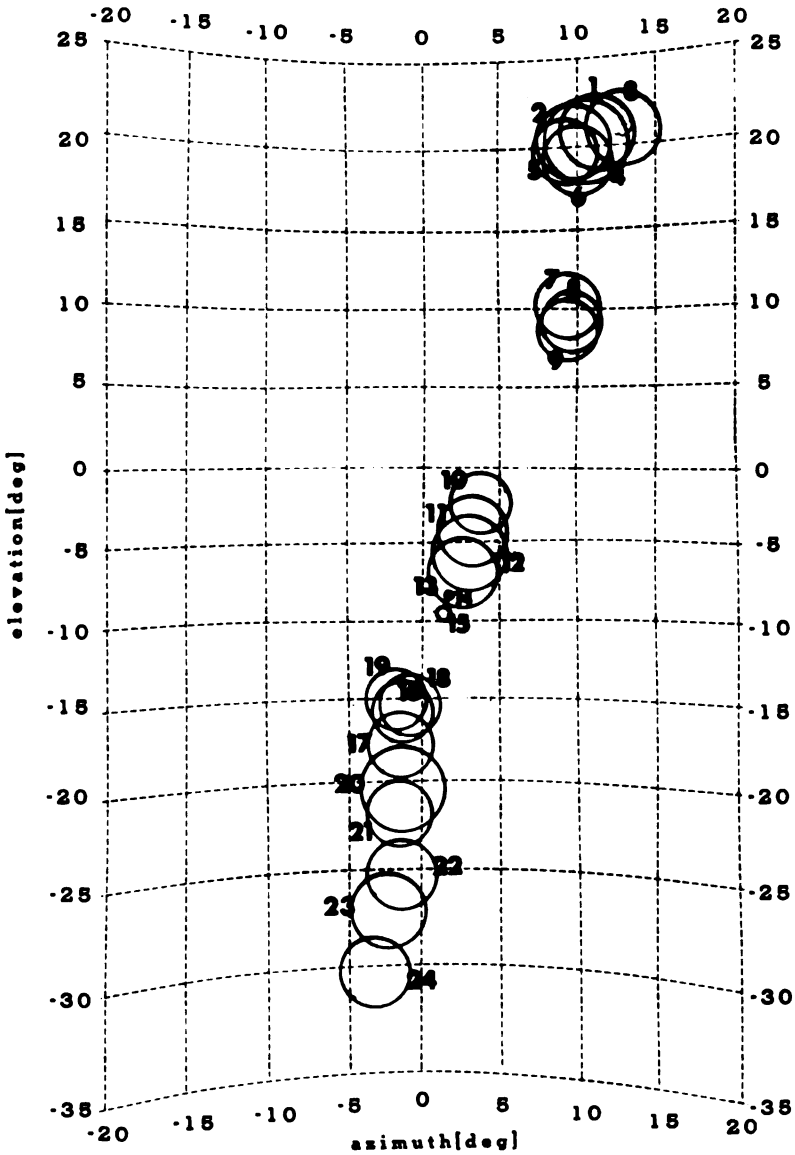
elevation[deg]
azimuth[deg]
-20 -15 -10 -5 0 5 10 15 20
25 20 15 10 5 0 -5 -10 -15 -20 -25 -30 -35

Discussion

The lateral geniculate nucleus of the ferret contains a single orderly map of the contralateral visual hemifield. Microelectrode recordings of multi-unit activity in the LGN revealed that the upper visual field is represented dorsally and rostrally in the nucleus, central receptive fields are found in the medial and caudal sections of the LGN, and peripheral fields are represented in the lateral LGN.

Comparison with cat. The organization of the ferret LGN may be compared to that of the more widely-studied cat LGN: the ferret map would become like the cat map if the ferret's right LGN were rotated approximately 110 degrees clockwise, as viewed from its medial aspect, in a parasagittal plane. (Compare Figure 6 of Sanderson, 1971 with Figure 8 here.) The ferret, having more laterally placed eyes, does not have as large a binocular representation of the visual field as does the cat. The volume of ipsilaterally-innervated territory is between an eighth and a fifth of that innervated by the contralateral eye. Recording sites in lamina A1 have receptive fields with azimuths as far as 30 degrees from the vertical meridian in the upper visual fields, and as far as 20 degrees at the horizontal meridian, a much less extensive ipsilateral representation than in the cat. Ipsilaterally-innervated sites in the cat LGN have been reported to have azimuths as far as 40 degrees from the vertical meridian (Sanderson, 1971). The visual field map is continuous between the LGN and PGN in the ferret, as in the cat (Sanderson, 1971).

Planes of section. The three standard planes of section are each useful for observing some aspect of geniculate organization. Although the laminar organization of the nucleus is obscure in coronal section, this plane is the most useful for viewing the pattern of isoazimuth and isoelevation lines representing a large part of the visual field. Lamination is easily seen when the LGN is sectioned parasagitally or horizontally. The parasagittal plane is also the most useful for observing the pattern of isoelevation lines relative to the laminae. The horizontal plane is the most useful for observing the pattern of isoazimuths relative to the laminar borders; however, this plane is not useful for histological reconstruction after electrophysiological studies.

Orienting the neurophysiologist. The summary map presented in Figure 6 and the data from the experiment illustrated in Figure 7 should aid in locating the position of a recording site in the LGN. Stereotaxic coordinates in these figures apply to female ferrets (700 - 800 g); we do not know by how much they would differ in the larger male animals. The precise position of the electrode along a line of projection may be determined by noting the eye preference and center-type of the receptive field. OFF-center receptive fields recorded through the ipsilateral eye are found in the outer leaflet of lamina A1 and ON-center ipsilateral fields map to the inner leaflet of A1. OFF-center contralateral fields are recorded in the outer leaflet of lamina A, and ON-center contralateral fields are found in the inner leaflet of lamina A (Stryker and Zahs, 1983). The C laminae may be recognized by the high spontaneous activity recorded there. Optic-tract fibres may contribute much of the high spontaneous activity evident in multi-unit recordings. Electrode penetrations located medial to the laminar LGN may encounter the medial interlaminar nucleus. Recording sites in the MIN are characterized by large multi-unit receptive fields, the borders of which are difficult to define using flashing or moving spots of light. The perigeniculate nucleus is located just rostral to the LGN. Although the visual field

map is continuous between the LGN and the PGN, there should be no difficulty in determining when an electrode has passed from one nucleus to the other: Multi-unit responses recorded in the PGN are less vigorous than those recorded in the LGN, and responses in the PGN can be elicited through either eye.

Fixation point and relation of the visual field meridians to the retinal axes. Our estimate of the elevation of the fixation point depends on the elevations of the smallest receptive fields. This estimate is subject to error because the size of central fields did not change dramatically with elevation (for example, see Fig. 4). However, our estimate of the fixation-point elevation is supported by two observations. First, this determination of the zero elevation, in relation to the elevation of the projection of the optic disc, was consistent from animal to animal. Second, from an analysis of retinal wholemounts retrogradely labelled by injections of HRP into the LGN, Vitek et al. (1985) have demonstrated that in the ferret, as in the cat, the line connecting area centralis to the optic disc makes an angle of 112 deg with the line of decussation. The line connecting our estimate of the fixation point and the projection of the optic disc is inclined at 96 deg to the vertical. If this estimate of the fixation point is correct, then the results of Vitek et al. indicate that the line of decussation should be projected to an angle of 16 deg (112 deg - 96 deg) to the vertical. Such an inclined projection of the line of decussation is consistent with our finding that the most medial receptive fields within the LGN formed an angle of between 10 and 20 deg with the vertical (for example, see Fig 4).

We have not been able to estimate the angle the vertical meridian makes with a vertical line passing through the fixation point. To determine this would require measurement of the horizontal separation between the two receptive fields of binocular recording sites at extremes in the upper and lower fields. In these experiments focusing on the LGN, so few binocular receptive fields at extreme elevations were encountered that this determination was not possible.

Bridges. An unexpected finding in this study was the occurrence of discontinuities in the ipsilateral projection onto lamina A1 and the contralateral projection onto lamina C. Sections from the double-labelled animal allowed us to observe bridges of label from the contralateral eye spanning these gaps in the ipsilateral innervation of lamina A1. Similarly, bridges of label between laminae A1 and C1 were seen to fill the gaps in the contralateral innervation of lamina C. To our knowledge, the electrode never passed through one of these bridges during the electrophysiological mapping experiments; we did not find any responses that were elicited through the "wrong" eye when recording in the A laminae. We do not know how the bridges relate to the retinotopic map in the LGN or the effects of the bridges on the cortical maps. Whatever the source of such irregularities in laminar pattern, the invariable outcome appears to be a strict segregation of the terminal fields of ipsilateral and contralateral eye afferents. Such an outcome suggests that the developmental mechanism responsible for the segregation of the two eyes' afferents operates more powerfully than any mechanism that tends to confine each eye's afferent terminals to particular laminae of the LGN.

These malformations of a smooth geniculate laminar pattern are reminiscent of, but much less pronounced than, those resulting from the Siamese and other pigment abnormalities (Guillery, 1969; Guillery and Kaas, 1971; Shatz, 1977; Cucchiaro and Guillery, 1982). Although the bridges described here were found in the LGNs of normally-pigmented ferrets, it is possible that these animals carried an albino allele. However, disruptions of the geniculate laminae have also been observed in normally-pigmented individuals of other species (cat, Polley and Guillery, 1980, Anderson et al., in preparation; non-human primates, Kaas, et al., 1978; humans, Hickey and Guillery, 1979). In cats, at least, such disruptions may be fairly common: Polley and Guillery observed anomalous islands of ipsilateral retinogeniculate input to lamina A in 6 of 13 normally-pigmented cats examined. It is not known whether afferents from the contralateral eye were excluded from these islands. Interestingly, these islands

occupied similar positions within the monocular segment of lamina A in all of the LGNs that contained such islands. Too few brains have been examined to determine whether bridges occupy stereotyped locations in the ferret LGN. A more complete study of the bridges may prove interesting, since their occurrence is clearly related to the question of how the retinogeniculate afferents sort themselves into the appropriate geniculate laminae during development.

Chapter III

The projection of the visual field onto primary visual cortex of the ferret

Introduction

Knowledge of the organization of the cortex in normal, adult animals is prerequisite to further investigations into geniculostriate and cortical development. This chapter describes the topographic organization of the primary visual cortex (area 17) of the adult, pigmented ferret (*Mustela putorius furo*). Other results from our laboratory regarding ocular dominance and orientation columns within the ferret's primary visual cortex will be reported elsewhere (Law et al., in preparation; Waitzman and Stryker, in preparation).

Transneuronal autoradiography following an intraocular injection of ^{3}H-proline has been used to locate area 17 within the occipital cortex of the ferret (Law et al., in preparation). In the present study, electrophysiological recordings were used to study the projection of the visual field onto area 17. The results reported here describe the orientation of the visuotopic map in area 17, an expanded representation of the projection of the horizontal meridian, the location of the representation of the monocular segment of the visual field within area 17, and the location of the boundary between areas 17 and 18 on the dorsal surface of the cortex.

Methods

Animals.

Two normally-pigmented adult ferrets (700 - 800 gm females, Marshall Farms, New Rose, N.Y.) were used in the electrophysiological mapping experiments. Data from an additional three animals concerning the anatomical localization of area 17 and the extent of the binocular visual field have also been included.

Electrophysiological recording.

Ferrets were prepared for physiological recording using the techniques described in Chapter 2. In these animals, a skull screw was placed over the hemisphere contralateral to that studied electrophysiologically, and the electroencephalogram (eeg) was monitored throughout the experiment. Intravenous thiopental sodium was administered at the first sign of desynchronization of the eeg.

Area 17 was made accessible by a large craniotomy extending from Horsley-Clarke anterior-posterior -2 mm to the caudal pole of the hemisphere (approximately Horsley-Clarke -8 mm), and from Horsley-Clarke lateral-medial 2 mm to the lateral margin of the skull (approximately Horsley-Clarke 11 mm).

Lacquered tungsten microelectrodes (Hubel, 1957) were used to record multi-unit activity in the cortex. Rows of electrode penetrations were made in the parasagittal plane.

Penetrations were spaced at 500-μm or 1-mm intervals within a row, and rows were spaced at 1-mm intervals. The entry points of the penetrations were recorded on photographs of the cortical surface, using blood vessels as reference points. The electrodes were advanced vertically in 100-μm steps until layer IV was encountered. Afferents from the lateral geniculate nucleus contribute to the multi-unit activity recorded within layer IV and can be recognized by their brisk responses to non-oriented, rapidly-moving stimuli.

Multi-unit receptive fields were plotted within layer IV, using spots and oriented bars of light. Responses could often be elicited through either eye. Receptive fields were always determined through the dominant eye at each recording site, and were usually determined through each eye. After recording in layer IV, the electrode was advanced and receptive fields were often plotted again within layer VI. The electrode was then advanced through the white matter until the ventral tier of gray matter was recognized by a change in background activity. Within the ventral tier, receptive fields were plotted at recording sites in layer VI and again in layer IV. Due to the folding of the cortex, vertical electrode penetrations are not normal to the laminae in the ventral tier of grey matter. Some of the most rostral penetrations travelled almost parallel to the laminae within the caudal bank of the splenial sulcus, and recording sites were spaced at 100-μm intervals here.

Histological reconstruction of electrode penetrations.

Electrolytic lesions (5 μA x 5 sec) were used to mark recording sites. At the end of the recording session, 0.5 to 1.0 μl of the dye fast green was injected into each of 2 or 3 sites in the cortex to serve as additional markers. The dye was injected, at a depth of 1 - 2 mm, through a 26 ga needle attached to a 5-μl Hamilton syringe. Dye marks were placed

between electrode penetrations within selected rows to help distinguish between rows of penetrations. The ferret was then deeply anesthetized with an intravenous injection of sodium pentobarbital. One animal was then perfused through the heart with 0.1 M phosphate buffer (pH 7.4) followed by 4% paraformaldehyde, 1% gluteraldehyde in 0.1 M phosphate buffer, while the second animal was perfused with 0.9% saline, followed by 10% formol saline. The head was placed in the fixative for 1 to 2 weeks. A block of brain containing area 17 was removed and sunk in 30% sucrose-formalin. The block was then embedded in an albumin-gelatin mixture, before being sectioned at 40 μm in the parasagittal plane on a freezing microtome. All sections were collected, mounted on gelatinized slides, and stained with cresyl violet.

Camera lucida drawings and photomicrographs were made of sections containing electrode tracks. Recording sites were assigned by referring to the Horsley-Clarke coordinates of the electrode penetrations, microdrive readings at the lesion sites, and the locations of the dye marks.

The receptive-field position at each recording site was noted on the photographs and drawings. The location of each receptive field was expressed as two angles, azimuth and elevation, using the system of spherical polar coordinates described in Chapter 2. The fixation-point azimuth was determined for each eye as described earlier. In order to make the cortex maps consistent with the LGN maps, the fixation-point elevation for each eye was placed 3.5 deg below the projection of the optic disc. The uncertainty in assigning the fixation-point elevation has been discussed in Chapter 2 and will be further considered later.

Graphically unfolding the cortex.

The drawings of the reconstructed electrode penetrations were used to create unfolded representations of area 17 and neighboring visual areas after building a physical 3-dimensional model. In these reconstructions, data from 4-10 serial 40-μm sections were collapsed onto a drawing of a single section. Sections were selected for drawing at approximate 1-mm intervals. Drawings were mounted on cardboard and assembled in accurate 3-dimensional register. Strips of foil were then laid along the border between layers IV and V, and the positions of the recording sites were projected radially onto these strips.

For all but the most medial and most lateral sections, the width of the strip of foil was the average distance between the section and its two neighbors of the series. Since, for both animals, the mapped region extended approximately to the medial border of area 17, the width of the most medial strip was chosen to be half the distance between the two most medial sections. For one animal (F81), electrode penetrations had been placed quite far laterally, and recording sites were found in the sharply-curved region of cortex, where the parasagittal plane is nearly tangential to the plane of layer IV. A tracing was made of the most lateral section of the series from F81, and this tracing was opened along an antero-posterior cut hinged at the caudal pole. In the second animal, sections containing recording sites did not extend as far laterally, and the most lateral section was represented as a strip half the width of the distance between it and its nearest neighbor of the series.

The strips were then laid flat and aligned so the caudal poles of the sections were in the correct relative anterior-posterior positions. Isoazimuth and isoelevation lines were drawn by connecting recording sites with receptive fields having the same azimuths or elevations, respectively. In drawing these lines, interpolations were sometimes made. (For

example, a 10 deg isoelevation line might be drawn between recording sites with receptive field elevations of 9 deg and 11 deg.)

Area measurements and areal magnification factors.

The area encompassed by area 17 was measured on each unfolded map using a Summagraphics bitpad connected to a MicroVaxII computer. Areal magnification factors were derived from measurements of these flattened maps. Each area of cortex bounded by a pair of isoazimuth lines and a pair of isoelevation lines was measured; areas bounded by isoazimuth or isoelevation lines drawn from long interpolations between recording sites were excluded from these calculations. This area value was then divided by the area of visual field represented in that area of cortex to give the areal magnification factor in units of mm^2 of cortex per deg^2 of visual field.

Results

Location of area 17.

The location of area 17, as revealed by electrophysiological recordings, is shown in Figure 11. Area 17 occupies most of the posterior lateral gyrus, the caudal portion of the splenial gyrus, and part of the caudal bank of the splenial sulcus. The representation of the vertical meridian forms the dorsal rostral border of area 17 and is seen as a line that roughly follows the contour of the posterior lateral gyrus. The exact rostrocaudal position of this line varies among animals and may extend dorsally onto the lateral gyrus. Inferior elevations are represented dorso-medially along this line and superior elevations map ventro-laterally. Isoazimuth lines are oriented nearly parallel to the long axis of the posterior lateral gyrus, and isoelevation lines run roughly perpendicular to the isoazimuth lines. Area 17 wraps around the posterior lateral gyrus at the posterior pole of the hemisphere, traverses the occipitotemporal sulcus (Lockard, 1982) and splenial gyrus, and terminates on the caudal bank of the splenial sulcus. The occipitotemporal sulcus is a shallow sulcus that takes the same position with respect to area 17 as the suprasplenial sulcus in the cat (Tusa et al., 1978). This sulcus is not always apparent in parasagittal sections through the cortex, and its rostral extent varies greatly among animals. The splenial gyrus forms the tentorial surface of area 17.

Figure 11. The location of area 17 on the surface of the ferret brain. The brainstem at the level of the medulla and the cerebellum have been removed. A) Lateral view showing the visual field projection onto area 17. *Solid lines* indicate isoazimuths and *dashed lines* indicate isoelevations. Labelling of sulci and gyri after Lockard, 1982. B) Caudolateral view of area 17. *Heavy arrows* show lateral-medial level of cut in left hemishpere in (E). C) Caudomedial view of area 17. D) Dorsal view of area 17. E) Relation of the surface appearance of area 17 to its appearance in section. The left hemisphere was cut in the parasagittal plane at the level shown in (B), the cortex lateral to the cut was removed, and the cut surface was outlined. Compare this figure to section 4 of Figure 13.

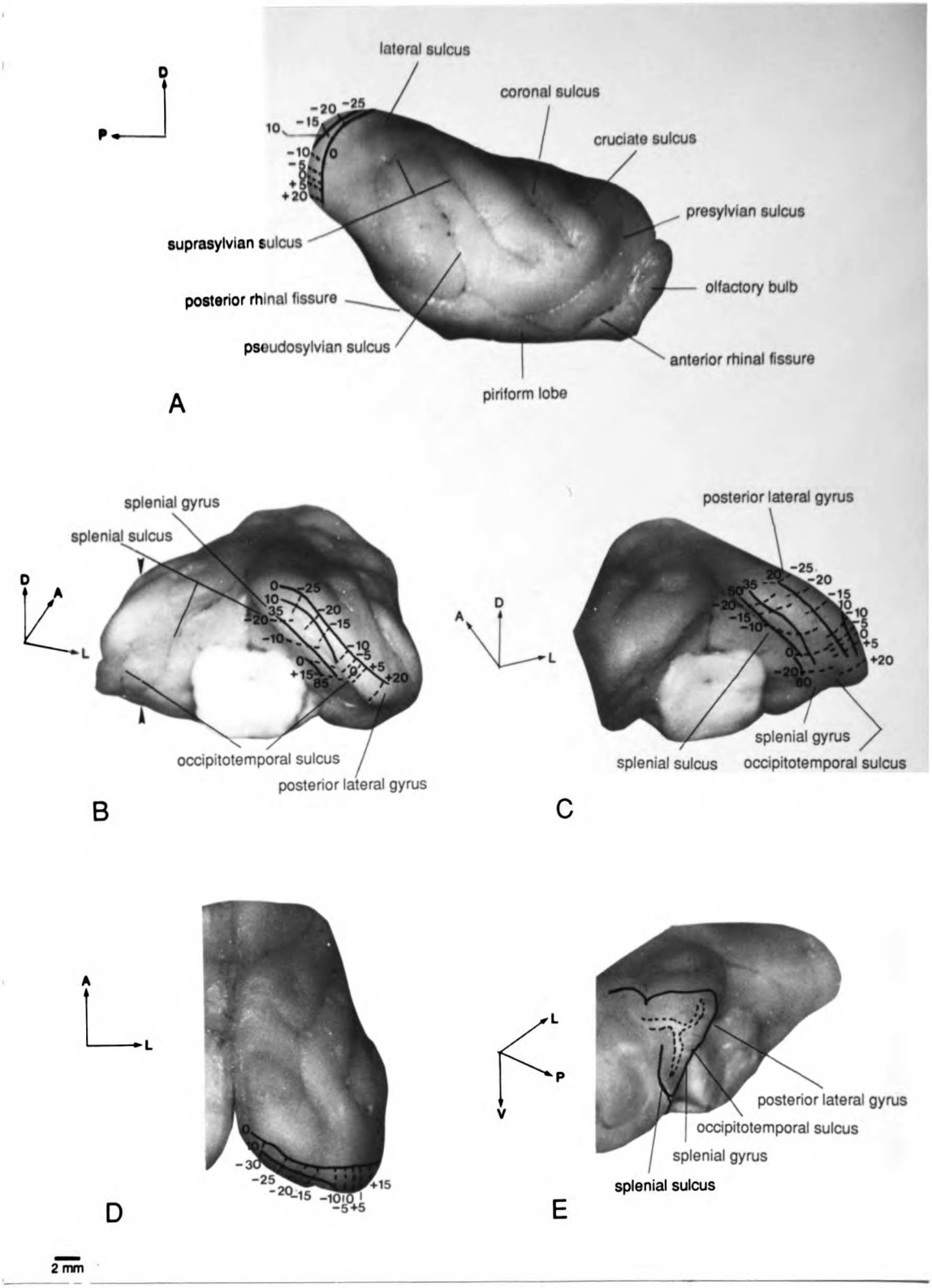
lateral sulcus
coronal sulcus
cruciate sulcus
presylvian sulcus
olfactory bulb
anterior rhinal fissure
piriform lobe
pseudosylvian sulcus
posterior rhinal fissure
suprasylvian sulcus
D
P
A
splenial gyrus
splenial sulcus
occipitotemporal sulcus
posterior lateral gyrus
B
posterior lateral gyrus
splenial gyrus
splenial sulcus
occipitotemporal sulcus
C
L
D
E
V
2 mm

Topographic organization of area 17.

Receptive fields were determined at 143 sites in 54 electrode penetrations in one animal (F81) and at 134 sites in 41 penetrations in a second animal (F91). Electrode penetrations were reconstructed from serial parasagittal sections stained by a Nissl method. Figure 12 shows the centers of the receptive fields of the multi-unit clusters recorded in F81. Because the location of area 17 is more easily seen in autoradiographically-labelled sections than in Nissl-stained sections, the mapping data from F81 were superimposed on a series of sections from another animal. This animal had received an injection of ^{3}H-proline into one eye a week prior to a terminal recording experiment in which the boundary between areas 17 and 18 was determined electrophysiologically. The locations corresponding to the recording sites from the more extensive mapping experiment of Figure 12 were placed on these sections, illustrated in Figure 13, using the Horsley-Clarke coordinates of each site. The position of the 17/18 border and receptive field elevations confirmed, respectively, the correct anterior-posterior and lateral-medial placements of the mapping data onto the sections.

Within a parasagittal section, area 17 may be traced caudally from its boundary with area 18 around the crown of the posterior lateral gyrus, then rostroventrally along the splenial gyrus to the caudal bank of the splenial sulcus. Receptive-field locations of units encountered along this route follow an arc from central and inferior to peripheral and superior in the contralateral visual hemifield. The elevations of receptive fields increase and the arcs become steeper in more lateral sections.

In order to gain a sense of the overall organization and continuity of the visuotopic map, it is desirable to "unfold" the cortex to view it as a flat sheet. We did not find it possible to reconstruct electrode penetrations in a cortex that had been physically unfolded.

Figure 12. The receptive-field centers of 143 multi-unit clusters recorded in area 17 and neighboring visual areas in F81. Locations marked with *circles* are receptive fields of sites recorded in area 17, locations marked with *squares* are receptive fields of sites recorded in area 18, locations marked with *triangles* are fields recorded in other visual area(s). Numbers and letters within the symbols refer to recording sites shown in Figures 13 and 14. The receptive field at the site marked 8g (8 deg azimuth, +40 deg elevation) is designated as being from "other visual areas" in Figures 12 and 14 on the basis of the response characteristics of the units recorded at the site. These sites appear to be well within area 17 on the section illustrated, an artifact of superimposing data on this particular representative section.

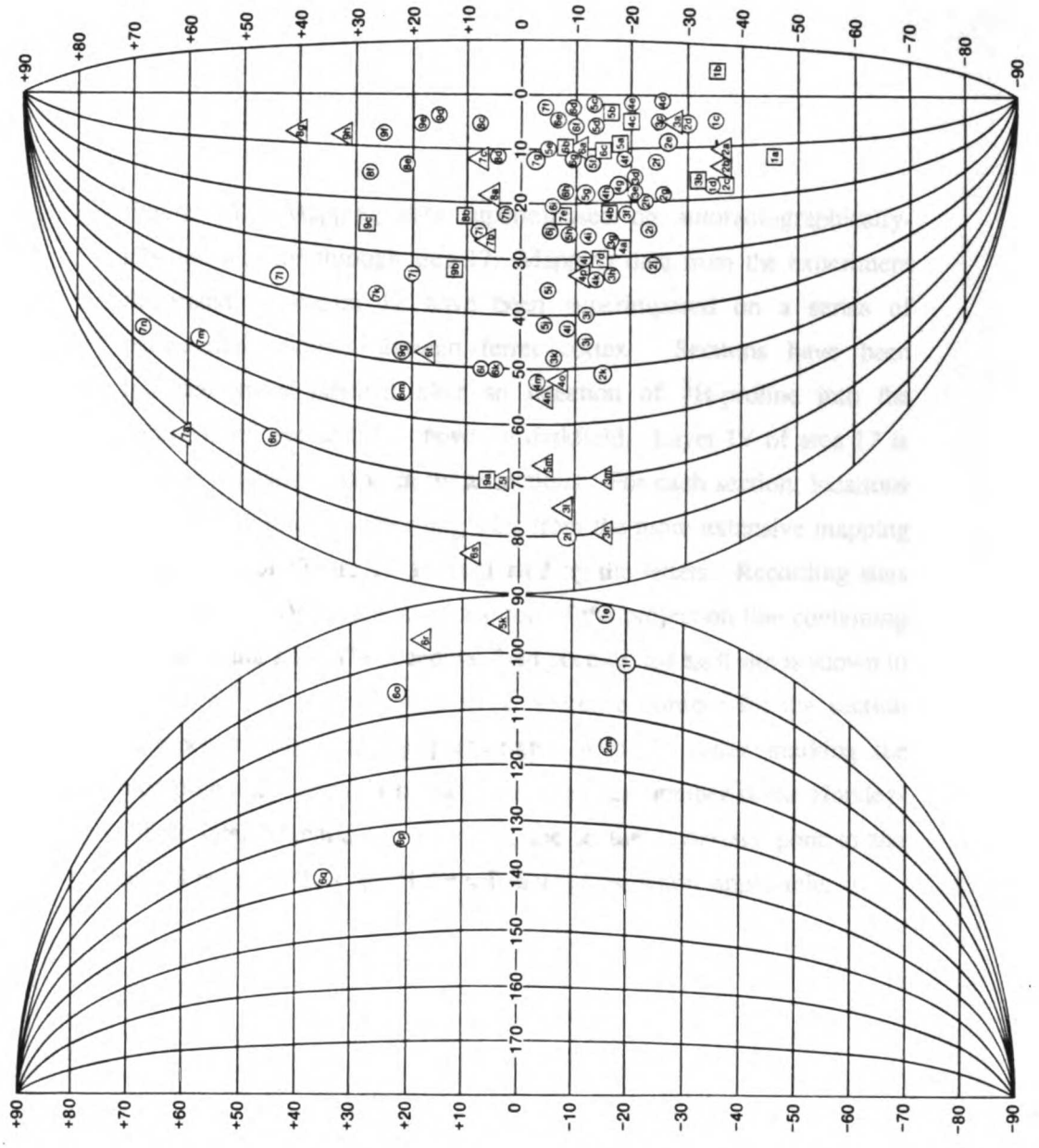
+90
+80
+70
+60
+50
+40
+30
+20
+10
0
-10
-20
-30
-40
-50
-60
-70
-80
-90
0
10
20
30
40
50
60
70
80
90
100
110
120
130
140
150
160
170

Figure 13. Mapping data superimposed on autoradiographically-labelled sections through area 17. Mapping data from the experiment illustrated in Figure 12 have been superimposed on a series of parasagittal sections through ferret cortex. Sections have been transneuronally labelled after an injection of ^{3}H-proline into the contralateral eye and are shown in darkfield. Layer IV of area 17 is seen as a labelled band in these sections. For each section, locations corresponding to the recording sites from the more extensive mapping experiment of Figure 12 are indicated by the letters. Recording sites were in layer IV; letters mark the top of the projection line containing the recording site. The receptive field position for each site is shown in Figure 12 and is designated by a reference number for the section (number in white circle) postscripted with the letter marking the recording site. Number beneath the reference number is the Horsley-Clarke lateral-medial coordinate of the section. *Arrows* pont to the caudal pole and the edge of the splenial sulcus, where applicable.

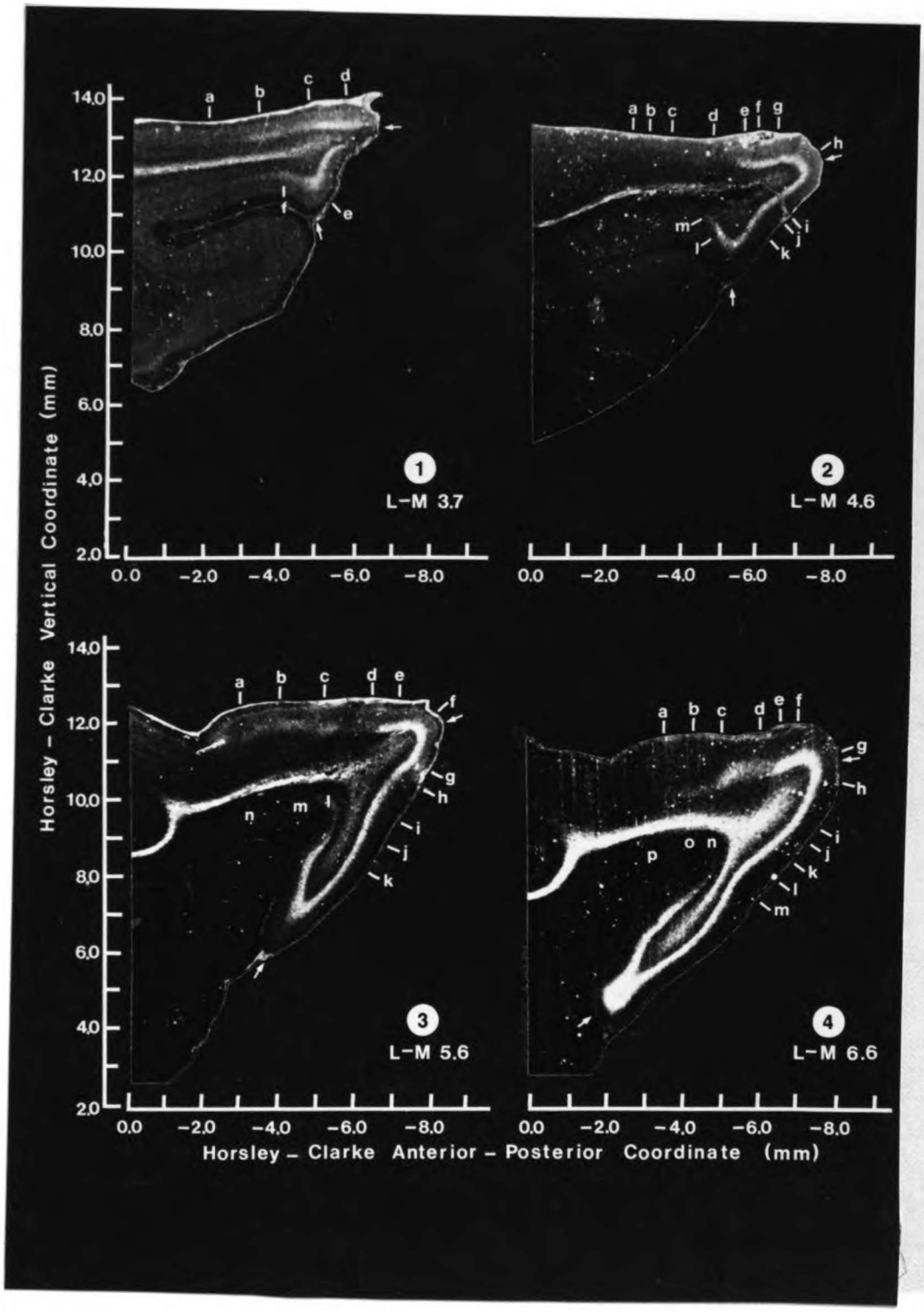
Horsley – Clarke Vertical Coordinate (mm)
14.0
12.0
10.0
8.0
6.0
4.0
2.0
0.0
-2.0
-4.0
-6.0
-8.0
a
b
c
d
e
f
g
h
i
j
k
l
m
n
o
p
1
L-M 3.7
2
L-M 4.6
3
L-M 5.6
4
L-M 6.6
Horsley – Clarke Anterior – Posterior Coordinate (mm)

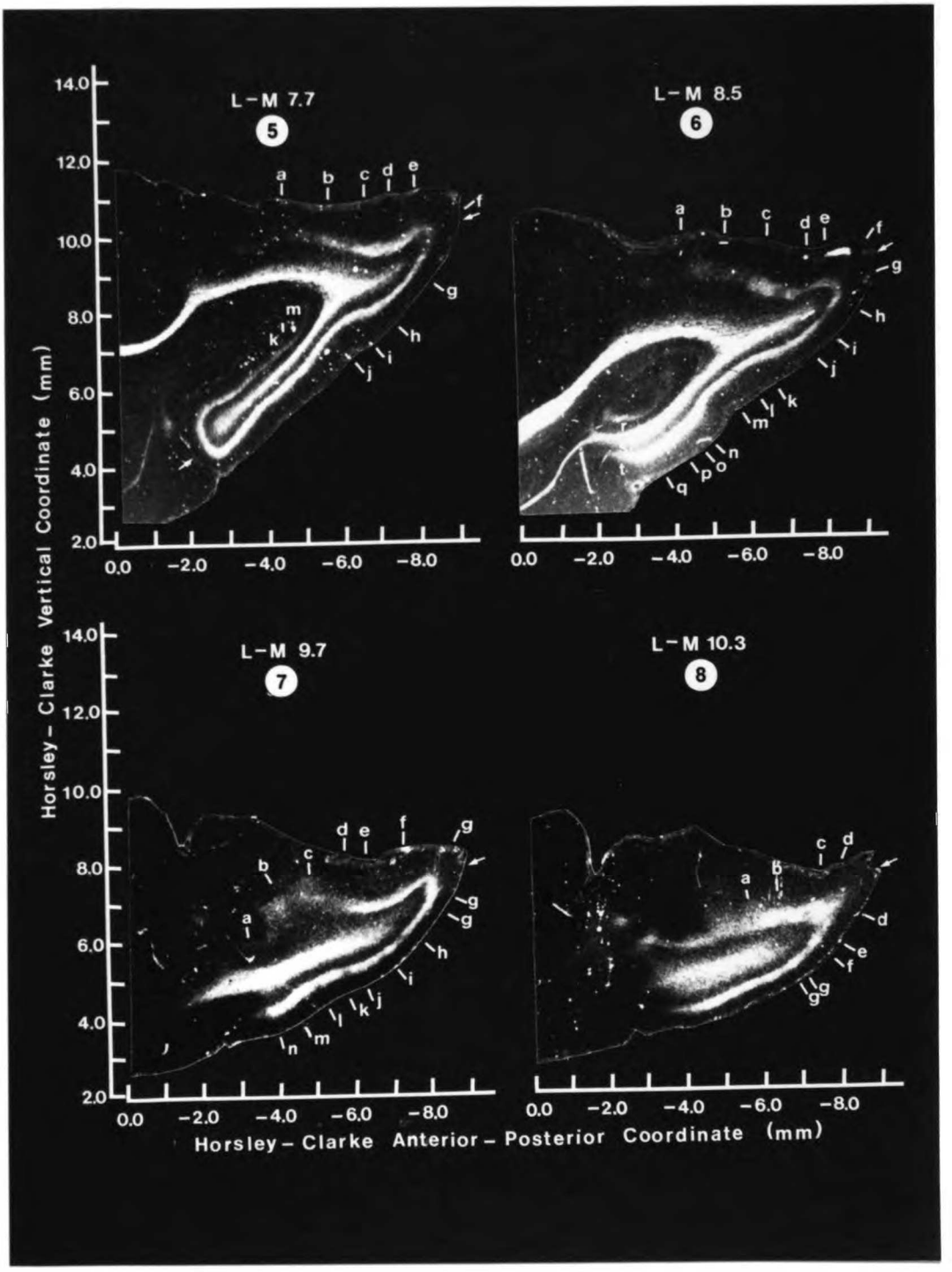
L-M 7.7
5
L-M 8.5
6
L-M 9.7
7
L-M 10.3
8
Horsley-Clarke Vertical Coordinate (mm)
Horsley-Clarke Anterior-Posterior Coordinate (mm)
14.0
12.0
10.0
8.0
6.0
4.0
2.0
0.0
-2.0
-4.0
-6.0
-8.0

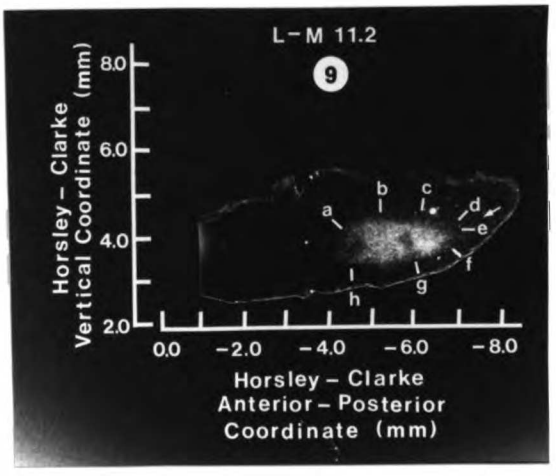
L-M 11.2
9
Horsley – Clarke
Vertical Coordinate (mm)
8.0
6.0
4.0
2.0
a
b
c
d
e
f
g
h
0.0
-2.0
-4.0
-6.0
-8.0
Horsley – Clarke
Anterior – Posterior
Coordinate (mm)

However, it was possible to graphically unfold the cortex after locating recording sites in sections. The unfolded map constructed from the mapping data of F81 is shown in Figure 14. A second unfolded map, constructed from the data obtained from F91, is shown in Figure 15. The receptive-field centers of the sites recorded in this animal are shown in Figure 16.

Several features of the visuotopic map in area 17 are apparent in Figures 14 and 15. Isoazimuth lines run roughly parallel to each other and are crossed at approximately right angles by isoelevation lines. The variability among animals in the exact location of area 17 is illustrated by these maps. In F81 (Figure 14), the region of area 17 representing the central 10 to 15 degrees of azimuth occupies approximately 2 mm on the dorsolateral surface of the posterior lateral gyrus. The most peripheral visual field (azimuths as large as 120 deg) maps to the crown of the splenial gyrus. Figure 15 illustrates the less frequently observed, but not rare, case in which area 17 is shifted back so that only the central 5 degrees of azimuth are represented on the dorsal surface of the cortex, and the very far periphery (azimuths larger than 85 deg) comes to be represented on the caudal bank of the splenial sulcus. Such variability in position is significant when one considers that the entire extent of area 17 (extending along the representation of the horizontal meridian) is no more than 10 mm.

Figure 14. Flattened representation of the visual-field projection onto area 17 (F81). Flattened representation of area 17 and neighboring visual areas constructed from the mapping data displayed on the sections of Figure 13. *Circles* indicate recording sites in area 17, *squares* indicate sites in area 18, and *triangles* show sites in more rostral visual area(s). These symbols correspond to the sites in Figure 13 and the receptive fields of Figure 12. *Thin solid lines* are isoazimuths, *dashed lines* are isoelevations. *Heavy lines* mark the caudal pole and edge of the splenial sulcus.

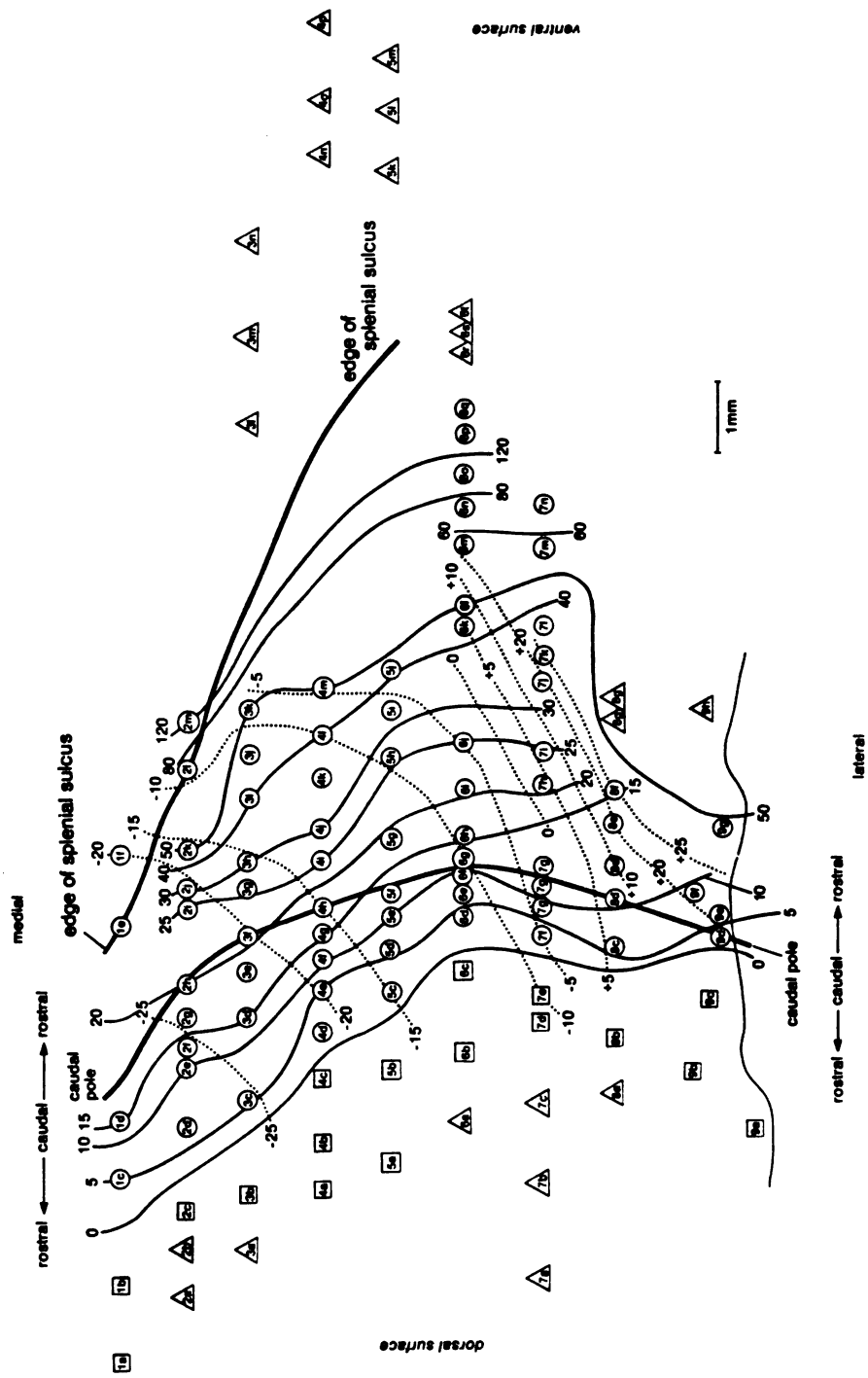
edge of splenial sulcus
edge of splenial sulcus
caudal pole
caudal pole
1mm
rostral ← caudal → rostral
medial
lateral
dorsal surface
ventral surface

Figure 15. Flattened representation of area 17 and neighboring visual areas constructed from mapping data from F91. Conventions the same as for Figure 14. Receptive fields of theses multi-unit clusters are shown in Figure 16.

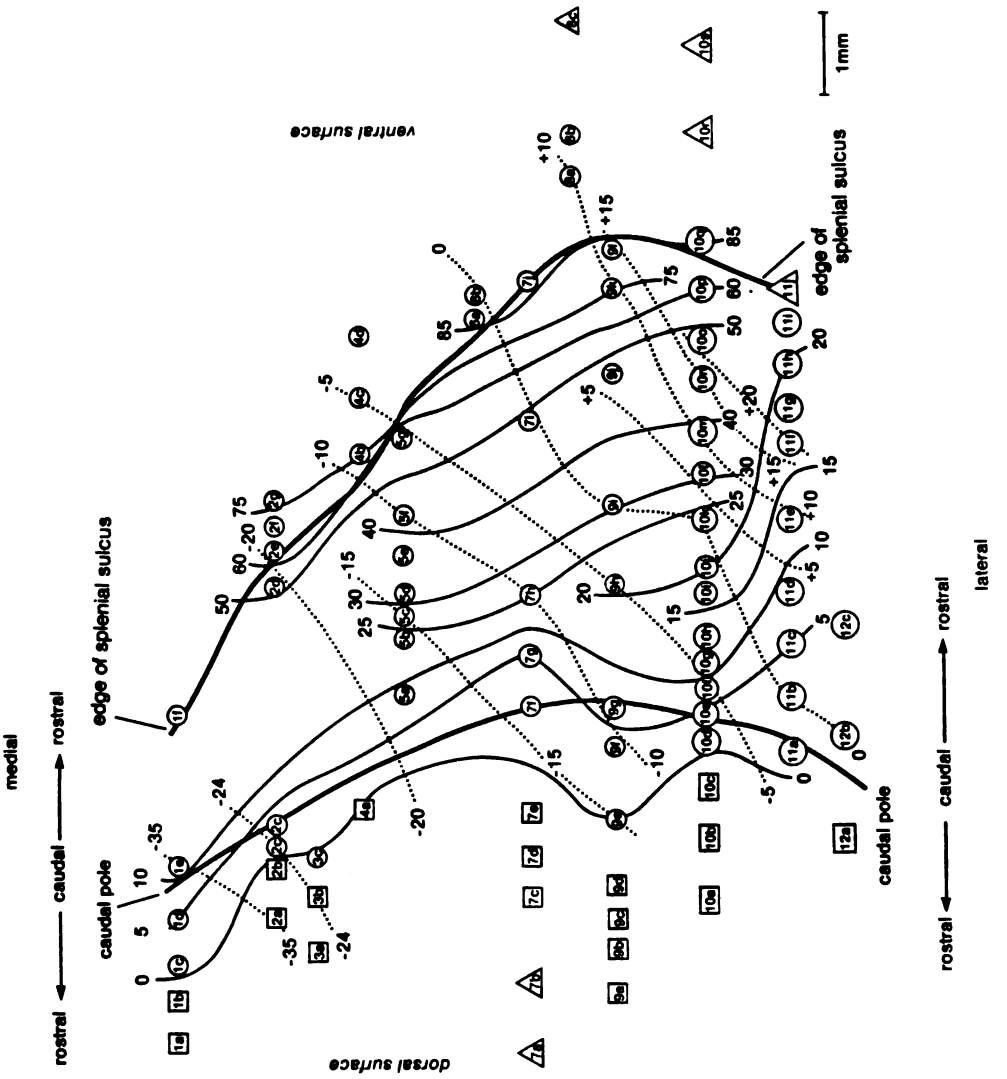
medial
rostral
caudal
rostral
edge of splenial sulcus
caudal pole
dorsal surface
ventral surface
edge of splenial sulcus
caudal pole
1mm
rostral
caudal
rostral
lateral

Figure 16. Receptive-field centers of 134 multi-unit clusters recorded in area 17 and neighboring visual areas of F91. Conventions are the same as in Figure 12. Receptive field 9c was omitted to reduce crowding; it lay between 9b and 9d.

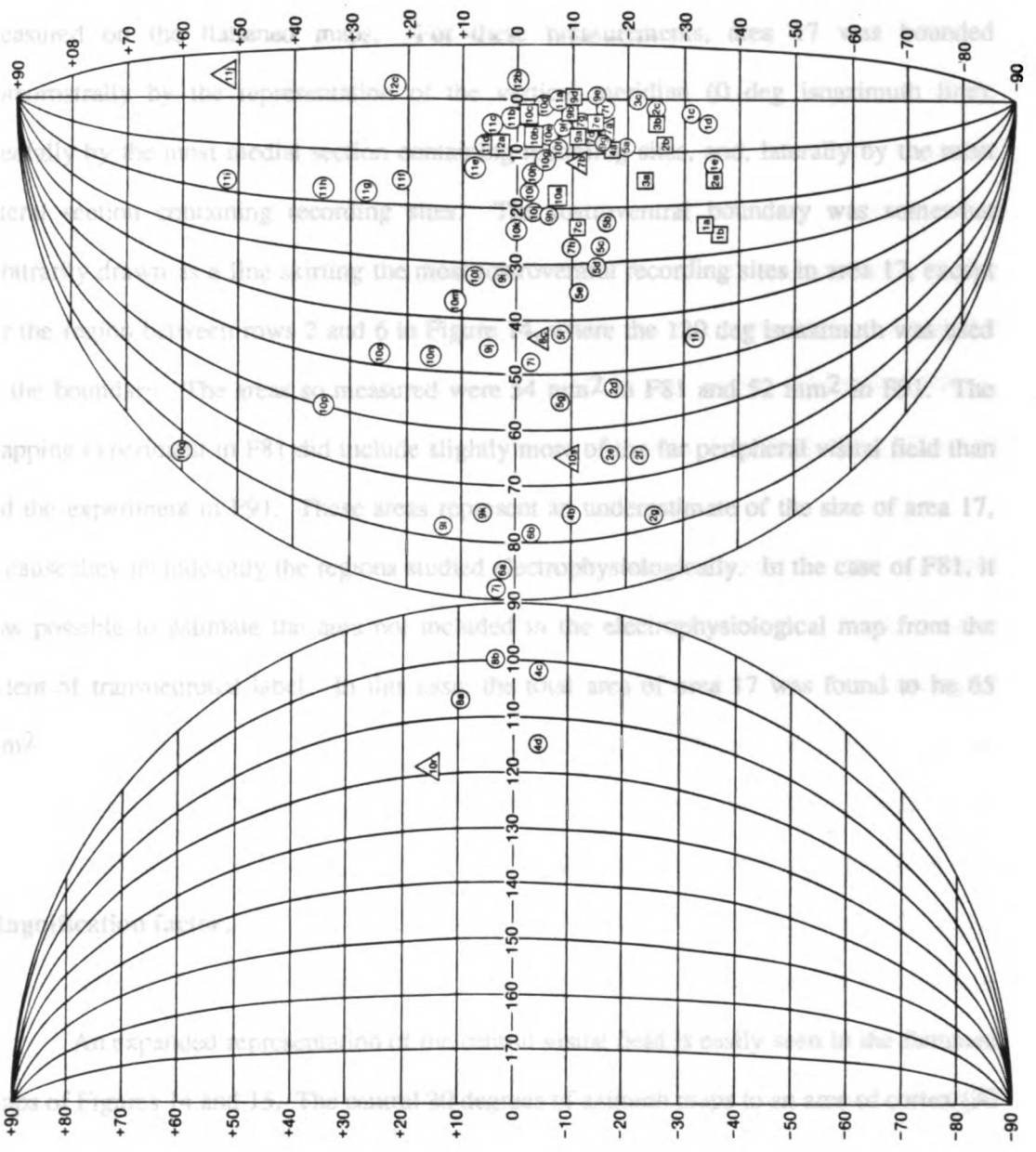
+90
+80
+70
+60
+50
+40
+30
+20
+10
0
-10
-20
-30
-40
-50
-60
-70
-80
-90
10
20
30
40
50
60
70
80
90
100
110
120
130
140
150
160
170

Size of area 17.

The area encompassed by the electrophysiologically-identified area 17 was measured on the flattened maps. For these measurements, area 17 was bounded dorsorostrally by the representation of the vertical meridian (0 deg isoazimuth line), medially by the most medial section containing recording sites, and, laterally by the most lateral section containing recording sites. The rostroventral boundary was somewhat arbitrarily drawn as a line skirting the most rostroventral recording sites in area 17, except for the region between rows 2 and 6 in Figure 14, where the 120 deg isoazimuth was used as the boundary. The areas so measured were 54 mm^2 in F81 and 52 mm^2 in F91. The mapping experiment in F81 did include slightly more of the far peripheral visual field than did the experiment in F91. These areas represent an underestimate of the size of area 17, because they include only the regions studied electrophysiologically. In the case of F81, it was possible to estimate the area not included in the electrophysiological map from the extent of transneuronal label. In this case, the total area of area 17 was found to be 65 mm^2.

Magnification factor.

An expanded representation of the central visual field is easily seen in the flattened maps of Figures 14 and 15. The central 30 degrees of azimuth maps to an area of cortex (30 mm^2 in F81, 24 mm^2 in F91) approximately equal to that representing the peripheral 90 degrees (24 mm^2 in F81, 27 mm^2 in F91). A greater area of cortex appears to be devoted to the inferior visual field (34 mm^2 in F81, 34 mm^2 in F91) than to the superior visual field

(20 mm^2 in F81, 18 mm^2 in F91), but this conclusion depends on the assignment of the fixation-point elevation. The assignment of elevation in the cortical maps was made to be consistent with maps of the lateral geniculate nucleus (see Chapter 2). This assignment was based on the distribution of geniculate receptive-field sizes as a function of elevation, a function that changed little between -30 and +20 deg of elevation. Inspection of the flattened maps reveals that the elevations near -10 deg have the most expanded representation, suggesting that the true horizontal meridian may be closer to the elevation labelled -10 deg in the maps than to that labelled 0 deg. If the line labelled -10 deg represents the projection of the horizontal meridian more accurately than the line labelled 0 deg, then the representation of the superior visual field (31 mm^2 in F81, 33 mm^2 in F91) is larger than that of the inferior visual field (23mm^2 in F81, 19mm^2 in F91). This issue will be considered more fully in the *Discussion.*

The expanded representation of the central visual field may be expressed quantitatively as the magnification factor (Daniel and Whitteridge, 1961). Areal magnification factors were calculated as described in *Methods.* Because of the spacing of the electrode penetrations during the recording sessions, as well as the expansion of the central visual field which occurs in the visuotopic map in area 17, smaller areas of the visual field were represented in areas of cortex measured in the central representation than in the peripheral representation. Areas of cortex devoted to 5 deg x 5 deg areas of the visual field were measured for the region of area 17 representing 0 to 20 deg azimuth, -20 to +25 deg elevation. For the region representing 20 to 50 deg azimuth, -20 to +10 deg elevation, areas of cortex were measured representing areas of the visual field not exceeding 50 deg^2. Visual-field areas did not exceed 100 deg^2 for even the most peripheral visual field (azimuths greater than 50 deg, or elevations less than -20 deg).

Figure 17. Areal magnification factors in area 17 of the ferret. A) Areal magnification versus eccentricity. Pooled data from F81 and F91. Smooth curve is the second-order polynomial that best fits these points. A single datum (eccentricity = 3.5, magnification factor = 7.48) has been omitted from this figure to save space, but this point was included when fitting the curve. B) Areal magnification versus azimuth. Mean and standard error of the mean (SEM) at each azimuth were calculated from the pooled data from F81 and F91 at all elevations. Number above each error bar is the number of areas that contributed to the mean. C) Areal magnification versus elevation. Mean and SEM at each elevation were calculated from the pooled data from F81 and F91 at all azimuths.

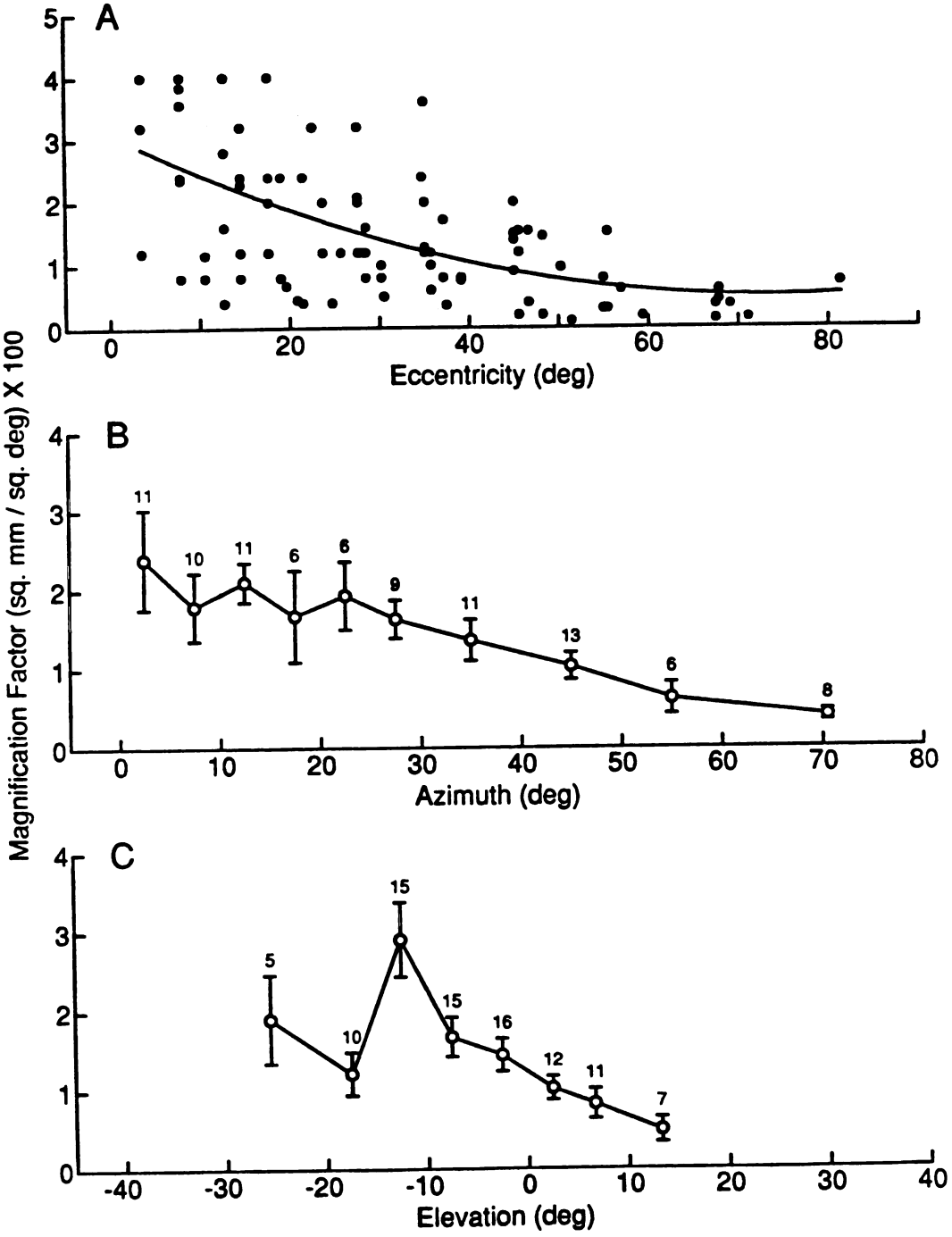
A
B
C
Magnification Factor (sq. mm / sq. deg) X 100
Eccentricity (deg)
Azimuth (deg)
Elevation (deg)
11
10
11
6
6
9
11
13
6
8
5
10
15
15
16
12
11
7

Figure 17A shows a scatter plot and best-fitting smooth curve of the relation between magnification factor and eccentricity, defined as the square root of the sum of the squares of azimuth and elevation. In calculating eccentricity, 10 degrees was added to the values of elevation shown on the maps, since the data presented here suggest that the -10 deg isoelevation line is closer to the true representation of the horizontal meridian than is the 0 deg line. Magnification falls off quite gradually by this analysis, in which azimuthal and elevational changes are combined.

Magnification also changes gradually as a function of azimuth, as shown in Figure 17B. Values on the abscissa indicate the center of the visual field areas represented. Magnification remains fairly constant across the central 25 degrees of azimuth, and then declines steadily. This trend, observed when data are pooled across elevations as shown, is also present when magnification factor versus azimuth is plotted for a series of elevations (not shown).

Figure 17C shows magnification factor plotted as a function of elevation. Magnification is greatest at -12.5 deg and decreases sharply above and below this elevation. When magnification factor versus elevation is plotted separately for each of a series of azimuths spaced at 5-deg intervals, a series of curves with peaks at -12.5 deg is obtained (data not shown).

Monocular segment.

One purpose of these experiments was to determine the location of the monocular segment of area 17. Figure 18 shows the eye through which each area 17 receptive field was plotted in F81, F91, and two additional ferrets in which area 17 was studied

electrophysiologically. Units responding to stimulation through the ipsilateral eye had receptive fields with azimuths as great as 38 deg. Based on the sample of receptive fields illustrated in Figure 18, the monocular segment of area 17 encompasses the region of cortex representing the visual field beyond 40 deg azimuth and occupies at least 17 mm^2 (17 mm^2 in F81, as measured on the physiologically-defined area 17, 26 mm^2 as measured on the anatomically-defined area 17; 22 mm^2 as defined phsyiologically in F91) on the ventromedial half of the splenial gyrus and the caudal bank of the splenial sulcus.

Figure 18. Monocular and binocular segments of the visual field represented in area 17. *Closed* and *open* symbols indicate receptive fields of units responding to stimulation through the contralateral and ipsilateral eyes, respectively. Receptive fields shown are those found in the mapping experiments in F81 and F91, as well as fields found in two additional ferrets in which area 17 was studied electrophysiologically.

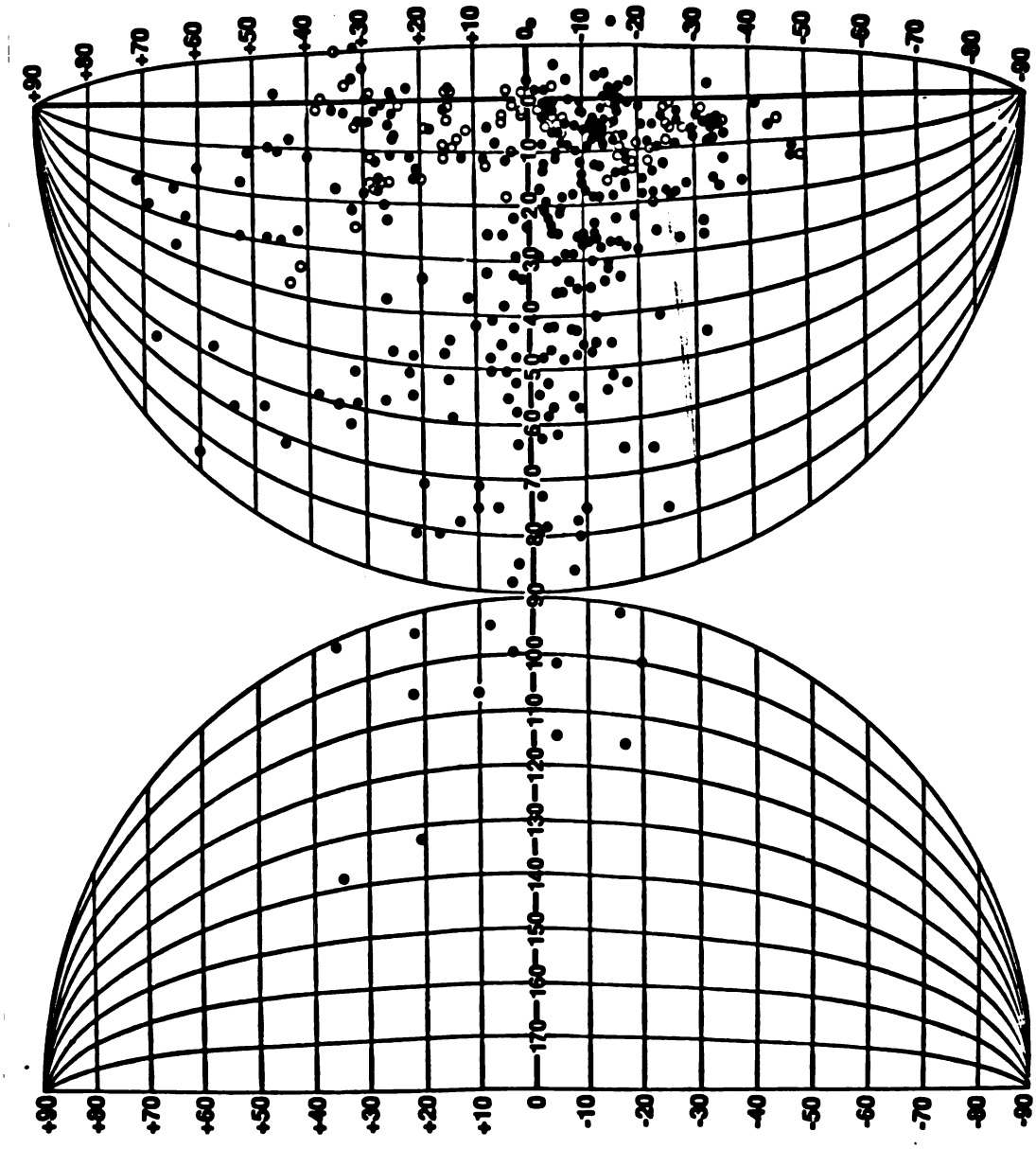
+90 +80 +70 +60 +50 +40 +30 +20 +10 0 -10 -20 -30 -40 -50 -60 -70 -80 -90
10 20 30 40 50 60 70 80 90 100 110 120 130 140 150 160 170

Discussion

Electrophysiological mapping techniques were used to determine the topographic organization of primary visual cortex in ferrets. From its border with area 18 on the posterior lateral gyrus, area 17 extends around the occipitotemporal sulcus and over the splenial gyrus to the caudal bank of the splenial sulcus. The visuotopic map is oriented with the isoazimuth lines approximately parallel to the long axis of the posterior lateral gyrus and the isoelevation lines approximately perpendicular to the isoazimuths.

An estimated 83% of area 17 was mapped electrophysiologically in each of the two animals described here. This value is based on a comparison of the mapped areas (54 mm^2 in F81) to the area of the anatomically-defined area 17 (65 mm^2 in the sections upon which the mapping data from F81 were superimposed). The unmapped area includes the ventromedial splenial gyrus and the ventral portion of the caudal bank of the splenial sulcus. It can be inferred from Figures 14 and 15 that this region of area 17 contains the representation of the superior peripheral visual field. The extent of the visual field represented in area 17 is best illustrated in Figure 18. Receptive fields of units in area 17 have been found with azimuths as great as 135 deg and elevations ranging from at least -40 deg to +70 deg. Based on the sample of receptive fields illustrated in Figure 18, the ferret's binocular visual field extends to at least 38 deg azimuth in the superior visual field and to at least 20 deg azimuth in the inferior visual field. This estimate of the extent of the binocular visual field is consistent with that found in mapping studies of the LGN.

There is a disproportionately large representation of the central visual field within area 17 of ferrets. Such central magnification has been described in several other species

(cat, Tusa et al., 1978; macaque, Malpeli and Baker, 1975; grey squirrel, Hall et al., 1971). In cats, cortical magnification factors appear to be determined by retinal ganglion cell densities (Tusa et al., 1978). However, central magnification in macaque striate cortex appears to be greater than that which would be predicted on the basis of retinal ganglion cell densities or lateral geniculate nucleus volumes (Malpeli and Baker, 1975). This study provides insufficient data to estimate the precise extent to which magnification factors in ferret cortex are determined by retinal ganglion cell densities. However, magnification factor in cortex does change in parallel with ganglion cell density in retina: cortical magnification factor changes more rapidly as a function of elevation than as a function of azimuth, just as retinal ganglion cell density changes more rapidly along the inferior-superior axis than along the nasotemporal axis (Vitek et al., 1985)

Use of the maps.

These mapping experiments were undertaken in part to provide a guide for future studies of ferret area 17. Figures 12 - 14 should aid the neurophysiologist in relating locations in the visual field to sites in the cortex. In order to locate a site in the cortex representing a known location in the visual field, the physiologist should refer to Figure 12 to find the reference number of the receptive field closest to the desired visual-field location. The reference number can then be used to find the corresponding cortical site in the parasagittal sections of Figure 13 or in the flattened representation of area 17 in Figure 14. Similarly, to find the receptive field of a recording site more rapidly when the Horsley-Clarke coordinates of that site are known, the physiologist should first refer to Figure 13 to get the reference number of the appropriate receptive field, next look at the flattened

representation in Figure 14 to find the approximate azimuth and elevation of that receptive field, and, finally, refer to Figure 12 for a more precise location of the receptive field. When it is necessary to adjust an electrode position, the following guidelines may be helpful. Caudal movement of the electrode results in a peripheral-superior (the main effect of the electrode movement on the receptive-field location is given first) shift in the receptive fields of sites recorded in the dorsal surface of area 17, and in a central-inferior shift in the receptive fields of sites on the tentorial surface. Lateral movement of the electrode results in a superior-central shift in the receptive-field location for sites recorded on either surface.

Fixation-point elevation.

Consideration of cortical magnification factors suggests that the true fixation-point elevation is below that assigned in Figures 12 - 18. In this study, the fixation point was chosen to make the cortical maps consistent with the LGN maps (see Chapter 2). When constructing the LGN maps, the fixation-point elevation was placed 3.5 deg below the elevation of the projection of the optic disc on the basis of the smallest receptive fields found in two geniculate mapping experiments. There was, however, little change in the sizes of geniculate receptive fields between elevations 34 deg below and 16 deg above the optic-disc projection, leaving the precise elevation of the fixation point relatively uncertain. Attempts to label retinal ganglion cells corresponding to known regions of the visual field failed to more precisely define the location of the fixation point.

Because of the presence of a visual streak in the ferret (Vitek et al., 1985), it is reasonable to assume that magnification factor in ferret area 17 is greatest along the

representation of the horizontal meridian. If this assumption is valid, the real fixation-point elevation is approximately 12 deg below that assigned in the figures, or 15 deg below the elevation of the optic-disc projection. This location is well within the range of elevations provided by a consideration of receptive-field sizes and the results of the retinal labelling experiments. This estimate is also consistent with that expected from relating the retinal wholemount data of Vitek et al. (1985) to the measurements of the visual field obtained in our studies of the cortex and LGN. The distance along the horizontal meridian from the optic disc to the area centralis averages 2.6 mm in the wholemounts *(see Figure 6 of Vitek et al.)*; this distance corresponds to an average of 31 deg of the visual field *(see Chapter 2)*. A distance of 1 mm on the retina therefore corresponds to 12 deg in the visual field. In the wholemounts, the optic disc is located approximately 1 mm inferior to the horizontal meridian; the projection of the optic disk onto the visual field is therefore approximately 12 deg above that of the projection of area centralis.

Neighboring visual areas.

During these experiments, electrode penetrations were made into visually-responsive areas rostral to area 17. Areas were distinguished by differences in the most effective stimuli for eliciting responses and by reversals in the visuotopic map when penetrations crossed from one area to another. Two visual areas were encountered rostral to area 17 on the dorsal surface of the posterior lateral and lateral gyri; these areas are presumed to be areas 18 and 19. Visual responses were also recorded on the caudal bank of the splenial sulcus rostral to area 17. This area may be analogous to area 20b in the cat, described by Tusa et al. (1978) as being located in the posterior portion of the splenial

sulcus abutting the representation of the upper visual field in area 17. Alternatively, it may be analogous to the splenial visual are of Kalia and Whitteridge (1973).

Comparison with the cat.

The topographic organization of ferret area 17 may be compared to that of the cat, a much more widely-studied carnivore. Viewed from its caudal aspect, the cat's brain could be made to resemble the ferret's brain by spreading the caudal poles upward and outward from a hinge at the dorsal midline. The medial bank of area 17 in the cat thus becomes the tentorial surface in the ferret. Area 17 is also shifted ventrally in the ferret relative to the cat, so the representation of the fixation point, which is found near the caudal-medial pole of the lateral gyrus in the cat, is found approximately 2/3 of the way down the dorsolateral surface of the posterior lateral gyrus in the ferret.

The ferret's visual field extends farther along the horizontal meridian than does the cat's, as would be expected from the ferret's more laterally-placed eyes. Recording sites were found in ferret area 17 with receptive fields having azimuths as great as 135 deg; the cat's visual field extends to the 90 deg azimuth. The visuotopic map in area 17 of both species contains an expanded representation of the central visual field. However, cortical magnification factor changes much more sharply as a function of azimuth in cats than in ferrets, probably reflecting the cat's well-developed area centralis (Stone, 1978) versus the ferret's visual streak (Vitek et al., 1985).

Chapter IV

ON and OFF sublaminae

in the lateral geniculate nucleus of the ferret

Introduction

In higher mammals, information about lightness and darkness in the retinal image appears to be conveyed from the eye to the brain in parallel channels of ON- and OFF-center retinal ganglion cell axons (Kuffler, 1953). In the retina, segregation of center-types is accomplished by the arborization of depolarizing bipolar cells to contact ON-center ganglion cells within a different sublamina of the inner plexiform layer from that in which hyperpolarizing bipolar cells contact the OFF-center cells (Nelson et al., 1978). These ON and OFF channels remain at least largely separate through the synapses of the lateral geniculate nucleus (LGN) (Hubel and Wiesel, 1961; Cleland et al., 1971).

Reports from Schiller's laboratory of a strict laminar segregation of center-type in the LGN of the tree shrew (Conway et al., 1980) led us to wonder whether the subtle sublamination of the main (A) laminae of the ferret LGN, noted by Sanderson (1974) and Guillery and co-workers (Linden et al., 1981) and termed "leaflets," might provide a substrate for the maintenance of separate ON and OFF channels. Microelectrode recordings now reveal that each leaflet consists of geniculate cells of a single center-type. These results have been reported previously (Stryker and Zahs, 1983).

Methods

Animals.

Eight adult ferrets were obtained from Marshall Farms, New Rose, New York, and housed in the vivarium at the University of California, San Francisco for 1 to 8 weeks. During the ferrets' stay in the vivarium, the light cycle was 14 hr light : 10 hr dark. For all but two experiments, the animals were females weighing between 700 and 850 gm; the others were 1.1- to 1.2-kg males.

Labelling the retinal afferents.

In three ferrets, retinal afferents to the LGN were labelled autoradiographically by intravitreal injections of 200 to 2000 μCi of ^{3}H-proline (Amersham TRK.439, specific activity 40 Ci/mmol). After survival times of one to two weeks, the animals were killed with an overdose of sodium pentobarbital (50 mg/kg i.p.), and perfused through the heart with 0.1 M phosphate buffer (pH 7.4), followed by 4% paraformaldehyde in the same buffer. Blocks of brain containing the LGNs were sectioned at 40 microns on a freezing microtome. Two of the brains were sectioned in the coronal plane; the third brain was sectioned parasagitally. Sections were processed for autoradiography using standard techniques. Retinal afferents in two other ferrets were labelled by injecting the vitreous humor of one eye with 0.25 mg of wheat germ agglutinin conjugated to horseradish peroxidase (Sigma, L9008) 3 to 5 days before perfusion.

After sectioning in the parasagittal plane, the LGNs were reacted for the presence of HRP using the tetramethylbenzidene method (Mesulam, 1978).

Electrophysiological recording.

Eight ferrets were prepared for physiological recording using the techniques described in Chapter 2. Microelectrodes were advanced into the LGN on a vertical axis in five ferrets, or on an axis in the parasagittal plane inclined 40 to 45 deg pointing anterior from the vertical in three ferrets. Such angled penetrations were expected to traverse the LGN approximately perpendicular to the laminar borders (follow a line of projection). Vertical penetrations were expected to remain within a single leaflet for relatively long distances.

Assignment of recording sites to leaflets.

One or more electrolytic lesions were made along the course of each electrode penetration by passing -4 to -6 μA for 4 to 6 sec. Nissl-stained sections containing the electrode tracks were projected at a magnification of X 47, and tracings, including all sublaminar boundaries, were made without knowledge of or reference to the physiological findings. It was then possible, by reference to microdrive readings at the lesions and at the entry point into the LGN, to reconstruct the locations of all recording sites on these tracings. This procedure located the point of transition between responses from the two eyes accurately at the border between laminae A and A1. Only after assigning each recording site to the C

laminae or to one of the leaflets of laminae A or A1 (or to the border zone between the leaflets) were the physiological ON or OFF responses assigned to each site and recorded on the tracings.

Two penetrations were made into caudal and medial regions of the LGN where we were unable to identify the borders of the leaflets anatomically. Although ON and OFF responses were segregated here as they were elsewhere, data from the 28 recording sites along these penetrations are excluded from the present analysis.

Data from the initial three of the eight animals used in this study were not available for this correlation, because the first two were used only to obtain stereotaxic coordinates and the third was sectioned in the wrong plane for reconstruction of the penetrations. Data from three of the animals contributed to the mapping results reported in Chapter 2.

Results

Identification of the leaflets.

In sections through the LGN in which the retinal afferents were labelled, either autoradiographically or with WGA-HRP, an unlabelled or extremely lightly labelled gap was clearly seen between two tiers of label in both laminae A and A1. Following Sanderson (1974), we took the gap in the labelled afferents to indicate the dividing line between the sublaminae, or "leaflets." The distribution of retinal afferents labelled autoradiographically by intraocular injection of ^{3}H-proline is shown in parasagittal section in in the upper half of Figure 19. Two tiers of label were found in each of laminae A and A1. The overall pattern of labelling was similar in sections labelled after an intraocular injection of wheat germ agglutinin-horseradish peroxidase, except that fascicles of peroxidase reaction product were seen in the border zone between the leaflets (lower half of Figure 19).

In parasagittal sections labelled by either method, the dense labelling at the outsides of each leaflet was sometimes discontinuous in one or both tiers. Such discontinuities occurring across an entire lamina are similar to the unlabelled gaps that correspond to the bridges described in Chapter 2. We do not know the significance of the non-uniformities in the label that occur in only one sublamina; the electrode never passed through such a site in a labelled LGN. It is possible that this occasional discontinuity is an artifact due to incomplete labelling of or damage to the retinal ganglion cells which would supply input to the unlabelled area.

Leaflets were also easily visible in the more rostral coronal sections of autoradiographically-labelled series; here the coronal plane is approximately perpendicular to

Figure 19. Leaflets in labelled parasagittal sections. *Upper row*, parasaggital sections ipsilateral (*left*) and contralateral (*right*) to an eye in which the vitreous humor had been injected with ^{3}H-proline. Note two tiers of label in both lamina A (contralateral) and A1 (ipsilateral). Dorsal is up; rostral is to the right for ipsilateral section (*left*), to the left for contralateral section (*right*). *A*, lamina A; *A1*, lamina A1; *i*, inner leaflet; *o*, outer leaflet. *Lower row*, similar parasagittal sections through the LGN ipsilateral (*left*) and contralateral (*right*) to an eye in which the vitreous humor had been injected with wheat germ agglutinin conjugated to horseradish peroxidase. Sections have been reacted with tetramethyl benzidene and are unstained. Note two tiers of label in both laminae A and A1. Conventions are the same as for *upper row*. *Scale bar* is 300 um.

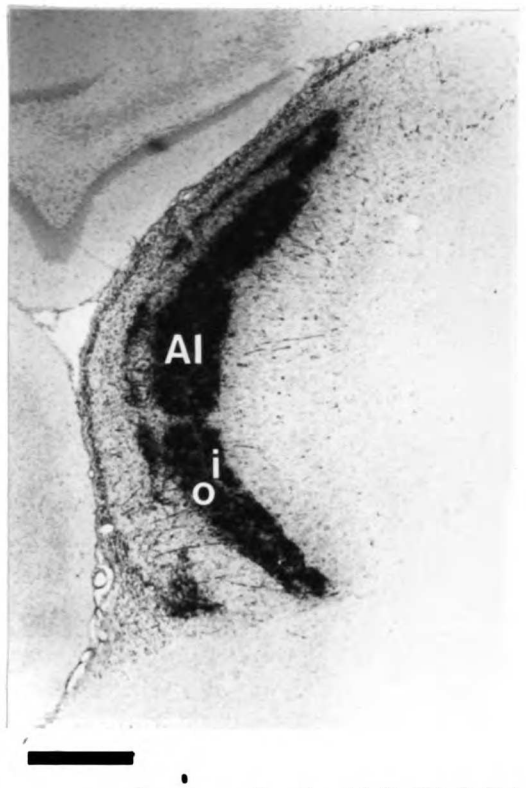
AI
i
o


A
i
o


AI
i
o


A
i
o

Figure 20. Leaflets in autoradiographically-labelled coronal section. Autoradiograph shown in brightfield of a coronal section through an LGN contralateral to an eye in which the vitreous humor had been injected with ^{3}H-proline. The section has been lightly stained with cresyl violet. Note two nearly continuous tiers of label in lamina A. A_O, outer leaflet; A_i, inner leaflet; *C*, C laminae; *M*, medial interlaminar nucleus. The *arrowhead* points to a lightly labelled gap between the leaflets. Dorsal is *up*, medial is *right*. The *scale bar* is 500 um.

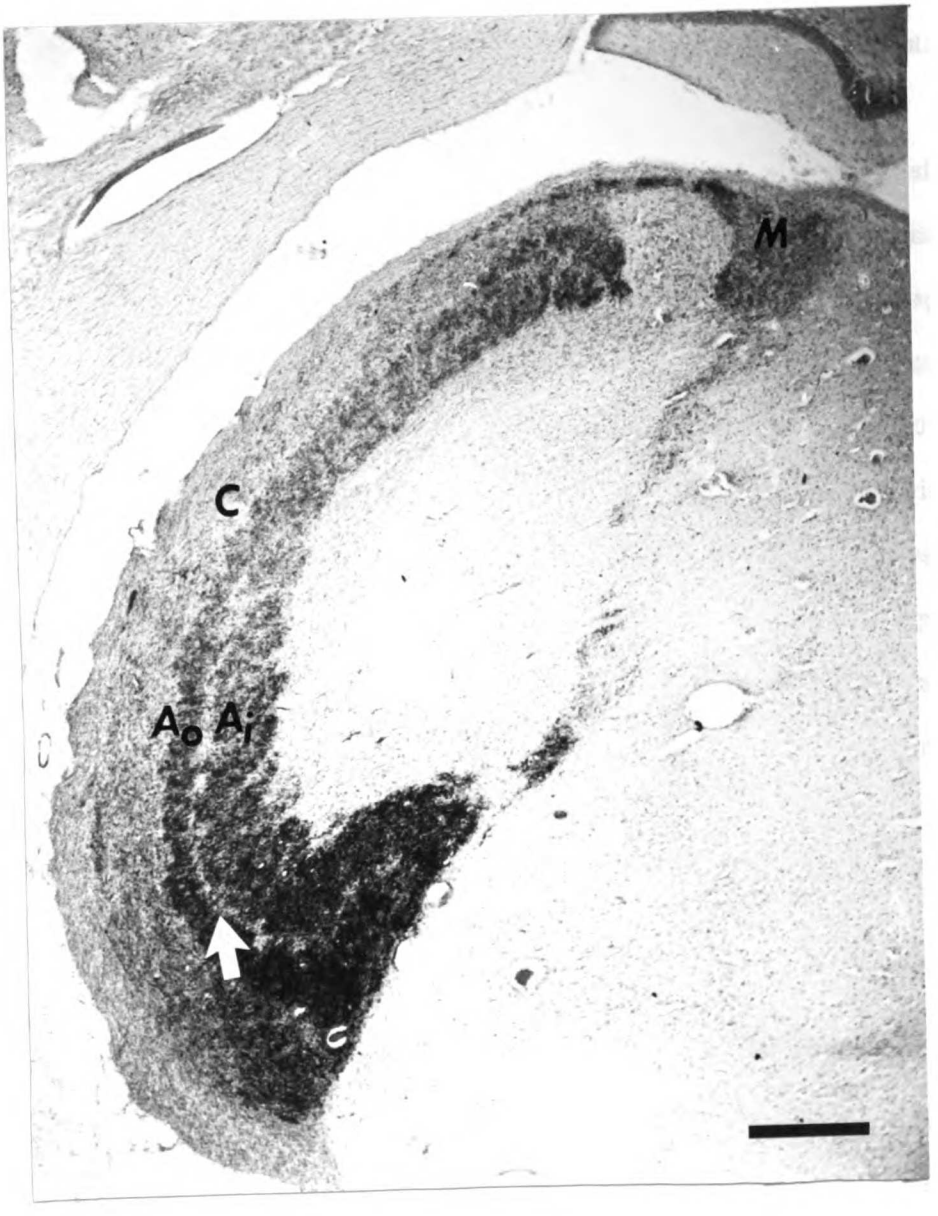
M
C
A_o A_i

the plane of the laminae. One such section is shown in Figure 20. This section includes the rostrolaterally placed monocular segment of the LGN, which receives retinogeniculate afferents from the contralateral eye only. The two tiers of label in lamina A were found to be nearly continuous, and the overall pattern of labelling was similar to that described by Guillery (1971) and Linden et al. (1981). The principal difference between our results and theirs was that it was necessary for us to cut the brains coronally or parasagitally rather than horizontally, so that entire electrode tracks could be traced in one or a few sections.

Inspecting such labelled sections along with neighboring sections stained by a Nissl method eventually allowed us to discern the locations of the leaflets in most stained sections without reference to the labelled ones. Although the ferret's LGN lacks a cell-sparse plexus between the leaflets, knowledge of the form taken by the leaflets in labelled sections at each level guided us in picking out the subtle differences in neuronal architecture that mark the boundaries of the leaflets. A comparison of the labelled section of Figure 20 with the Nissl-stained section from another animal shown in Figure 21A will make clear that it was possible to do this. However, in the most caudal coronal sections and the most lateral parasagittal sections, determining the borders of the leaflets on unlabelled sections by reference to our atlas series of labelled sections was sometimes difficult; rostrally and medially, near the border with the medial interlaminar nucleus, it was sometimes impossible.

Sublaminar distribution of ON and OFF responses.

A typical vertical penetration into the LGN is illustrated in Figure 21. When the electrode first passed into the nucleus, a region of high spontaneous activity and strong visual responses was invariably encountered. Histology later showed this region to be the C laminae

Figure 21. Reconstruction of a vertical electrode penetration in coronal section. A) Photograph of a coronal section containing a vertical microelectrode penetration into the LGN. Compare with autoradiograph shown in Figure 20. B) Drawing of electrode penetration superimposed onto the section shown in (A). The *solid arrowhead* indicates the lesion made beyond the point at which visual responses were obtained. *Open squares* indicate sites at which exclusive ON responses were recorded; *solid squares* indicate OFF responses; *half-filled squares* indicate mixed ON and OFF responses. The electrode passed through the C laminae, in which ON and OFF responses were mixed, and briefly through the outer leaflet of lamina A, in which OFF-center responses were encountered, before traversing a long series of ON-center sites. Conventions as in Figure 20. The *scale bar* is 100 um.

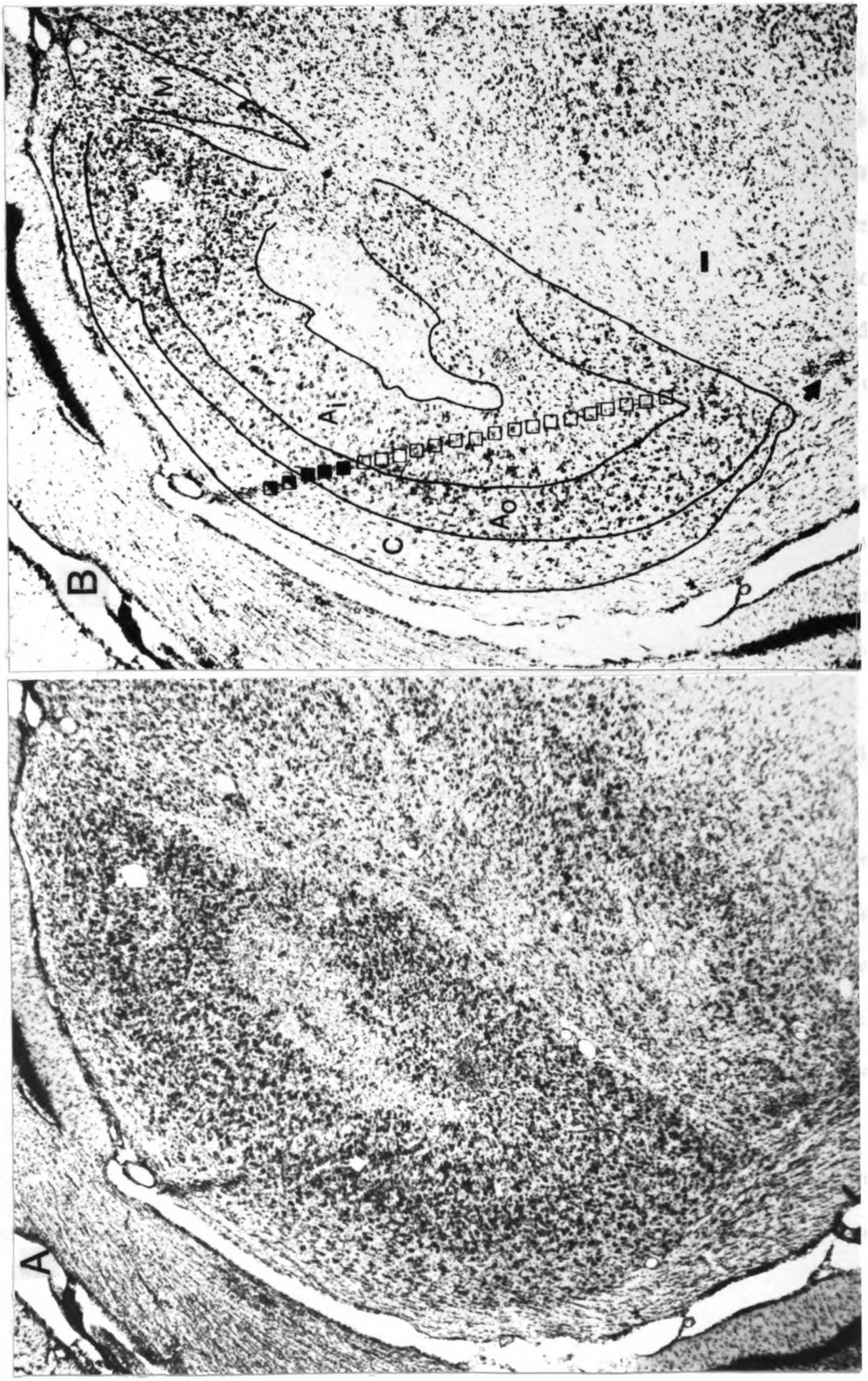
M
Ai
Ao
C
B
A

of the LGN. The unit clusters here were frequently responsive to both eyes, depending on the eccentricity of the receptive fields in the visual field, and were usually responsive to both the onset and offset of a spot flashed in the center of the receptive field. The single units isolated at these sites were always monocularly driven and of either ON- or OFF-center type, suggesting that in these laminae units of different types were intermingled within the resolving distance of the multi-unit microelectrode. Some unit clusters (38 of 138), however, were predominantly or exclusively of one sign of contrast, raising the possibility that a detailed organization may exist in these laminae beyond the resolution of our methods.

After a variable distance, the electrode next encountered a region of distinctly lower spontaneous activity and dramatically different response properties. Here, the unit clusters were driven exclusively by one eye, and, in 225 of 245 cases, exclusively by either the onset or offset of illumination in the receptive field. All single units isolated at such sites shared these properties of the cluster and were found to have approximately circular receptive fields with mutually antagonistic center-surround organization similar to that found in the cat (Hubel and Wiesel, 1961).

We noted the eye and center-type of unit clusters at 100-μm intervals along each penetration. As the penetration continued downward and receptive fields progressed downward in the visual field, the eye and center-type could change or could remain the same for distances greater than 1 mm. The penetration shown in Figure 21, for example, passed briefly through a region of contralateral-eye OFF responses before entering an extended region of ON responses. Receptive fields following the last one indicated in Figure 21 were not plotted because of their extreme inferior position in the visual field. Only in regions of transition between eyes or center-types did the electrode record mixed activity, and single units were always monocular and either ON- or OFF-center.

Figure 22. Responses at "ON" and "OFF" sites in the LGN. A) Vertical electrode penetration into the LGN drawn onto a photograph of a Nissl-stained parasagittal section. The *upper curved arrowhead* indicates the site at which the poststimulus histogram in (B) was obtained; the *lower curved arrowhead* indicates the site of the poststimulus histogram in (C). The *straight arrowhead* indicates the site of the electrolytic marking lesion. *P*, perigeniculate nucleus. Dorsal is *up*; rostral is *left*. The *scale bar* is 100 um. B) Poststimulus histogram for the site indicated by the *upper curved arrowhead* in (A). This histogram was compiled from a multi-unit record consisting of at least four single units. Note that all gave only an ON response. Tic marks indicate 500 msec (abscissa) and 10 spikes/sec (ordinate). The *heavy black line* on the *abscissa* indicates the period in which the stimulus light was on. C) Poststimulus histogram for the site indicated by the *lower curved arrowhead* in A. This histogram was compiled from multiple units, all of which responded only at OFF. Conventions as in B.

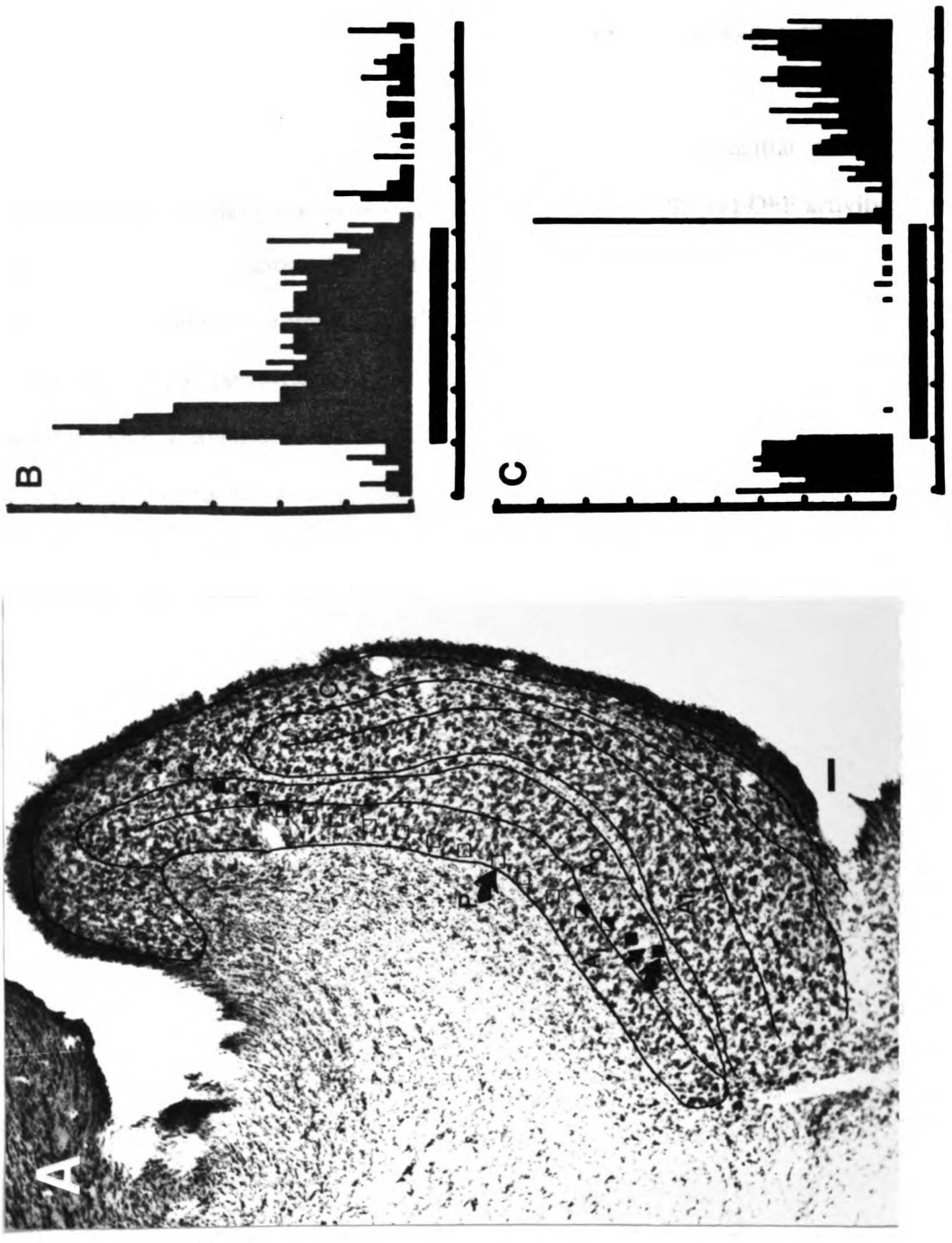
B
C
A
I

When such penetrations were located on histological sections by reference to electrolytic lesions made along their course, the ON and OFF regions were seen to correspond to the sublaminae, or leaflets, of layers A and A1 of the LGN.

Figure 22 shows a vertical electrode penetration in parasagittal section. This penetration passed through a region of high spontaneous mixed ON and OFF activity in the C laminae, followed by a region of OFF responses in the outer leaflet of lamina A before encountering ON responses in the inner leaflet of lamina A. It remained within this leaflet until nearly the end of the penetration, when it re-entered the outer leaflet of lamina A, again encountering OFF responses. Figure 22, B and C, shows poststimulus histograms for unit clusters, each containing at least four units, at two sites along the penetration. Note that only an ON response is seen in Figure 22B, recorded at the location in the inner leaflet indicated by the *upper curved arrow*, and only an OFF response, recorded at the location in the outer leaflet indicated by the *lower curved arrow*, is seen in Figure 22C. Such histograms show responses typical of more than 90% of the multi-unit responses in the A laminae.

The sublaminar distribution of 383 recording sites in 41 penetrations in five ferrets is shown in Table I. Note that within the A laminae, mixed ON and OFF responses were encountered primarily at recording sites located at the borders of the leaflets. Only 8% of recording sites had any contribution from responses of the opposite center-type.

The arrangement of the sublaminae was made clearer by making penetrations as nearly normal to the geniculate laminae as could be managed without removing the tentorium. Examples of two such penetrations are shown in Figure 23. The more dorsal penetration nearly followed the lines of projection of the visual field so that receptive field position changed very little along its course. The sequence of response types in such penetrations was invariably as follows: first, C laminae with high spontaneous activity and usually mixed responses; then, unless the receptive fields were in the monocular segment of the visual field, the outer leaflet of

Table 1

Visual Response Properties by Sublamina

	ON	ON >> OFF	MIXED	OFF >> ON	OFF	TOTAL
A_{outer}	1	0	0	2	53	56
A_{inner}	95	2	0	0	0	97
$A1_{outer}$	1	0	0	0	24	25
$A1_{inner}$	51	1	0	0	0	52
Border	0	0	13	2	0	15
C	7	2	100	21	8	138

Table 1: **Visual response properties by sublamina.** The distribution of LGN recording sites by sublamina and visual response properties. Sites characterized as "ON" were unanimously so: all audible units at those sites responded exclusively to the onset of a light spot of the appropriate size centered in the receptive field. At the sites classified as predominately ON (ON >> OFF), nearly all of the units responded to light onset, but a weak or distant response was also obtained to offset of the receptive field spot. It was not always possible to determine whether this OFF response emanated from an OFF-center geniculate cell or was a surround response of a small ON-center unit whose receptive field did not overlap those of the other simultaneously recorded units. The OFF and OFF >> ON categories were defined similarly. The "mixed" category includes all sites at which a substantial response was present at both ON and OFF; in most cases it was clear that such responses emanated from two separate populations of units. For the locations of the named sublaminae, refer to Figures 19, 20B, or 21B. "Border" refers to sites on the border of the two leaflets.

lamina A1, containing ipsilateral eye OFF-center units followed by the inner leaflet of A1 containing ipsilateral ON-center units; and finally, the outer leaflet of layer A with contralateral OFF-center units followed by the inner leaflet with ON-center units. The electrode usually then passed into the perigeniculate nucleus in which responses were much different.

Figure 23. Reconstruction of angled penetrations in parasagittal section. Two electrode penetrations inclined in the parasagittal plane drawn onto a photograph of a Nissl-stained section through the LGN. Note the sequence of responses encountered as the electrode passed through the leaflets. The *arrowhead* indicates the site of the electrolytic marking lesion. Other conventions as in Figure 22.


C
A1i
A1o
P
Ai
Ao

Discussion

The present findings indicate that ON- and OFF-center geniculate cells are segregated from each other in the A laminae of the ferret's LGN: responses at only 6 recording sites of 230 within anatomically-identified leaflets had any contribution of the inappropriate center-type. They suggest strongly that the terminal arbors of retinal afferents are also segregated by center-type; indeed, discovering the functional correlate of the stratification of the retinal afferents was the original goal of this study.

These results shed little light on whether ON- and OFF-center cells are segregated in the C laminae. Our multi-unit electrodes found only 38 of 138 sites to be predominantly or exclusively of one center-type, but such electrodes may sample over a distance that is considerable compared to the width of possible sublaminae in the C laminae.

ON- and OFF-center cells are segregated within the LGNs of several species, although the pattern of this organization varies among species. The organization of the mink's LGN appears to be identical to that of the ferret's LGN, except that the cellular sublamination is more distinct in mink than in ferrets (Guillery, 1971; Sanderson, 1974; Linden et al., 1981; LeVay and McConnell, 1982). ON- and OFF-center cells are found in separate laminae in tree shrews (Conway and Schiller, 1983), although the ordering of these layers is different in shrews than in ferrets or mink. ON-center and OFF-center cells are also segregated within at least a portion of the macaque's LGN (Schiller and Malpeli, 1978). Although there is not an obvious segregation of ON-center and OFF-center cells in the LGN of the cat (Sanderson, 1971), a functional segregation of ON and OFF channels is still present in the retinogeniculate projection. Individual relay cells in the LGN appear to receive input from retinal ganglion cells of only one center-type (Hubel and Wiesel, 1961; Cleland et al., 1971; Mastronarde, 1983; Horton and

Sherk, 1984). A partial layering of ON and OFF responses in the cat LGN has more recently been reported, with ON responses being more common near the tops of the layers (Bowling, 1983; Bowling and Schoel, 1983). Other investigators have reported a segregation of ON and OFF geniculate cells into columns normal to the laminar borders (Naporn et al., 1985). This matter remains to be resolved.

Despite the fact that ferrets lack the distinct interlaminar zones between the leaflets that are seen in mink, the segregation of ON and OFF geniculate cells revealed physiologically is as complete in the ferret as in the mink. This observation suggests that the segregation of the retinal afferents is as strict in ferrets as in mink. In ferrets (Linden et al., 1981), as well as in other species studied (tree shrews, Brunso-Bechtold and Casagrande, 1982; cats, Shatz, 1983), segregation of the initially-overlapping retinal afferents precedes the formation of interlaminar spaces. Perhaps the ferret's visual system is slightly more primitive than that of the mink: the formation of interlaminar spaces proceeds to a greater degree in mink than in ferrets, resulting in "interleaflet" spaces in the former species but not the latter.

It appears that retinal afferents have some role in the development of laminae in the LGN. Binocular encucleation before the geniculate laminae have begun to form results in a nucleus in which interlaminar spaces are absent. However, cytological differences among the presumed layers are apparent in binocularly-enucleated animals (tree shrew, Brunso-Bechtold and Casagrande, 1981; ferret and mink, Guillery et al., 1985). For example, in ferrets, early binocular enucleation results in an LGN that is severely shrunken and that has indistinct borders; however, the cells of the C laminae are characteristically elongated, while those of the A laminae are roughly spherical.

It is also interesting to ask what causes the afferents themselves to segregate. Stratification of retinogeniculate afferents does not require binocular competition. Leaflets appropriately distinct for their species form in the innervated layers of the LGNs of minks and

ferrets monocularly-enucleated before the time that the retinal afferents normally begin to segregate (Guillery et al., 1985). In addition, Shatz and Sretevan (1986) have shown that, in early monocular-enucleates, the terminal arbors of retinogeniculate axons appear to be "distributed in tiers" highly reminiscent of the distribution of axons serving the contralateral and ipsilateral eyes in normal animals. Finally, albino ferrets have an abnormally large contralateral retinogeniculate projection, so that most of layer A1 is innervated by the contralateral eye. In these animals, there are normally-appearing interlaminar plexuses between laminae A and A1 despite the fact that these geniculate laminae receive retinogeniculate axons from the same eye (Guillery, 1971). Perhaps not surprisingly, early monocular enucleation fails to disrupt the pattern of interlaminar spaces in albino ferrets (Guillery et al., 1985).

In the case of the monocularly-enucleated embryonic cats, it is not known on what basis the retinogeniculate axons sort. In the case of the albino ferrets, the retinal afferents lying across from each other in laminae A and A1 come from non-neighboring retinal ganglion cells. In monocularly-enucleated ferrets or mink, the tiers of afferents presumably reflect the segregation of ON and OFF retinogeniculate axons. The latter two findings could be explained if correlated activity among the retinal ganglion cells has a role in organizing their patterns of termination within the LGN.

Sublamination may be a general feature of organization by which different response properties can remain segregated from one another through stages of synaptic relay. The finding that ON-center and OFF-center cells are located in different layers or sublayers of the LGN in several species raises many questions: 1) What are the projections of the different (sub)laminae; are they kept separated up to the level of the cortex? This question will be addressed in the next chapter. 2) Are the sublaminae themselves organized with respect to other functional properties; for example, do X and Y cells cluster within each center-type sublayer? 3) What are the consequences for visual processing of maintaining anatomically separate ON

and OFF channels through the LGN? Schiller and Malpeli (1978) have suggested that the segregation of ON-center and OFF-center cells into separate geniculate laminae would permit the selective modulation of ON and OFF cells by non-retinal inputs to the LGN. 4) How does sublamination arise during development? These last two questions will be discussed at length in Chapter 6.

Chapter V

Physiological evidence for ON and OFF patches within layer IV of ferret visual cortex

Introduction

Within the mammalian central visual system, cells with different physiological properties are often segregated anatomically. The development and functional consequences of such segregation are questions of major interest.

Axons of the retinal ganglion cells from each eye terminate in separate laminae of the lateral geniculate nucleus (LGN) of the ferret (Sanderson, 1974; Guillery, 1971; Linden et al., 1981). This segregation is maintained in the projection from LGN to cortex, resulting in the ocular dominance columns seen with transneuronal labelling techniques (Law et al., in preparation). On-center and off-center cells are also found in separate sublayers of the ferret's LGN (Stryker and Zahs, 1983). The purpose of the present experiments was to determine if and how the axons of ON and OFF geniculate cells segregate within the primary visual cortex (area 17) of ferrets.

The segregation of the afferents serving the two eyes into separate geniculate laminae occurs in many species, and the segregation of on-center and off-center cells into separate geniculate laminae or sublaminae has also been reported in macaques (Schiller and Malpeli, 1978), tree shrews (Conway and Schiller, 1983), and mink (LeVay and McConnell, 1982). However, the arrangement of these laminae within the LGN and the organization of their projections to the cortex vary greatly among species. In macaques, segregation of the ON and OFF geniculocortical projections has not been reported. The axons of ON and OFF LGN cells terminate in different sub-layers of layer IV of the visual cortex in tree shrews (Conley et al., 1984), a species in which ocular dominance is also stratified (Kretz et al., 1986). In mink, a species which has ocular dominance columns, the evidence favors a patchy distribution of ON

and OFF afferents similar to ocular dominance patches in the plane of layer IV (McConnell and LeVay, 1984).

There were several reasons for undertaking these studies in ferrets. First, it is of general interest to know more about the detailed organization of thalamocortical projections. Some of the hypotheses about the mechanisms that give rise to precise topographic maps and ocular dominance patches imply that other functional properties important to the discharge patterns of geniculate cells should cause segregation. Second, ferrets are born relatively immature. The segregation of retinal ganglion cell axons into the appropriate geniculate laminae appears to be complete at the time of birth in macaques (Rakic, 1976), cats (Shatz, 1983), and tree shrews (Brunso-Bechtold and Casagrande, 1982). Ferrets, however, are born at a time when the axons from the retinal ganglion cells of the two eyes still overlap in the LGN (Linden et al., 1981) and should provide an especially useful model for studying visual system development. Mink (*Mustela vison*) development might be expected to follow a timecourse similar to ferret (*Mustela putorius furo*) development, but ferrets are more tractable than mink and breed easily in the laboratory year-round. Although the segregation of ON and OFF geniculate cells seen physiologically is as complete in ferrets as in mink, the ON and OFF sublayers are anatomically more distinct in mink. It was not clear to what degree, if any, ferret ON and OFF geniculate cells would segregate their projections to cortex.

In the present study, the organization of the geniculocortical afferents was revealed by microelectrode recordings from axonal arbors within layer IV of area 17. Afferent activity was easily recorded after eliminating the activity of cortical neurons with kainic acid, an excitatory neurotoxin that kills cells while sparing terminals and fibers of passage (McGeer et al., 1978). McConnell and LeVay (1984) also used kainic acid to eliminate cortical activity and record from geniculate afferents in mink. The present technique differs from theirs in that a larger area of cortex was silenced, and afferents could be recorded for longer periods. In minks, a patchy

distribution of ON and OFF afferents was inferred from the results of long penetrations made tangential to the cortical layers. The present method of kainate application permitted the construction of maps from multiple radial or vertical penetrations in order to show the distribution of afferent activity looking down onto the cortical surface.

The results obtained in kainate-treated ferrets suggest that LGN afferents do cluster according to center-type, and that this clustering results in patches of ON and OFF afferents in the plane of layer IV. These conclusions were strengthened by the results of quantitative analyses of the data using Monte Carlo techniques.

Methods

Animals.

Eleven adult sable ferrets were used in these studies. The animals were obtained from Marshall Farms (New Rose, N.Y.) and were maintained on a 14 hr light:10 hr dark cycle in the vivarium at the University of California, San Francisco.

Electrophysiological recording.

Animals were prepared for physiological recording using conventional techniques. The ferrets were initially anesthetized with a mixture of acepromezine (0.04 mg/kg) and ketamine (40 mg/kg) injected intramuscularly. Atropine (0.08 mg) was administered intramuscularly every 12 hours throughout the experiment. The femoral vein and trachea were cannulated, and surgical anesthesia was subsequently maintained with thiopental sodium administered intravenously as needed. All wound margins were infiltrated with lidocaine.

Each ferret was placed in a modified kitten stereotaxic apparatus, and the scalp was incised and retracted. A large craniotomy was performed, extending from Horsley-Clarke anterior-posterior -3.0 to the posterior pole of the cortex (approximately Horsley-Clarke anterior-posterior -8) and from Horsley-Clarke lateral-medial 1.5 to 8.5 . The dura was opened and the exposed brain was kept moist with 0.9% saline or lactated Ringer's solution. Neuromuscular blockade was then induced with gallamine triethiodide (1.0 ml/kg/hr, 10 mg/ml

in 0.45% saline with 2.5% dextrose), and the ferret was artificially ventilated with a mixture of 75% nitrous oxide, 25% oxygen at a rate and volume that maintained peak inspiratory pressure at 1.5 kPa and end-tidal carbon dioxide at 3.8-4.3%. The electroencephalogram (EEG) contralateral to the exposed cortex was continuously monitored, and thiopental sodium was administered at the first sign of desynchronization of the EEG. The animal's temperature was maintained at 37.5 deg Centigrade using a feedback unit, and the animal's heart rate was also monitored throughout the experiment.

The cortical surface was photographed with a Nikon 35mm camera mounted on either a bellows or to a Zeiss operating microscope. When these photographs were printed at a final magnification of 28X the cortical vasculature was represented in enough detail to provide a convenient and accurate means of recording the entry points of the electrode penetrations.

After completion of the photography, a piece of filter paper (Whatman No. 4, 2 mm x 7 mm) was soaked in kainic acid (Sigma, K0250, 10 mM in 0.9% saline) and placed over the caudalmost part of the exposed cortex. The same kainate solution was superfused onto this filter paper at the rate of 67 μliters/hr, using a piece of Silastic tubing attached to a syringe placed in an infusion pump. The anterior part of the exposed brain was covered with saline-soaked filter paper. Moist cotton was then placed around the exposure and covered with Saran Wrap, creating a damp chamber over the cortex. The cotton was repeatedly moistened with saline throughout the infusion without disturbing the chamber. The nictitating membranes were retracted with phenylephrine hydrochloride and plastic contact lenses were inserted to protect the corneas during the period of kainate application.

The kainate superfusion was continued for 12-14 hours, after which time the filter paper was removed, usually with no apparent damage to the cortical surface. A dental cement well was built around the exposure and filled with either 0.9% saline or 300-Stokes oil (dimethyl polysiloxane, Dow Corning 200).

The protective contact lenses were removed, and atropine was applied to dilate the pupils and paralyze accommodation. Plastic contact lenses (2.6 - 2.8 mm base curve, plano) were selected to focus the eyes on a tangent screen placed either 57 cm or 114 cm in front of the animal. Focus was checked by retinoscopy. The projections of the two optic discs were plotted on the tangent screen using a reversing beam ophthalmoscope.

Tungsten microelectrodes (Hubel, 1957) were used to record extracellularly from units in the cortex. The best electrodes for these experiments had impedances of 1.5 to 2.0 MOhm at 300 Hz and tapered to a very sharp point over 25 to 40 μm. The electrode was connected to a capacity-compensated pre-amplifier (Grass, P15), and the signal was filtered at 30 Hz to 10kHz and displayed on an oscilloscope (Tektronix 5115) and played on an audio-monitor (Grass AM8).

Receptive fields were plotted on the tangent screen using light spots or bars produced with a Zeiss handlamp or black discs held at the end of a wand. The screen had a background luminance of 6.2 cd/m^2; the light stimuli were 0.85 log units brighter than background, and the dark stimuli were 0.75 log units darker than background.

Vertical organization. In order to study the vertical organization of the afferents, radial penetrations were made into area 17 in 5 kainate-treated ferrets. The electrode was advanced in 40-μm steps and responses were sought at each depth using flashing or moving spots and bars of light and black discs. Single- and multiple-unit responses could be recorded with these electrodes. For each response, the center-type, receptive-field location and eye through which the response was elicited were recorded. Electrolytic lesions (5 μA x 5 sec) marked selected positions along the course of a penetration. In one animal, a stimulating electrode (lacquer-coated tungsten, 800 kOhm impedance) was placed in the LGN at a site where the receptive fields of the geniculate cells overlapped those of the units recorded in the cortex (Zahs and Stryker, 1985).

Horizontal organization. The horizontal organization of the afferents was studied in a series of surface mapping experiments. Many closely-spaced (100-150 μm) penetrations were made across the dorsal surface of area 17 in 3 kainate-treated ferrets. The entry point of each penetration was marked on a photograph of the cortical surface. For each penetration, the electrode was advanced in 40-μm steps until the first afferent responses were encountered. Center-type, eye of origin, and receptive-field location were determined for the units encountered at this depth and at two successive depths spaced at 40-μm intervals.

The horizontal organization of the afferents was further studied by making long penetrations tangential to the cortical layers. In two kainate-treated ferrets, one of which was also used in a surface mapping experiment, electrode penetrations were angled dorsomedial to ventrolateral in the coronal plane. Such penetrations were expected to travel approximately parallel to the cortical layers. Responses were recorded at 20-μm intervals for as long as the penetration remained within layer IV.

An initial two animals were not treated with kainic acid, and the distribution of ON and OFF activity was recorded in layer IV. These animals were prepared for recording in the manner described, except that recording began immediately after completion of the photography. In these cases, the electrode was rapidly advanced normal to the cortical layers until it reached layer IV, recognized by the presence of units which responded to rapidly-moving, non-oriented stimuli. Multi-unit responses to flashed spots or moving discs were recorded at one or two depths within each penetration. Many such penetrations were made across the surface of the cortex.

Histology.

The brains of the five animals used to study the vertical organization of the afferents were processed for histological reconstruction of the electrode tracks. At the end of the recording sessions, the ferrets were deeply anesthetized with an intravenous injection of sodium pentobarbital and perfused through the heart with 0.1 M phosphate buffer (pH 7.4) followed by 1.25% paraformaldehyde and 2.5% gluteraldehyde in this same buffer. The occipital cortex, including area 17, was removed, and the blocks were sectioned on a Vibratome at 40 μm in the coronal plane. All sections were collected, mounted on gelatinized slides, and stained with cresyl violet.

Quantitative analyses.

Data were subjected to quantitative analyses in order to answer four questions: 1) Do afferents of the same center-type tend to cluster? 2) If afferents do cluster, are there separate ON and OFF strata in layer IV, or 3) are there separate ON and OFF patches in the plane of layer IV? 4) If the afferents terminate in separate patches in the plane of layer IV, what is the size of the patches?

Clustering. In order to determine whether the afferents are clustered according to center-type, a Monte Carlo analysis was applied to the data from radial penetrations in which single-afferent responses were recorded in layer IV. Clustering was quantified using a *cluster index*[1] that expressed the probability that two successively-encountered units were of the same

1 Cluster Index = (1 - (s/t)) x 100, where *s* is the number of switches in center-type between successively-recorded units within a penetration, and *t* is the number of units minus the number of penetrations.

center-type. This value was calculated for the pooled data from the animals used to study the vertical organization of the afferents.

A MicroVaxII computer then simulated 1000 experiments in which responsive "units" were distributed among penetrations in the same way as occurred experimentally, except that the center-type of each "unit" was randomly reassigned from a pool of "responses" that contained the same total numbers of ON and OFF responses as were found experimentally. The value of the *cluster index* was calculated from the results of each of these simulations, allowing us to compare the degree of clustering observed experimentally to that which would be observed if ON and OFF afferents were randomly dispersed within layer IV.

Stratification. To test for stratification, penetrations were divided into thirds along their lengths. The frequency of units of each center-type was calculated for each segment, and, these frequencies were compared using the Friedman two-way analysis of variance (Siegel, 1956). Only penetrations in which units were recorded throughout the depth of layer IV were included in this analysis.

Patch analysis. Data from the surface mapping experiments were also analyzed with a Monte Carlo technique to determine whether there are ON and OFF patches in the plane of layer IV. For each map, the location of the entry point of each penetration was entered into the computer using a digitizing tablet. Each penetration was classified according to the center-type and eye of origin of the units it sampled. Boundaries were drawn around regions of common center-type or eye dominance using an algorithm that effectively placed a border half-way between neighboring penetrations that fell into different response classes. The number of regions thus formed was counted to give the number of patches for each map. There should be fewer patches in a cortex in which afferents of the same type are clustered than in a cortex in which the afferents are randomly dispersed, assuming that the spacing between electrode penetrations is less than the size of the patches and that most sites do not yield mixed responses.

For each animal, the number of patches found experimentally was compared to the values that resulted from 500 simulated experiments in which center-types or eye preferences were randomly redistributed over the penetration sites.

Patch-size analysis. A final Monte Carlo analysis was devised to estimate the sizes of the patches; this analysis was applied to both the center-type data and the eye preference data. Simulated maps were constructed, consisting of patches modeled as a repeating series of parallel stripes. The aim of this analysis was to determine what range of patch widths or periods in the simulated maps adequately fit the experimental data. For the center-type stripes, each cycle consisted of an ON stripe, followed by a MIXED stripe, followed by an OFF stripe, followed by a MIXED stripe. The relative widths of the stripes were determined by the proportions of responses in the pooled data from the surface mapping experiments[2]; kainate-treated and normal cortices were considered separately.

For each stripe period, 200 simulated maps (corresponding to a particular patch width) were created by randomly rotating and translating the original map before placing it on the field of stripes. Each penetration was then reclassified as ON-dominated, OFF-dominated, or MIXED according to the stripe on which it fell. Borders were then drawn around the regions containing penetrations of the same response category, using the same algorithm as described above, and the number of patches thus formed was counted, yielding a distribution of patch counts for each period. For each distribution, the percentile of the experimentally-obtained patch count was recorded. These percentile values were then plotted as a function of period.

---

2 *wON* : *wOFF* : *wMIXED* = *nON* : *nOFF* : *nMIXED*/2, where *wON* = width of the ON stripe, *wOFF* = width of the OFF stripes, *wMIXED* = width of the MIXED stripes, *nON* = total number of penetrations classified as ON-dominated from the surface mapping experiments in the kainate-treated (or normal) animals, *nOFF* = total number of penetrations classified as OFF-dominated in the surface mapping experiments in the kainate-treated (or normal) animals, and *nMIXED* = total number of MIXED penetrations in the kainate-treated (or normal) animals.

We reasoned that the period for which the experimentally-obtained patch count occurred at the 50th percentile was the most likely estimate of the period of the ON-MIXED-OFF-MIXED cycle.

The same type of analysis was applied to the ocular dominance patches, except, in this case, the patches were modeled as a cycle of contralateral-binocular-ipsilateral-binocular parallel stripes. The relative widths of the stripes were again determined by the relative proportions of the different types of responses in the pooled data from the surface mapping experiments.

The shortcomings of this analysis and the validity of the underlying assumptions will be considered in the *Discussion*.

Results

Surface maps in untreated ferrets.

In initial experiments, an attempt was made to study the distribution of ON and OFF afferents in layer IV of normal cortex. Many closely-spaced electrode penetrations were made into the exposed dorsal surface of area 17 in two ferrets, and multiple-unit responses were recorded within layer IV. At the beginning of each penetration, the electrode was quickly advanced until layer IV was recognized by an increase in background activity and the presence of units that responded to a light spot moved rapidly back and forth across the eyes. Once the electrode had reached layer IV, light flashes and rapidly-moving light or dark spots were presented on the tangent screen, within the appropriate receptive field, and we attempted to evaluate the responses of the geniculate afferents. Afferent responses differ in quality from cortical-cell responses on an audio monitor: afferent activity sounds like a high-frequency "swish" that reliably follows even rapidly presented stimuli; cortical units have relatively low frequency, habituating responses.

Afferent-like responses were rated on a 7-point scale (1(7) = pure ON(OFF) response, 2(6) = strongly ON(OFF)-dominated response, 3(5) = weakly ON(OFF)-dominated response, and 4 = equally MIXED ON-OFF response) analogous to that commonly used to describe ocular dominance (Hubel and Wiesel, 1962). The results of these experiments are shown in Figure 24. In this figure, classes 1 and 2 have been grouped together and designated as ON-dominated sites, classes 6 and 7 have been grouped together as OFF-dominated site, and classes 3, 4, and 5 have been grouped together as MIXED sites. Many penetrations encountered

Figure 24. Center-type surface maps in normal ferrets. The distribution of ON and OFF activity in layer IV was mapped in two ferrets that were *not* treated with kainic acid. In this figure, and all subsequent surface maps, the drawings represent the view of an observer looking down on the cortical surface onto which the responses recorded in layer IV have been projected. *Top*, surface map obtained from ferret F62. 130 penetrations were made into the dorsal exposed surface of area 17, and the multi-unit responses were rated on a 7-point "ON-OFF" scale (*see text*). Borders were drawn around regions in which responses were of a common type. The *lightly-shaded* areas contained ON-dominated responses (responses rated 1 or 2), *dark* areas contained OFF-dominated responses (ratings of 6 or 7), and MIXED responses (ratings of 3, 4, or 5) were found in the areas of *intermediate shading*. Spots of contrasting shading represent the entry points of the electrode penetrations. Bottom, surface map obtained in ferret F78 (60 penetrations). Conventions the same as for the upper map. Caudal is *up*; lateral is to the *right*. *Scale bar* = 150 microns.

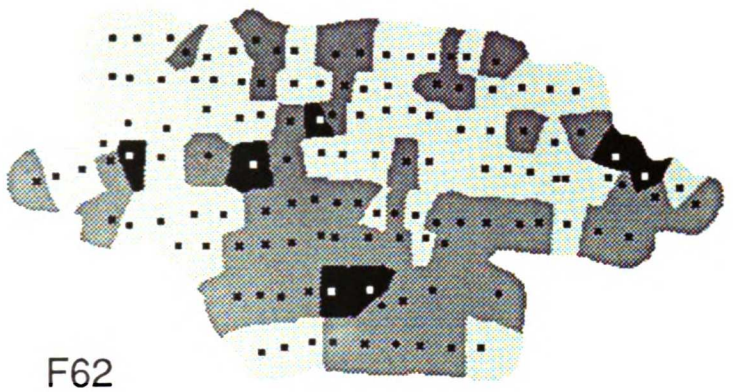

F62

F78

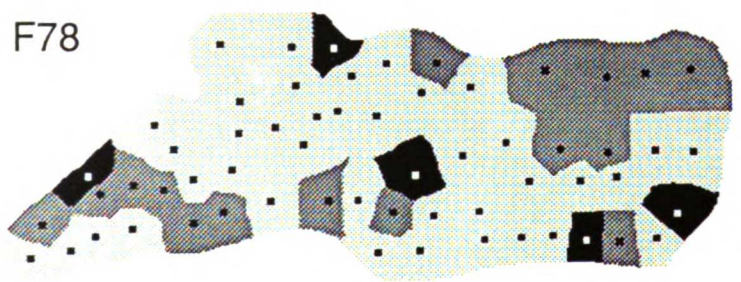

regions dominated by ON or OFF activity, but most regions gave mixed responses. Neighboring penetrations tended to be of the same response-type.

Despite the use of stimuli that should more effectively drive LGN afferents than cortical cells, cortical neurons contributed significantly to the responses. It was extremely difficult to attend to the geniculate-like responses in the presence of active cortical cells, and the ratings reported were contaminated by cortical-cell responses. We concluded from these experiments that cortical neurons would have to be silenced if afferent responses were to be recognized consistently.

General effects of kainic acid treatment.

Following 12-14 hours of superfusion with kainic acid, neuronal activity was eliminated in the upper layers of the cortex. Recordings after shorter exposures to kainate (6-8 hours) revealed seizure activity which prevented the study of visual responses. After the longer exposures, neither visually-evoked nor spontaneous activity was encountered until the electrode reached the top of layer IV. Within layer IV, spontaneous activity was high and multiple-unit responses were easily elicited. The single-units that contributed to this activity could be distinguished when the appropriate electrodes (see *Methods*) were used. These units, recorded after kainate treatment, had the response characteristics of geniculate cells (Stryker and Zahs, 1983; Zahs and Stryker, 1985): they were driven through one eye only, they responded to high-frequency light flashes or rapidly moving light or dark spots within receptive fields of the appropriate size, they showed no preferences for stimulus orientation, most gave sustained responses to small spots of the appropriate sign of contrast, and all of those tested showed

center-surround antagonism. Active units were also found within layer VI, but we did not attempt to study them further.

Although responsive units were abundant within layer IV, it was difficult to discriminate among them solely on the basis of differences in the sizes of their action potentials. The differences among single-unit waveforms were frequently discriminable when played through the audio monitor, however, and the ability to activate individual receptive fields with appropriate small spot stimuli made it possible to map single units during the few minutes that each produced the most distinct spike among the multiple units recorded by the electrode. It was almost never possible for us to hold the rare unit isolated using the window discriminator long enough to study its visual responses quantitatively. However, the units that remained isolated long enough to photograph their superimposed waveforms had very fast (< 200 μsec total duration), small (10-50 μV) action potentials, consistent with their identification as axons (Bishop, Burke, and Davis, 1962). In one animal, a stimulating electrode was placed in the LGN at a site where the receptive fields of the geniculate cells overlapped those of the units recorded in the cortex. The units recorded in layer IV could follow electrical stimulation at this site at frequencies as great as 400 Hz, providing further evidence that the responsive units in kainate-treated cortices were the axon terminals of geniculate cells.

When the cortical surface was viewed through the surgical microscope during the recording sessions, the area exposed to kainate initially appeared normal. After several hours of recording, an exudate was sometimes observed on the cortical surface; in the most severe cases, this exudate obscured the cortical vasculature. Histology revealed gross abnormalities in the kainate-treated cortices. Kainate-treated cortices were very pale-staining, and the thickness of the cortex was reduced. Only glia stained darkly, and the presumed neurons appeared ghost-like. All cell layers were affected in the areas that had been underneath the kainate-soaked filter paper. Although the laminar borders were less distinct than in normal tissue, laminae were still

Figure 25. Histological abnormalities in kainate-treated cortex. A) Coronal section through area 17 of a normal ferret. The section has been stained with cresyl violet. *Roman numerals* identify the cortical layers. B) Coronal section through area 17 of a kainate-treated ferret. Kainic acid was superfused onto the cortex for 14 hours (see *Methods*); the animal was perfused 12 hours after the kainate superfusion was discontinued. This section has been stained using the same protocol as the section shown in (A), and the photographs are printed at the same magnification. To aid in comparison, the sections in parts (A) and (B) have been positioned so that the IV/V borders are aligned. Note the shrunken, pale staining appearance, and that all cell layers are affected. Three electrolytic marking lesions (*arrows*) are seen at the border between layers IV and V in (B). *Scale bar* applies to both (A) and (B), equals 100 microns. The dorsal (pial) surface is *up*; lateral is to the *left*. C) Higher-power photomicrographs (printed at final magnification of 600X) of the appearance of cells in a kainate-treated cortex. *Roman numerals* refer to the cortical laminae; *arrows* point to ghost-like cells, believed to be neurons.

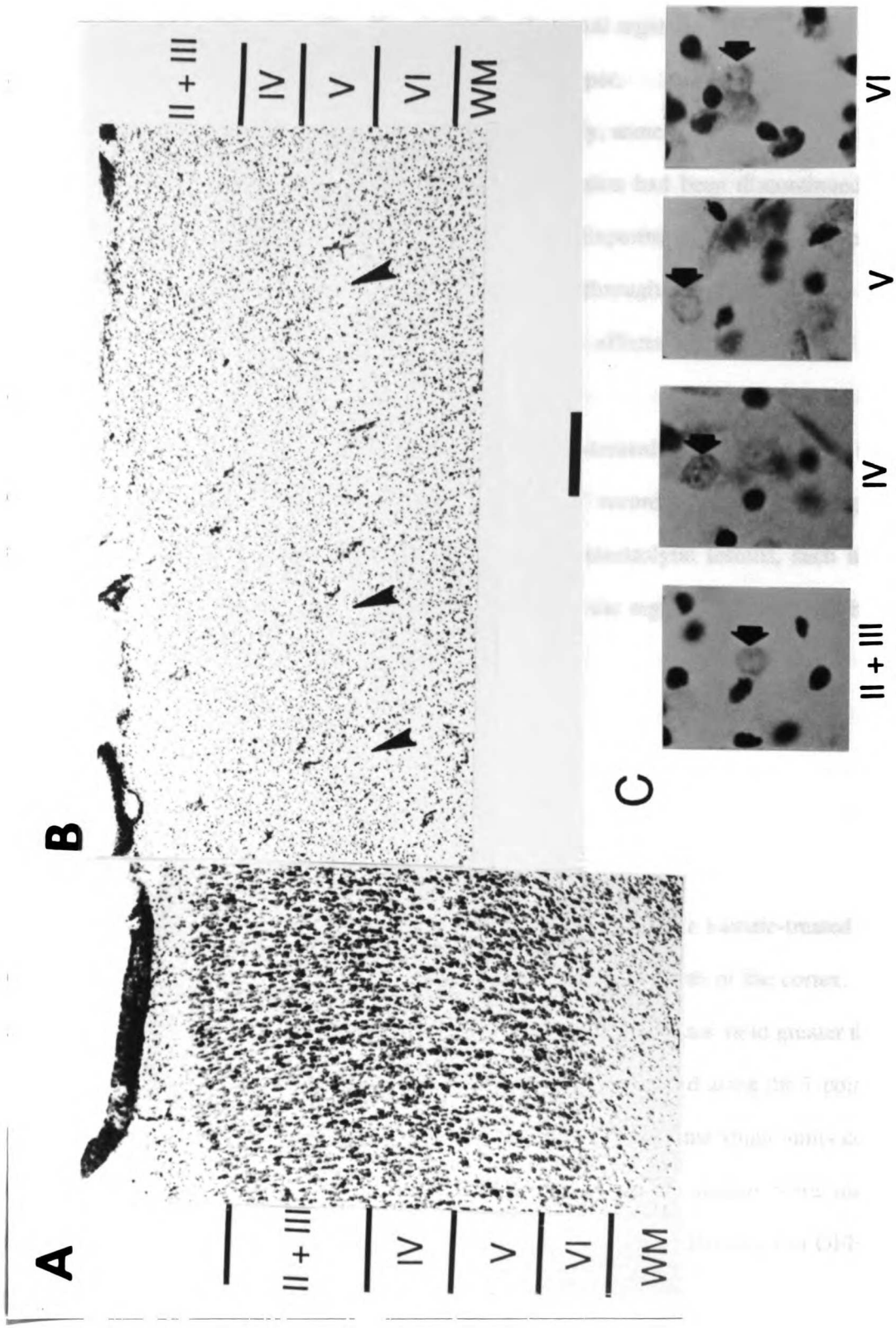
A
B
C
II + III
IV
V
VI
WM
II + III
IV
V
VI
WM
II + III
IV
V
VI

distinguishable cytoarchitectonically. Histologically abnormal regions had fairly sharp borders that extended less than 1 mm beyond the edge of the filter paper.

Despite the severity of the damage seen histologically, some cortical responses returned some (8 to more than 12) hours after the kainate superfusion had been discontinued. This responsiveness was often accompanied by seizure activity. Experiments were terminated when large, orientation-specific responses returned. A section through the cortex of one animal perfused at this time is shown in Figure 25. The chronic effects of this method of kainate application are not known.

Reconstructions of electrode penetrations in kainate-treated cortices confirmed that the units studied were within layer IV. Laminar position of recording sites was assigned by referring to microdrive readings at recording sites and at electrolytic lesions, such as those shown in Figure 25. These lesions, marking the bottom of the region from which units were recorded, are at the border between layers IV and V.

Vertical organization in kainate-treated animals.

Twenty-eight radial penetrations were made into area 17 of five kainate-treated ferrets, and recording sites were spaced at 40-μm intervals throughout the depth of the cortex. In the first animal (7 penetrations), stimuli were presented in an area of the visual field greater than the size of typical LGN receptive fields, and multi-unit responses were rated using the 7-point scale mentioned above. In subsequent experiments, however, it was found that single units could be easily distinguished by their distinct receptive fields when smaller stimuli were used and receptive fields were mapped carefully. Single units gave exclusively ON-center or OFF-center

responses. While the results from the first animal were consistent with those found later, only the *single*-unit recordings from the other four ferrets were considered further.

Afferent responses were recorded throughout the depth of layer IV in 16 electrode penetrations; responses were recorded over shorter (less than 200 μm) distances in an additional 5 penetrations. Reconstructions of 4 representative electrode penetrations are shown in Figure 26. At many depths it was possible to record from more than one unit. When the electrode was advanced, characteristically one or two single-unit responses could be discerned. After a few minutes, the responses of new afferents would be recorded, distinguished from the previous units by their receptive fields. These responses were from different afferents and did not not merely reflect changes in the receptive-fields of previously-encountered units caused by slippage of the eyes: the center-type as well as the receptive-field location of the response sometimes changed, and it usually remained possible to record responses from one or more previously-detected units to stimuli of the appropriate contrast presented within their original receptive field(s). We believe that small movements of the electrode relative to the surrounding axon terminals resulted in the appearance and disappearance of particular responses. If responses were elicited from the same receptive field at adjacent sites, only the first response was counted. It is therefore likely that a larger number of units were actually recorded than were counted. Of the 16 penetrations in which responses spanned layer IV, 6 contained only ON afferents, 2 contained OFF afferents exclusively, 2 contained a region of one center-type followed by a region of the second center-type, and 6 had units of both center-types interspersed throughout layer IV.

Figure 27 shows the receptive fields of the units illustrated in Figure 26. Fields of ON units are represented with open circles and those of OFF units are shaded. The numbers indicate the order in which the units were encountered. The receptive fields of successively-encountered units were frequently separated by distances of several field-diameters. The area

Figure 26. Reconstructions of 4 representative radial penetrations in kainate-treated cortices. Each dot represents a single afferent recorded in layer IV. Vertical scale shows the depth (microns) at which the response was recorded; for each penetration, the first site at which a response was encountered was assigned depth 0. A) Example of one of the 6 penetrations in which only ON responses were encounterd. B) Example of one of the 2 penetrations in which only OFF responses were recorded. C) Example of one of the 2 penetrations in which a region of afferents of one center-type was followed by a region of afferents of the opposite center-type. D) Example of one of the 6 penetrations in which ON and OFF afferents were interspersed throughout the depth of layer IV. Note that, even in this case, one center-type (OFF) predominates.

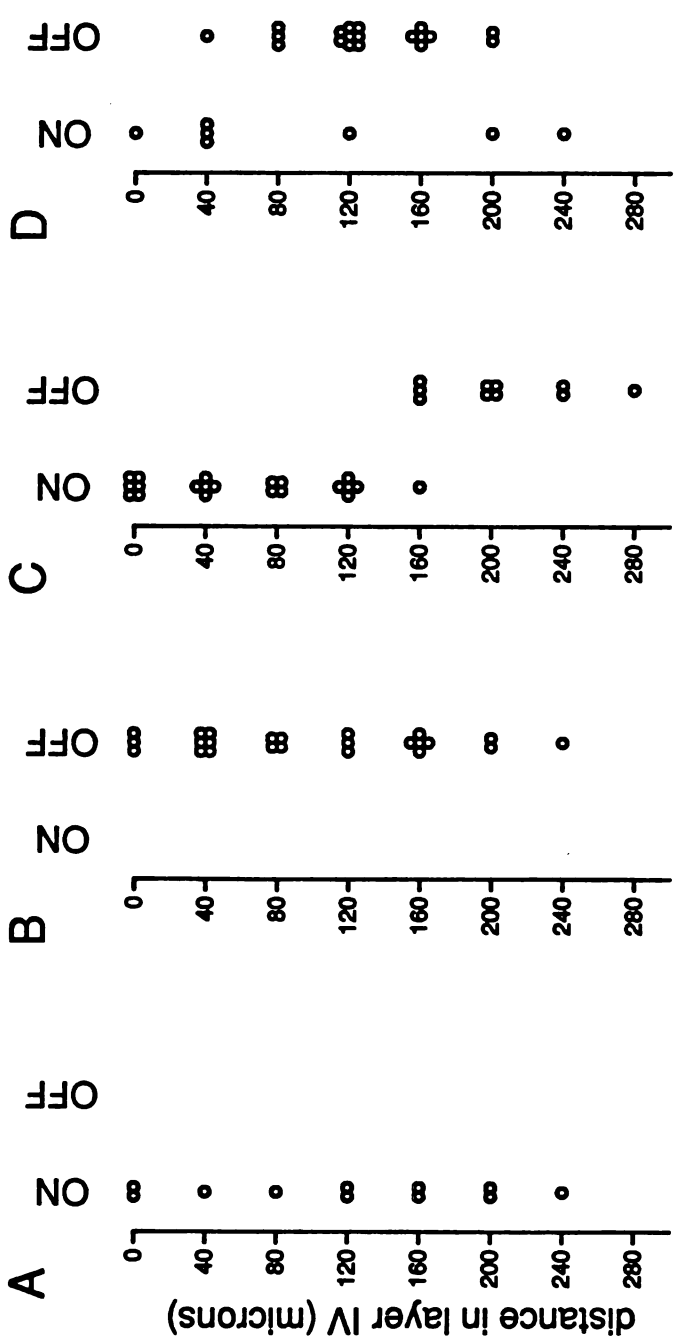
A
B
C
D
ON
OFF
0
40
80
120
160
200
240
280
distance in layer IV (microns)

Figure 27. Receptive fields of the units illustrated in Figure 26. Letters correspond to the penetrations of Figure 26. *Open circles* represent the receptive fields of ON-center afferents; *shaded circles* show the receptive fields of OFF-center afferents. Numbers indicate the order in which the receptive fields were encountered. *Up* is superior in the visual field; to the *left* is more central in the visual field. *Scale bar* = 1 deg. Note that the regions of the visual field represented by the ON and OFF afferents in parts (C) and (D) are largely non-overlapping.

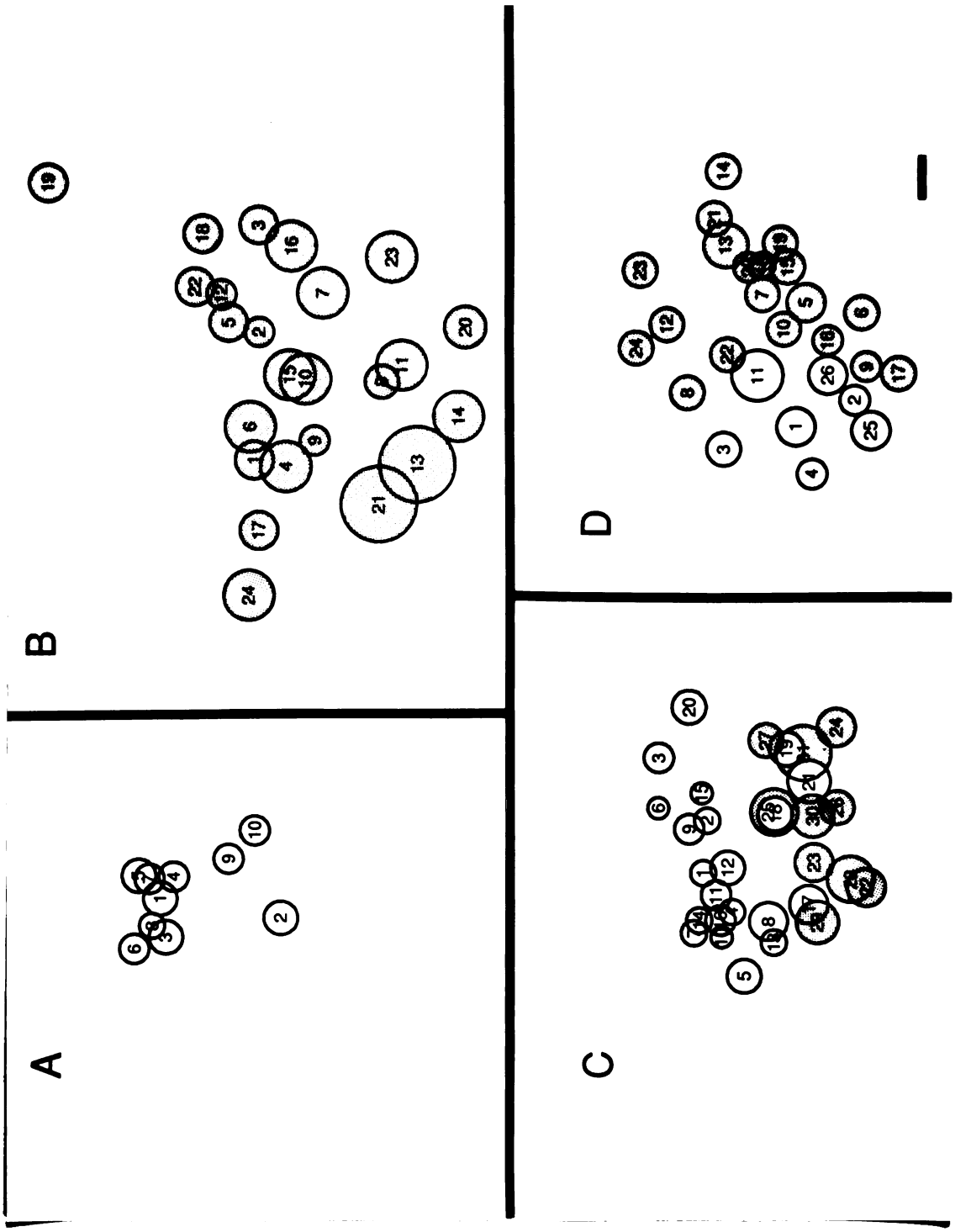
A
B
C
D

of the visual field covered by the receptive fields found in a single penetration was, however, within the range of receptive field sizes of cortical neurons representing this region of the visual field (Waitzman and Stryker, in preparation). Figure 27 also illustrates the common finding that the receptive fields of the ON and OFF units in a single penetration covered largely non-overlapping (6/8 penetrations, exemplified in Figure 27C) or only partially-overlapping (2/8 penetrations, see Figure 27D) regions of the visual field.

Inspection of the reconstructed penetrations lead to the conclusion that geniculate afferents with the same center-type tend to cluster within layer IV of area 17. This conclusion was supported by the results of the Monte Carlo analysis illustrated in Figure 28. The value of the cluster index (87) calculated from the experimental results was outside the range (40 - 59) of values calculated from each of 1000 computer-simulated experiments (see *Methods*) in which ON and OFF afferents terminated randomly within layer IV. Thus the probability of encountering ON and OFF geniculate afferents clustered to the degree found experimentally in a randomly-organized projection was less than 0.001.

Clustering of axons of the same center-type could reflect either of the two patterns of segregation of ON and OFF afferents reported in other species: 1) stratification of ON and OFF afferents within layer IV or, 2) separation of ON and OFF axons into patches in the plane of layer IV. These data provided evidence against stratification. The reconstructed penetrations were divided into thirds along their lengths, and the proportions of ON and OFF units encountered in each segment were calculated. There was no tendency for units of either center-type to be found preferentially in the top, middle, or bottom of layer IV, as shown in Figure 29.

Figure 28. Monte Carlo analysis of clustering. Distribution of values of the *cluster index* obtained in 1000 computer simulations in which ON and OFF responses were randomly redistributed among the experimentally-obtained recording sites. *Arrow* shows the value of the index calculated from the experimentally-obtained data from kainate-treated cortices. The arrow is outside the range of values for the random cases, indicating that ON and OFF responses are segregated to a greater degree than is probable ($p < 0.001$) if the afferents were randomly distributed.

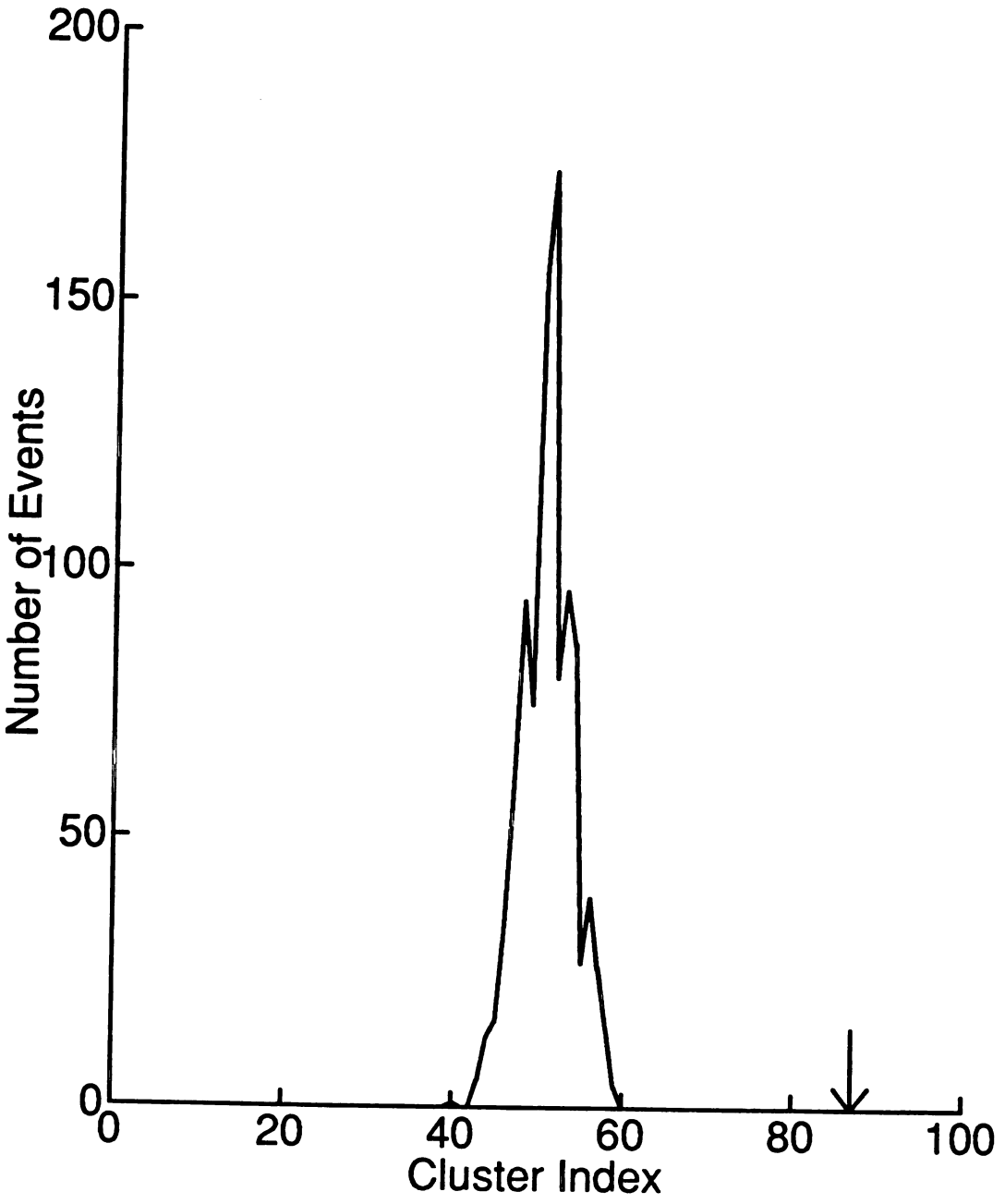
200
150
100
50
0
Number of Events
0
20
40
60
80
100
Cluster Index

Figure 29. Distribution of ON and OFF responses throughout the depth of layer IV. Reconstructions of 16 penetrations in which responses were recorded over a distance of at least 200 microns were divided into thirds along their lengths, and the fractions of responses that were ON (*left* side of figure) and OFF (*right*) were calculated. Graph shows mean $\pm$ standard error of the mean. There was no tendency for units of either center-type to be distributed preferentially in the top, middle or bottom of layer IV.

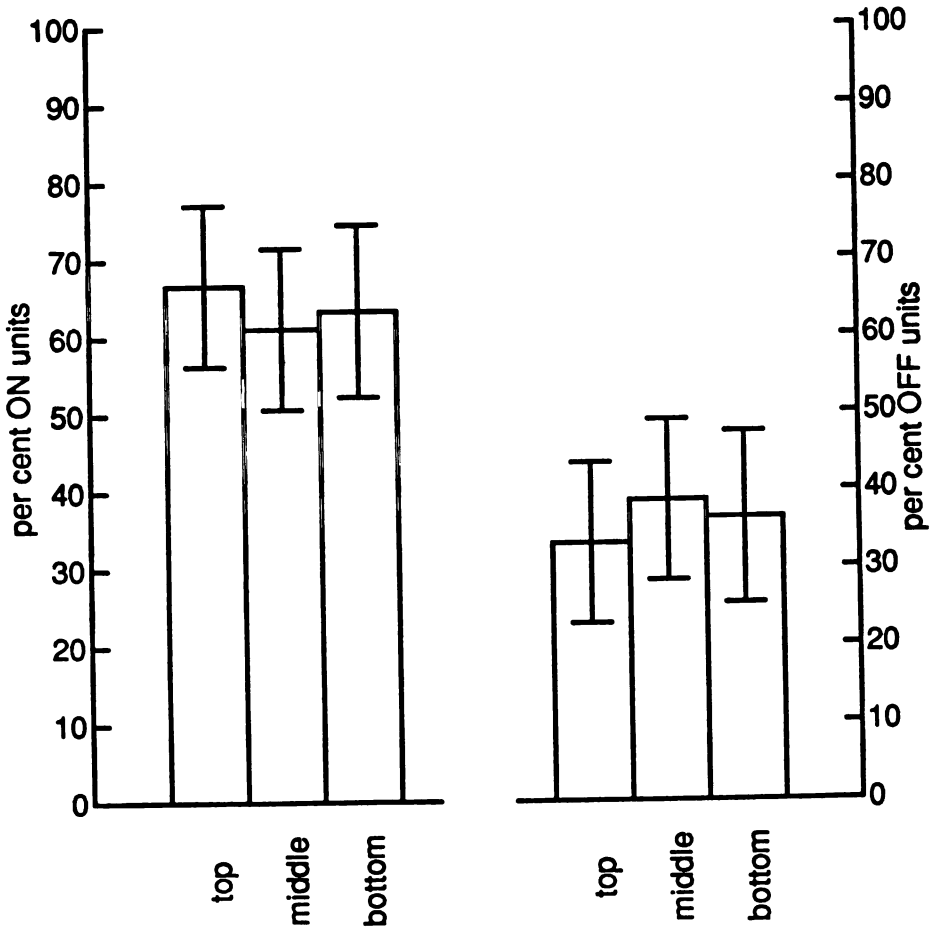
100
90
80
70
60
50
40
30
20
10
0
per cent ON units
top
middle
bottom
100
90
80
70
60
50
40
30
20
10
0
per cent OFF units
top
middle
bottom

Horizontal organization in kainate-treated ferrets.

In order to study the horizontal organization of the ON and OFF projections, many closely-spaced penetrations were made across the dorsal surface of area 17 in three kainate-treated ferrets. Multi-unit responses were recorded near the top of layer IV, at three depths spaced at 40-μm intervals. Each multi-unit response was rated using our 7-point ON/OFF scale and the 7-point ocular dominance scale of Hubel and Wiesel (1962). Ratings at the three sites were averaged to give single response ratings for center-type and for ocular dominance for each penetration.

The surface maps of ON and OFF activity obtained in the three experiments are shown in Figure 30. When constructing these maps, responses rated 1 and 2 were classified as ON-dominated, responses rated 3, 4, and 5 were classified as MIXED, and responses rated 6 and 7 were designated OFF-dominated. It can be seen that neighboring penetrations tended to have encountered afferents of the same center-type. When borders were drawn around regions in which all penetrations are in the same category, the surface of layer IV appeared as a patchwork of ON and OFF afferent activity.

Figure 31 shows surface maps of eye preference constructed from the same afferents as were used to make the ON/OFF surface maps of Figure 30. As when making the center-type maps, the original 7 response classes have been compressed into three categories: contralateral-dominated (groups 1 and 2), binocular (groups 3, 4, and 5), and ipsilateral-dominated (groups 6 and 7). Afferents serving the contralateral and ipsilateral eyes also appeared to terminate in separate patches in the plane of layer IV. Ocular dominance patches have been previously demonstrated in ferret area 17 by transneuronal labelling techniques (Law and Stryker, 1983), so their appearance here was expected.

Figure 30. Center-type surface maps in kainate-treated ferrets. Surface maps of ON and OFF activity in 3 kainate-treated ferrets, F110 (61 penetrations), F113 (18 penetrations), and F116 (51 penetrations). Conventions the same as in Figure 24.


F110


F113

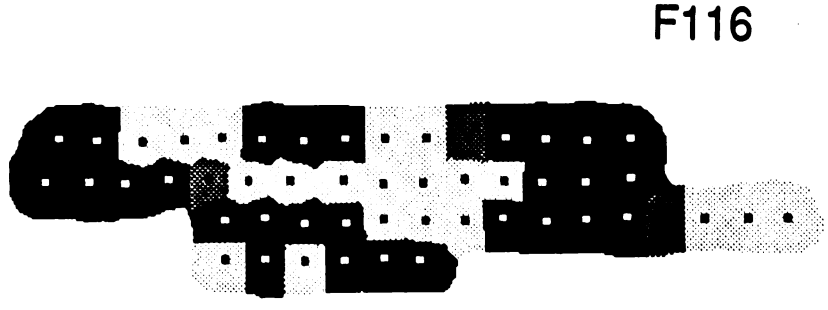
F116

Figure 31. Ocular-dominance surface maps in kainate-treated ferrets. Surface maps of the distribution of afferents serving the two eyes constructed from the same recordings as were used to make the center-type maps of Figure 30. Regions in which responses were dominated by the contralateral eye (responses rated 1 or 2, using the 7-point ocular dominance scale of Hubel and Wiesel (1962)) are *lightly-shaded*, regions dominated by the ipsilateral eye (responses rated 6 or 7) are *dark*, and regions in which afferents serving both eyes were intermingled (ratings 3, 4, or 5) are shown with *intermediate shading*. All other conventions are the same as in Figure 24.

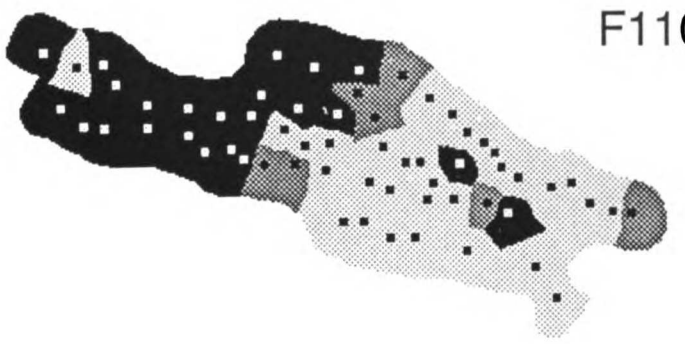
F110

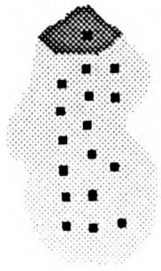
F113

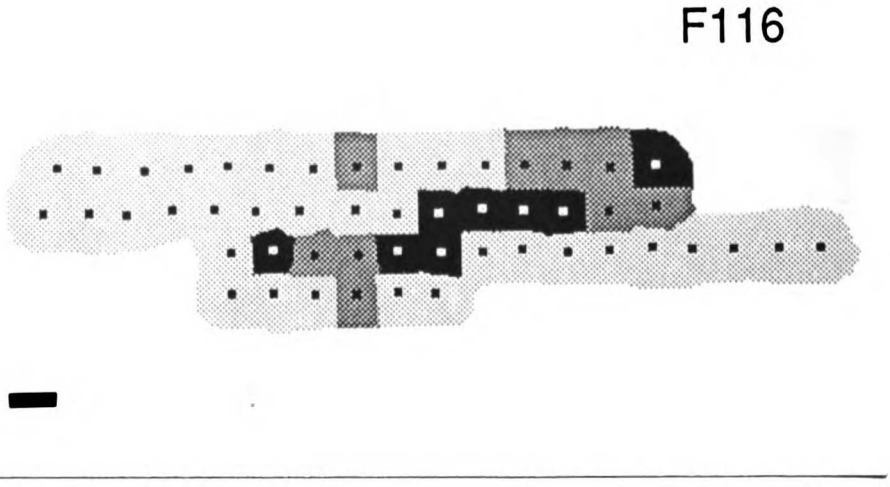
F116

The mapping data were analyzed using a Monte Carlo technique to determine whether the patchy appearance of the maps resulted from significant segregation of the afferents. The degree of segregation was evaluated by counting the number of patches in each map; the more segregated the ON and OFF projections and the larger the patches in relation to the spacing between penetrations, the fewer patches will be found in a given map. For each animal, 500 simulated maps were generated by randomly redistributing the center-types among the penetration sites, and the number of patches in each of these maps was counted. Figure 32 shows the distributions of the numbers of patches obtained from the simulated maps for each animal. In each case, the number of patches found experimentally is at the lower extreme of the distribution of values found for the simulated random cases. The probability of obtaining the experimental results if the afferents were dispersed randomly in the plane of layer IV is less than 0.01 for ferrets F110 and F113 and less than 0.05 for ferret F116.

This Monte Carlo analysis was also applied to the ocular dominance maps from F110 and F116. The third map (F113) contained only one penetration in which units were driven through the ipsilateral eye; simulations would therefore result in patch counts of two for all of the randomly-generated maps. Figure 32 shows the distribution of the number of patches found in 500 computer-simulated maps, for each animal, in which eye preference was randomly reassigned. In both cases, the number of patches found experimentally is outside the range of values generated by the simulations. These results demonstrate that this analysis was capable of confirming non-random organization in a system in which there is independent anatomical evidence for segregation of the afferents.

Figure 32. Monte Carlo analyses of the horizontal organization of the afferents. Distributions of the number of patches obtained in 500 computer simulations for each animal in which center-type (left) or eye preference (right) was randomly redistributed over the penetrations, as described in *Methods*. A *"patch"* was defined as a continuous area in which all penetrations were given the same classification. In each case, the *arrow* shows the number of patches found in the experimentally-obtained surface map; the numbers in the upper right corner give the probablility of the experimentally-obtained value occurring in a cortex in which the geniculocortical afferents were randomly distributed with regard to center-type or eye preference.

CENTER - TYPE

EYE

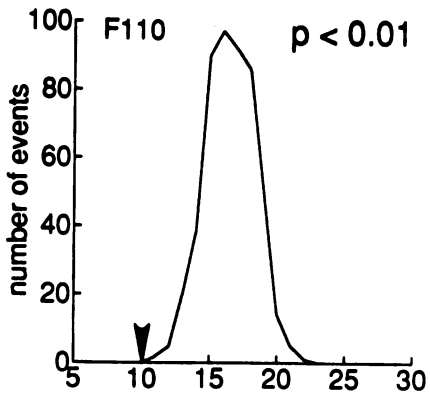

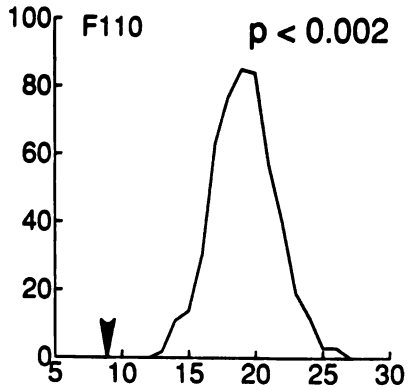

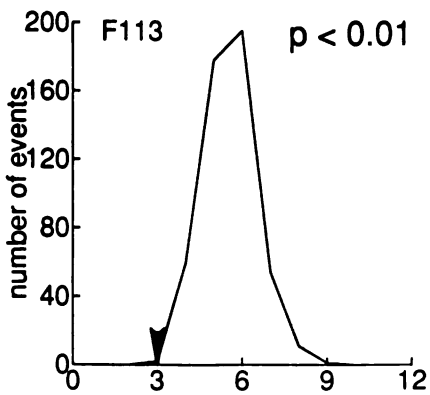

F113

analysis not applicable

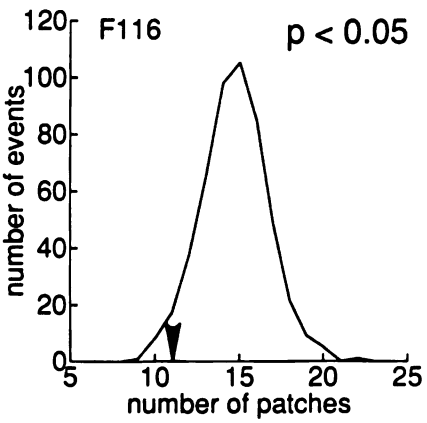

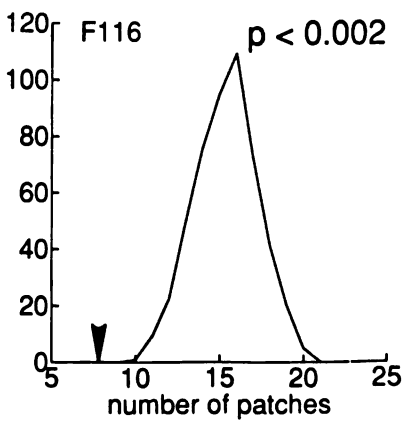

Correspondence of ocular dominance patches and center-type patches.

Eye patches and center-type patches generally do not share the same borders, as can be seen by comparing Figures 30 and 31. When the center-type changed between penetrations, the eye through which responses were elicited usually stayed the same. When the eye through which units were driven changed between penetrations, the center-type usually remained the same.

Patch size.

The complete borders of only a few patches were defined, making it impossible to draw any firm conclusions about the size of the center-type patches. Center-type patches as large as 700 μm across and smaller than 300 μm across were observed. Eye patches ranged from less than 190 μm across to greater than 490 μm across. We considered the possibility that the real patches might be much smaller than those observed when penetrations were spaced at 100-150 μm intervals. If this were the case, the observed patches might result from aliasing. Observations in 2 kainate-treated animals showed that this was not the case. In these two animals, electrode penetrations were made tangential to layer IV, and activity was sampled at 20-μm intervals. The results obtained in one of these animals are shown in Figure 33. The electrode traveled within layer IV in four penetrations. In two of these penetrations, the electrode encountered single- and multiple-units of only one center-type for as long as it remained within layer IV, a distance of 500 μm in Pass 2 and 450 μm in Pass 3. The penetrations shown are in register, so the ON patch traversed in Pass 3 extended at least another 100 μm in the coronal plane, as seen in Pass 4.

Figure 33. Reconstructions of 4 tangential penetrations made into area 17 of a kainate-treated ferret (F113). The multi-unit response at each recording site is represented by a symbol: *open circles* indicate ON-dominated responses (responses rated 1 or 2 on the scale described in the text), *closed circles* represent OFF-dominated (ratings of 6 or 7) responses, and *half-filled circles* represent MIXED (ratings 3, 4, or 5) responses. *Scale bar* = 100 microns. *Inset* shows the angle of the penetration with respect to a coronal section through area 17. *D*, dorsal; *V*, ventral; *L*, lateral; *M*, medial; *A*, anterior; *P*, posterior.

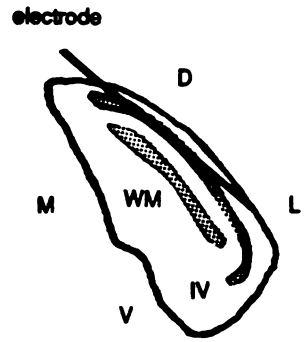
electrode
D
M
WM
L
IV
V

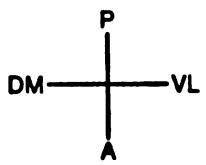
P
DM
VL
A

A final Monte Carlo analysis (see *Methods*) was applied to both the center-type and eye preference data in an attempt to obtain estimates of the sizes of the center-type and ocular dominance patches. Simulated maps were formed by placing the experimentally-obtained maps over a field of parallel stripes, reassigning the response classification of each penetration according to the stripe upon which it fell, and drawing borders around regions with common responses. These simulated maps were similar in appearance to the maps obtained from the experimental data: the maps looked patchy, and, in many cases, unless the periods were very large, there was no hint of the underlying striped pattern. The appearance of the maps was thus seen to depend on where responses were sampled, as well as on the actual organization of the cortex.

If the ON and OFF (or contralateral and ipsilateral) projections are organized into a series of parallel stripes, simulated maps should result in patch counts like those found experimentally when 1) the period of the simulated stripes equals the actual period, and 2) the maps are oriented so the real stripes are aligned with the simulated stripes. Simulations were performed for a set of periods ranging from 100 μm to 3200 μm. Two hundred simulated maps were produced for each period, and the number of patches in each of these maps was counted. A distribution of patch counts was thus produced for each period, and the percentile occupied by the experimentally-obtained patch count was recorded. If the experimental value occurred at a very low percentile, simulations at that period resulted in many more patches than occurred experimentally, and the period was likely to be too small. If the experimental value occurred at a very high percentile, the period was likely to be too large. The range of periods in which the experimental value occurred between the 16^{th} and 84^{th} percentiles ($\pm$ 1 standard deviation) should provide a generous range of estimates for the period of the patches.

We were guided by the anatomical data on ocular dominance columns when interpreting the results of this analysis. In all cases the anatomically-derived estimate of the

period of the ocular dominance columns (approximately 1 mm; Law et al., in preparation) fell into the range of values of the period for which the experimental patch count fell between the 16th and 84th percentiles. However, application of this analysis to some of the maps resulted in a range of estimates for the period that was too large to be useful. Plots of the percentile that contains the experimentally-obtained patch count versus period are sigmoid-like curves that are linear between upper and lower bounds. The slope of the linear part of these curves determines the utility of this analysis: the steeper the curve, the more restricted the range of estimates for the most likely period. When the curves obtained for each animal were compared, it was found that this slope increased as the number of experimentally-observed patches increased.

When estimating the size of the patches from these results, we decided to restrict our attention to those curves with the relatively steep slopes: we chose to consider only the data from maps containing 9 or more patches. This value was chosen, albeit somewhat arbitrarily, for two reasons: first, higher cutoffs, which would have given us a more restricted range of estimates for the period, would have left us with fewer than two curves from which to consider the ocular dominance results, and, second, the estimate of the period of the ocular dominance columns obtained from the two steepest ocular dominance curves is in good agreement with that obtained from anatomical experiments (Law et al., in preparation).

The results of the patch-size analysis are summarized in Table 2. We reasoned that the period for which the experimental value occurred at the 50th percentile of the patch count distribution is the most likely estimate for the value of the real period. From these results, the most likely estimates of the period of the ocular dominance cycle (contralateral-binocular-ipsilateral-binocular) were 950 and 1050 μm. Such values are in good agreement with the sum of the widths of the contralateral (650 μm) and ipsilateral (350 μm) eye patches measured in transneuronally-labelled cortices (Law et al., in preparation). The most likely estimates of the ON-MIXED-OFF-MIXED cycle were between 425 and 800 μm.

Table 2

Patch-Size Analysis

Animal	# patches	16^{th}-84^{th} range (μm)	50^{th} (μm)
Ocular dominance			
F62	13	550 - 1250	950
F110*	9	600 - 1425	1050
Center-type			
F62	22	150 - 550	425
F78	13	100 - 900	550
F116*	11	300 - 1050	700
F110*	10	400 - 1150	800

* Kainate-treated

Table 2: **Patch-size analysis.** A Monte Carlo analysis (see *Methods*) was applied to both the center-type and eye preference data in an attempt to obtain estimates of the sizes of the center-type and ocular dominance patches. Simulated maps were formed by placing the experimentally-obtained maps over a field of parallel stripes, reassigning the response classification of each penetration according to the stripe upon which it fell, and drawing borders around regions with common responses. Simulations were performed for a set of periods (complete cycle of ON-MXED-OFF-MIXED or CONTRALATERAL-BINOCULAR-IPSILATERAL-BINOCULAR) ranging from 100 μm to 3200 μm. Two hundred simulated maps were produced for each period, and the number of patches in each of these maps was counted. A distribution of patch counts was thus produced for each period, and the percentile occupied by the experimentally-obtained patch count was recorded. The first column gives the animal from which surface maps were obtained, and the second column shows the number of patches found experimentally. Only the maps from which 9 or more patches were found experimentally are considered (*see text*). The third column gives the range of periods in which the experimental value occured between the 16^{th} and 84^{th} percentiles ($\pm$ 1 standard deviation). The fourth column gives the the period in which the experimental value occurred at the 50^{th}- percentile, the most likely estimate of the period of the cycle. The upper part of the table summarizes the results of the analysis of the size of the ocular dominance patches, while the lower half shows the results for the center-type patches.

Discussion

Recordings of afferent terminals within area 17 of kainate-treated cortices revealed that the axons of on-center and off-center geniculate cells are found in separate patches in the plane of layer IV. These recordings also confirmed the segregation of afferents serving the contralateral and ipsilateral eyes that had been previously observed using anatomical tracing techniques (Law et al., in preparation).

Did kainate treatment allow mapping of geniculocortical afferent organization?

Evidence presented in *Results* indicates that the recordings obtained were from geniculocortical afferents. There is no reason to doubt that the recordings sampled from the normal complement of afferents. We cannot, exclude, however, the possibility that a sub-population of afferents was damaged by kainic acid and rendered unresponsive or inaccessible to the electrode.

It is also possible that the geniculocortical arbors were reshaped as a consequence of the changes induced in the membranes of their target cells by kainate treatment. A reorganization of the retinogeniculate afferents has been reported following degeneration of their geniculate target cells after ablation of visual cortex (Ralston and Chow, 1973). However, these changes occurred after much longer times (4 - 12 months) than were allowed in the present, acute experiments. It also seems likely that any such reorganization would obscure, rather than create the illusion of, patches. Perhaps the strongest evidence that the results obtained in the kainate-treated cortices are not artifactual is that the ocular dominance data are completely consistent with anatomical results in normal cortices: the size of the ocular dominance patches, the relative sizes of projections serving the contralateral and ipsilateral eyes, and the degree of overlap between afferents serving the two eyes are exactly what would be expected from transneuronal-

labelling studies (Law et al., in preparation). Thus, it is likely that the distribution of the afferents found in kainate-treated cortices accurately reflects the normal organization of the afferents.

How segregated are the ON and OFF afferents? Monte Carlo analyses of the surface mapping data allowed us to reject a Null Hypothesis that the afferents are randomly-dispersed in the plane of layer IV with greater certainty for the ocular dominance maps ($p < 0.002$ in the two cases in which the analysis was applicable) than for the center-type maps ($p < 0.01$ for two of the maps, $p < 0.05$ for the third map). There are at least two possible explanations for this difference.

First, afferents may indeed segregate more nearly completely on the basis of ocular dominance than on the basis of center-type. Since the eye-specific geniculate laminae are more sharply-defined anatomically than are the center-type leaflets, the terminal zones of the laminae within layer IV (eye patches) might be expected to be more distinct than the terminal zones of the leaflets (center-type patches). This hypothesis is unlikely, since only 9 % of the penetrations from the surface mapping experiments were classified as MIXED, while 12% were classified as binocular. Overlap between the patches serving the contralateral and ipsilateral eyes has previously been inferred from measurements of the volume of layer IV labelled autoradiographically after an injection of ^{3}H-proline into an eye: in the hemisphere contralateral to the injected eye, approximately 77% of the most binocular region of area 17 was occupied by label, while 49% of the corresponding region was labelled ipsilaterally. The sum of these 2 figures, 126%, would indicate that there is some degree of overlap between afferents serving the two eyes, although the precise extent of this overlap cannot be deduced from such measurements made in different hemispheres.

Alternatively, the difference in the results of the Monte Carlo analyses may arise because the center-type patches are smaller than the ocular dominance patches. A given area of cortex would then be likely to contain more center-type patches than ocular dominance patches, as was indeed the case in all 5 surface maps from both the normal and kainate-treated ferrets. Our measure of segregation, the number of patches per map, depends on the size of the patches relative to the area mapped. Because relatively small areas of cortex were mapped in these experiments, the Monte Carlo analysis could not so strongly demonstrate segregation for the center-type patches as for the ocular dominance patches. This hypothesis is likely to be correct, since the results of the Monte Carlos analyses of the patch sizes yielded larger estimates for the period of the ocular dominance cycle than for the period of the center-type cycle.

Patch sizes. The Monte Carlo analysis of the patch sizes is based on the assumptions that 1) the patches can be modeled as a series of parallel stripes, in which afferents of opposite types occupy alternate bands with some areas of overlap, and 2) the relative widths of these bands is reflected in the proportions of the responses sampled.

The first assumption is probably valid for the ocular dominance patches, which do appear as a series of roughly parallel bands in reconstructions of transneuronally-labelled cortices (Law et al., in preparation). We do not know how the center-type patches are patterned. However, even if the center-type patches do not appear as a series of parallel stripes throughout the extent of area 17, stripes may be a good approximation of their appearance over the small areas of cortex mapped. This would be true, for example, for the orientation maps revealed with 2-deoxyglucose (Hubel et al., 1978) or voltage-sensitive dyes (Blasdel and Salama, 1986).

The second assumption also seems to be valid for the ocular dominance stripes. As mentioned above, 63% of the penetrations in the surface maps in kainate-treated cortices were classified as contralateral-dominated, 24% were classified as ipsilateral-dominated, and 13%

were classified as binocular. For an ocular dominance cycle with a period of 1 mm, the contralateral stripes would have a width of 630 μm, ipsilateral stripes would have a width of 240 μm, and areas of overlap (binocular) would be 65 μm wide. If such stripes were measured in a transneuronal labelling experiment, labelled bands 695 μm wide would be seen contralateral to the injected eye, and bands 305 μm wide would be seen in the hemisphere ipsilateral to the injection. These values are in fairly good agreement with those measured experimentally: labelled bands contralateral to the injected eye were 650 μm wide, while bands ipsilateral to the injection were 350 μm wide in material prepared by Law et al. (in preparation). The ratio of the width of contralateral patches to the width of the ipsilateral patches is 2.3 for the stripe analysis and 1.9 for the labelled cortices, values differing by only 22%.

This analysis appears to yield estimates for the period of the ocular dominance patches that were in good agreement with the period measured on transneuronally-labelled cortices: the analysis yielded a range of 950 - 1050 μm for each contralateral-binocular-ipsilateral-binocular cycle, consistent with the sum of the widths of the ocular dominance patches labelled contralateral (650 μm) and ipsilateral (350 μm) to an eye which had been injected with ^{3}H-proline. However, this estimate of the period of the cycle may be slightly large; as mentioned above, it has been concluded from the anatomical data that there is some overlap between the patches serving the contralateral and ipsilateral eyes.

We also expect the Monte Carlo analysis to err towards overestimating the patch sizes. The number of patches obtained by rotating the maps on a field of parallel stripes is affected by the shape of the maps: the more elongate the maps in the direction *parallel* to the stripes, the more inaccurate will be the number of patches. It can be seen by examining Figure 30 that most of our maps are elongated along the lateral-medial axis. This direction of elongation is approximately perpendicular to the ocular dominance stripes, which run rostro-caudally in this

region of the cortex (Law et al., in preparation). We therefore expected that the analysis would yield accurate estimates for the period of the ocular dominance patches, which appears to be the case. We do not yet know the orientation of the maps relative to the orientation of center-type stripes or patches. For the worst case, in which the actual patches are elongated parallel to the long axis of the map, the mean number of patches obtained from the simulations will equal ((0.636 X L/W)) - 1) X (actual number of patches), where L is the length and W is the width of the map. When L/W is equal to 2.0, the simulations result in a mean number of patches 1.9 times greater than the real number; when L/W is equal to 3.0, the simulations err by a factor of 2.5.

This analysis resulted in a considerable range of estimates for the size of the center-type patches. We conclude from these results that the period of an ON-MIXED-OFF-MIXED cycle is on the order of hundreds of microns rather than tens of microns or millimeters, most likely between 425 and 800 μm. Center-type patches therefore are smaller than ocular dominance patches. A second conclusion to be drawn from this analysis is that more refined estimates of the patch sizes require the construction of much larger maps. Additional maps of the same size as those already obtained would not help answer this question. Since the maps from F110 and F116 are as large as we are able to construct during the time allowed by the kainate blockade, we believe that further progress on this question will require new techniques.

Relative sizes of the ON vs. OFF and contralaterally-driven vs. ipsilaterally-driven geniculocortical projections. The results of these experiments suggest that there may be a larger ON than OFF projection from ferret LGN to cortex. In the animals used to study the vertical organization of the afferents, 158 (55%) ON units and 131 OFF (45%) units were recorded. In the surface mapping experiments, the aggregate activity in a total of 73 (56%)

penetrations was classified as ON, 45 (35%) penetrations were classified as OFF, and 12 (9%) penetrations contained nearly equally mixed ON and OFF activity. Such findings are consistent with the results of multi-unit recordings in the A laminae of the LGN in which more ON-dominated sites (151, 62%) were encountered than OFF-dominated sites (81, 33%). The remaining sites, found at the borders between leaflets, had mixed ON/OFF activity (Stryker and Zahs, 1983).

Recordings in kainate-treated cortices also revealed a predominance of afferents serving the contralateral eye, even though such recordings were all well within the binocular segment of area 17. In the surface mapping experiments, 82 (63%) penetrations were classified as contralateral-dominated, 31 (24%) were classified as ipsilateral-dominated, and 17 (13%) penetrations were approximately equally binocular. Such contralateral dominance is consistent with the results of the transneuronal labelling experiments mentioned above, as well as with the finding in intact cortices that 2 to 4 times as many multi-unit recording sites are dominated by the contralateral eye as are dominated by the ipsilateral eye, depending on the region of the binocular segment in which responses are sampled (Law et al., in preparation).

General organization of center-type and ocular-dominance patches. The experiments reported here were limited to a small area on the dorsal exposed surface of area 17, a region representing the central 15 deg of azimuth and -5 to -20 of deg elevation. The pattern of of the ON and OFF patches throughout area 17 was not accessible using present electrophysiological methods: the duration of the kainate-induced blockade of cortical cell activity is insufficient to allow us to map large areas of the cortex. In previous studies (Law et al., in preparation), the pattern of ocular dominance patches throughout area 17 was made apparent using transneuronal labelling techniques. No such purely anatomical technique appears to be available to exclusively label the terminals of either the ON or OFF geniculocortical axons. We are

currently attempting to selectively label the OFF geniculocortical projection by combining the 2-deoxyglucose technique with administration of 2-amino-4-phosphono butyric acid, a glutamate analog that selectively blocks the ON retinogeniculate pathway (Schiller, 1982; Horton and Sherk, 1984).

Within the areas of cortex mapped in this study, the center-type patches and ocular dominance patches generally do not share the same borders. This independence of center-type and ocular dominance patches is similar to that which has been reported for ocular dominance and orientation columns in macaque striate cortex (Hubel et al., 1978). Such an arrangement would allow each point in the visual field to be represented by both on-center and off-center afferents and, within the binocular segment, afferents serving both the contralateral and ipsilateral eyes. Complete coverage of the visual field by both ON and OFF cells occurs among the alpha ganglion cells in the cat's retina: each retinal point is covered by the dendritic tree of at least one on-center and one off-center alpha retinal ganglion cell (Wassle et al., 1981). It is reasonable to suppose that this coverage is maintained in the projection from retina to LGN, and then from LGN to cortex.

A question that arises is how the visuotopic maps within the ON and OFF and contralateral-eye and ipsilateral-eye projections interdigitate. Within a single penetration, regions of the visual field represented by ON afferents and OFF afferents are often largely non-overlapping. This disparity is to be expected if the organization of the cortex is a compromise between maintaining retinotopy and segregating the ON and OFF (or contralateral and ipsilateral) afferents. Within each patch, there should be an orderly progression in receptive fields until the border with the next patch is reached; the microtopography should then be repeated in the new patch. Unfortunately, the surface mapping results do not shed any light on this question; the scatter in receptive field locations within a penetration prevents the construction of accurate topographic maps from the few multi-unit responses recorded at the top

of layer IV. A similar displacement in the receptive field locations of cells driven by the contralateral and ipsilateral eyes has been observed at the borders between ocular dominance columns in layer IV of monkey striate cortex, and the size of this displacement has been shown to be a function of the widths of the columns and the local magnification factor (Hubel et al., 1974).

Now that we are able to map the distribution of geniculocortical afferents, it is exciting to consider the kinds of questions that can be addressed in the future: which aspects of cortical organization are determined by the organization of the afferents and which come about through intracortical connections? For example, single cortical cells can exhibit excitatory responses to both light onset and light offset. Although it is likely that cortical cells in layer IV are in a position to receive convergent input from ON and OFF afferents, as will be discussed in the next chapter, it is possible that the on and off responses of single cortical cells come about through intracortical connections. Another question, prompted by the observation that there is scatter in the receptive-field locations of neighboring afferents, is whether the topographic organization of the afferents is less orderly than is the topographic organization of the cortical-cell receptive fields. More detailed mapping of the receptive fields of both the afferents and the cortical cells is required to answer this question.

These results, together with the results reported in Chapter 4, demonstrate that ON-center and OFF-center cells are segregated within the lateral geniculate nucleus of the ferret, and that this segregation is maintained in the geniculocortical projection. The significance of these findings will be discussed at length in the final chapter.

Chapter VI

Conclusions and Discussion

Since Guillery and colleagues (Linden et al., 1981) drew attention to their potential value as subjects for developmental studies, ferrets have become increasingly popular models in investigations of the mammalian visual system. The studies reported here characterized several aspects of the organization of the primary visual system of adult ferrets. In particular, we were interested in the functional definition of the geniculate sublaminae, and in the pattern of the projections of these sublaminae to primary visual cortex. Additional experiments examined the topographic organization of the lateral geniculate nucleus and primary visual cortex of adult ferrets.

The lateral geniculate nucleus (LGN) and primary visual cortex (area 17) each contain a single orderly representation of the contralateral visual hemifield. Both the LGN and area 17 contain expanded representations of the central visual field and large and accessible monocular segments. Although the topographic mapping studies did not yield any unexpected results, they are prerequisites to more interesting work on the development and organization of the ferret's primary visual system.

Electrophysiological recordings revealed that the geniculate sublaminae represent the segregation of on-center cells and off-center cells. Segregation is preserved in the projection from geniculate to cortex: the ON and OFF geniculocortical axons terminate in separate patches in the plane of layer IV. Ferrets also have ocular dominance patches in area 17, as revealed by transneuronal labelling experiments (Law et al., in preparation) and further demonstrated by the recordings of geniculocortical afferents described here. Thus, in ferrets, the center-type sublaminae segregate their projections to cortex in the same manner as do the eye-specific laminae.

These results raise questions concerning the significance of segregating on-center and off-center cells in separate geniculate sublaminae and of segregating the ON and OFF geniculocortical projections. This chapter contains speculations about two such questions: 1) What are the functional consequences, if any, of maintaining anatomically separate ON and OFF channels in the retinogeniculocortical pathway? and 2) How does such segregation of the ON and OFF pathways arise during development?

During the period in which these experiments were conducted, separate ON and OFF channels have been described in the primary visual system in several other species. In attempting to understand the significance of the results reported here, it is useful to compare the organization of the ON/OFF channels in ferrets to that in other species and to consider the organization of the receptive fields of the cortical neurons of each species.

ON and OFF channels in the primary visual systems of other species.

Mink. Mink, like ferrets, are members of the genus *Mustelidae.* The organization of the mink's LGN appears to be identical to that of the ferret's LGN, except that the cellular sublamination is more distinct in minks than in ferrets (Guillery, 1971; Sanderson, 1974; Linden et al., 1981; LeVay and McConnell, 1982; Stryker and Zahs, 1983). Thus, ON and OFF sublayers alternate within the A laminae of the LGN in the two species of mustelids studied. This organization is illustrated schematically in Figure 34.

McConnell and LeVay (1984) recorded afferent activity in area 17 of mink after microinjections of kainic acid into the cortex and observed at least a partial segregation of the ON and OFF afferents. Their results are consistent with a patchy, rather than sublaminar, segregation of the geniculocortical axons into separate ON and OFF domains within layer IV.

LeVay and his colleagues (1987) have recently examined the receptive field organization of cortical cells in area 17 of minks. Nearly all cortical cells were orientation-selective, and most cells could be classified as simple (having receptive fields composed of one or more spatially-distinct ON or OFF excitatory subfields) or complex (excitatory response to light onset or light offset throughout the cell's receptive field), using the terminology of Hubel and Wiesel (1962). Simple cells comprised the majority of cells studied in layers IV and VI; complex cells predominated in layers II + III and V, while the simple cells found in these layers were found near the border with layer IV.

This study also addressed the question of the contributions of ON and OFF geniculate input to cortical-cell responses. LeVay et al. recorded from single cortical units and assessed the relative strengths of the responses to the onset and offset of light slits presented in various regions of the receptive field. Half of the units studied responded at least twice as vigorously to one sign of contrast as to the other, and 15% of the units showed quite a strong (9X) preference. Units with a common contrast preference were reported to be arranged in columns.

Tree shrews. There are separate ON and OFF channels in both the retinogeniculate and geniculocortical projections in the tree shrew (genus *Tupaia*), but the organization of these projections differs from that observed in mustelids. The LGN of the tree shrew contains six cellular laminae; laminae 1 and 5 (using the conventions of Brunso-Bechtold and Casagrande, 1982) receive input from the ipsilateral eye, and the remaining layers receive projections from the contralateral retina. Layers 3, 4, and 5 contain OFF-center cells, layers 1 and 2 contain ON-center cells, and layer 6 contains a mixture of ON-center, OFF-center, and ON-OFF cells (Conway and Schiller, 1983). Thus, cells of the same center-type are found in adjacent layers of the LGN, as illustrated schematically in Figure 34.

The ON and OFF layers of the LGN project to separate strata of layer IV. Using anatomical tracing techniques, Conley et al. (1984) showed that LGN layers 4 and 5 (OFF)

Figure 34. Comaparison among species of center-type organization of the primary visual system. Schematic illustration of the locations of ON-center and OFF-center cells within the LGNs of several species (*lower*), and of the patterns of termination of the ON and OFF geniculocortical axons within layer IV of primary visual cortex (*upper*). In all cases, *white* areas are regions of ON-dominated activity, *black* areas are regions of OFF-dominated activity, and *shaded* areas are regions of MIXED ON and OFF activity. *FERRET, MINK*: ON and OFF cells are found in different sublayers of the A laminae of the LGN (ferret, present study; mink, LeVay and McConnell, 1982). Geniculocortical afferents terminate in ON and OFF patches, similar to ocular dominance patches, in the plane of layer IV. *TREE SHREW*: ON and OFF cells are found in different layers of the LGN (Conway and Schiller, 1983). ON and OFF geniculocortical afferents are stratified within layer IV (Conley et al., 1984; Kretz et al., 1986). Numbering of geniculate laminae using the conventions of Brunso-Bechtold and Casagrande, 1982. *MACAQUE*: OFF cells are found in the ventral parvocellular layers of the LGN; ON cells are found in the dorsal parvocellular layers (Schiller and Malpeli, 1978). The distribution of ON and OFF geniculocortical afferents within layer IV has not been directly examined in this species. *CAT*: Distribution of ON and OFF activity within the LGN is controversial (*see text*). ON and OFF geniculocortical afferents are intermingled in layer IV of striate cortex (LeVay et al., 1987).

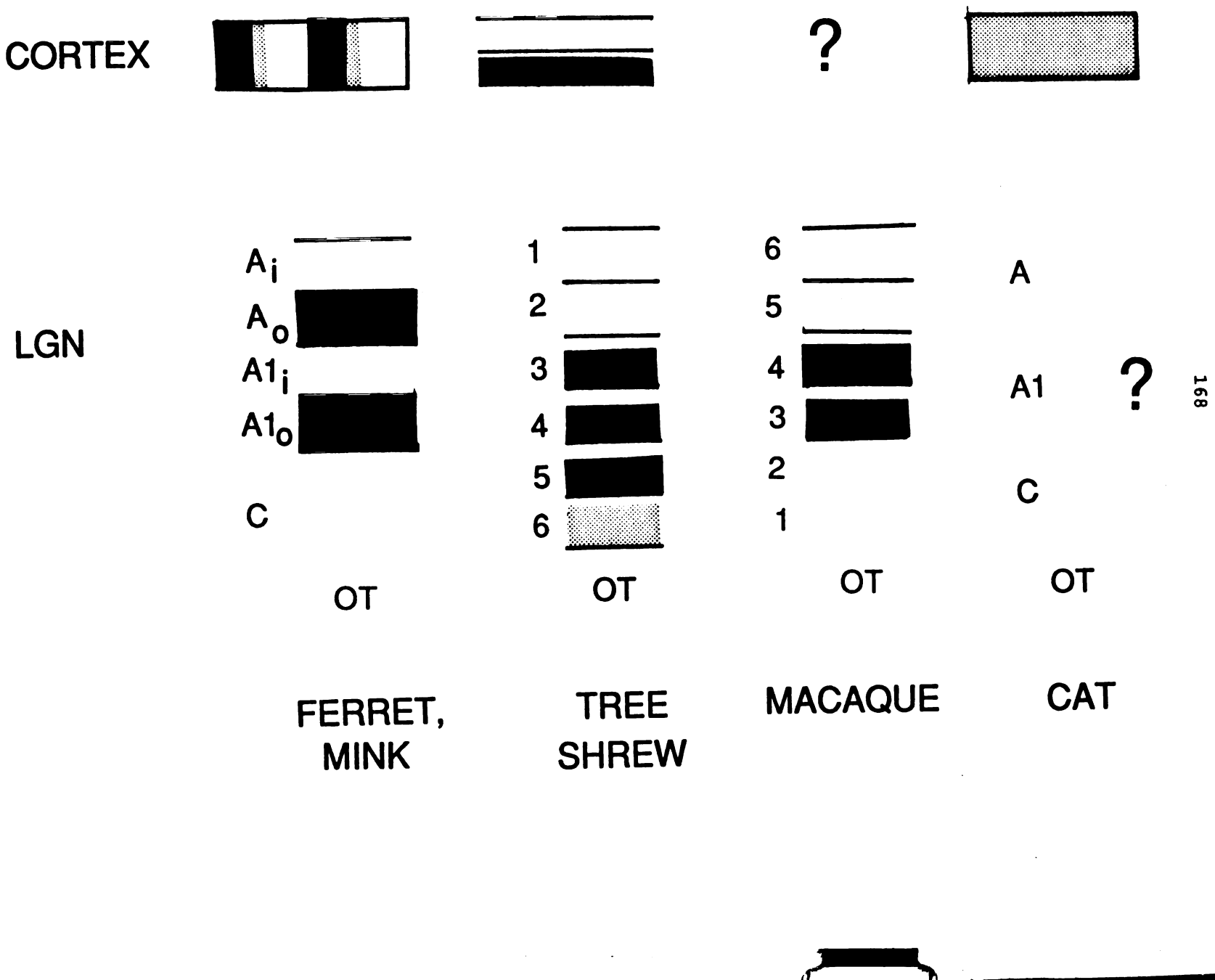
CORTEX
?
LGN
A_i
A_o
$A1_i$
$A1_o$
C
1
2
3
4
5
6
6
5
4
3
2
1
A
A1
?
C
OT
OT
OT
OT
FERRET, MINK
TREE SHREW
MACAQUE
CAT
168

project to cortical layer IVb, and layers 1 and 2 (ON) project to layer IVa. Electrophysiological recordings from cortical neurons revealed that cortical cells in layer IVa respond to the onset of light, while cells in IVb respond to light offset (Kretz et al., 1986). Thus, ON and OFF channels remain separate at least up to the level of the first synapse in the primary visual cortex of tree shrews. It is interesting to note that tree shrews do not have ocular dominance columns in the cortex, but that there is some vertical separation of the geniculocortical afferents subserving the two eyes: While most cells in layer IV are binocular, there is an absence of ipsilateral eye responses from the region of the cell sparse cleft between layers IVa and IVb (Kretz et al., 1986).

It is not possible draw any conclusions about the laminar distribution of receptive-field classes from the published studies of responses of cells in the cortex of the tree shrew. Kaufmann and Sonjen (1979) studied the receptive field properties of neurons within area 17 of the tree shrew and reported that most cells were orientation-selective and could be classified as either simple or complex. The laminar distribution of receptive field types was not reported, however. Kretz et al. (1986) used only flashing spots as stimuli and recorded multi-unit responses in layer IV.

Macaque. On-center cells and off-center cells are found in separate laminae in the macaque's lateral geniculate nucleus, but there is no evidence that this segregation is maintained in the projection from LGN to cortex.

The LGN of the macaque contains two ventral magnocellular laminae (one for each eye) and four parvocellular laminae in the portion of the nucleus representing the central 15-20 deg of the contralateral visual hemifield. The parvocellular layers contain color-opponent cells. The dorsal pair of parvocellular laminae contain mostly red or green ON-center cells. The majority of cells in the ventral pair of parvocellular layers are red or green OFF-center cells, although blue ON cells are found only in the ventral parvocellular layers. (See Figure 34.) In

the four-layered portion of the LGN, there is only one magnocellular and one parvocellular layer for each eye. Each layer contains both ON and OFF cells, but layering of ON and OFF cells within each parvocellular lamina may occur (Schiller and Malpeli, 1978).

Simple, complex, and hypercomplex cells are found in the macaque's striate cortex, and most cells are orientation-selective (Hubel and Wiesel, 1968). However, within layer IV, there exists a population of units with receptive fields with color-opponent, center-surround organization; it is possible that these units are geniculocortical axons.

Cat. Although there is not an obvious segregation of ON-center and OFF-center cells in the LGN of the cat (Sanderson, 1971), a functional segregation of ON and OFF channels is still present in the retinogeniculate projection. Individual relay cells in the LGN appear to receive input from retinal ganglion cells of only one center-type (Hubel and Wiesel, 1961; Cleland et al., 1971; Mastronarde, 1983; Horton and Sherk, 1984). A partial layering of ON and OFF responses in the cat LGN has more recently been reported, with ON responses being more common near the tops of the layers (Bowling, 1983; Bowling and Schoel, 1983). In addition, the terminal arbors of Y-OFF retinal ganglion cells have been found to have more boutons in the lower halves of the A laminae than in the upper halves (Bowling and Michael, 1984). Other investigators have reported a segregation of ON and OFF geniculate cells into columns normal to the laminar borders (Naporn et al., 1985). This matter remains to be resolved. Interestingly, a non-uniform pattern of labelling of retinal afferent terminal arbors is seen in the LGNs of embryonic cats in which microinjections of horseradish peroxidase (HRP) are made into the optic tracts (Sretevan and Shatz, 1987). Terminal arbors appear as patches elongated normal to the laminar borders; labelled regions are separated by non-labelled gaps. A similar pattern of labelling has been observed after bulk injections of HRP into the optic tracts of adult cats (Mason and Robson, 1979). While the significance of this pattern is not known, it is tempting to speculate that it represents the labelling of axons of similar functional type that

travel together within the optic tract. The retinogeniculate projection could then be thought of as a series of interdigitating maps formed by axons of different types (Sretevan and Shatz, 1987).

In cats, the terminals of ON and OFF geniculocortical axons intermingle within layer IV of area 17, as demonstrated by recordings from geniculate afferents in kainate-treated cortices (LeVay et al., 1987). These authors also carefully examined the ON and OFF responses of cortical neurons in cat striate cortex using the same methods described earlier for mink: flashing bar stimuli were presented over discrete regions of a cell's receptive field; the responses to light onset were then averaged over all regions of the receptive field and compared to a similarly-derived measure of the response to light-offset. Sixty-seven per cent of the units studied showed less than a 2:1 preference for one sign of stimulus contrast over the other, and only 4% responded almost exclusively to either the onset or offset of a light stimulus. There did not appear to be any tendency for cells with similar contrast preferences to cluster in this species.

Neurons within area 17 may be classified as simple, complex, and hypercomplex. Simple cells are found in cortical layers III, IV, and VI, while complex cells are found in layers II, III, V, VI, and rarely, in layer IV (Hubel and Wiesel, 1962).

Functional significance.

The inter-species variability in the pattern of organization of the ON and OFF channels raises several questions about the functional significance and development of each pattern. There does not appear to be a simple correspondence between the pattern of the geniculocortical projection and the receptive-field types of the cortical neurons in area 17: orientation-selective

simple, complex, and hypercomplex cells are found in all of the species reviewed above, despite major differences in the organization of the geniculate laminae and the pattern of geniculocortical terminations of ON and OFF cells. However, differences in the proportions and laminar distribution of each cell type and subtle differences in the organization of cells with different types of subfields may not have been revealed in most of the studies cited. LeVay et al. (1987) have reported just such species-differences in cats and minks: cortical neurons with similar contrast preferences cluster in minks but not in cats.

Schiller and Malpeli (1978) have suggested that the segregation of on-center cells and off-center cells into separate geniculate laminae would permit the selective modulation of ON and OFF cells by non-retinal inputs to the LGN. LeVay, et al. (1987) have proposed that a similar explanation could apply to the ON and OFF patches in the cortex.

The parcelling of layer IV into separate ON and OFF domains would provide a convenient anatomical substrate for the construction of simple-cell receptive fields according to the model originally proposed by Hubel and Wiesel (1962). However, as attractive as this proposal is, a patchy distribution of on-center and off-center afferents is clearly not necessary for the formation of such receptive fields: ON and OFF axons appear to be intermingled in layer IV of area 17 of the cat (LeVay et al., 1987), the species in which "simple" receptive fields were originally described.

The present experiments do not address the question of whether the ON and OFF geniculate axons converge onto single cortical neurons in ferrets. However, three observations suggest that some convergence does occur: 1) In untreated ferrets, where cortical cells contributed significantly to the multi-unit activity, recordings in layer IV yielded many more mixed ON-OFF responses than did recordings from kainate-treated animals. 2) Ferrets have cortical simple cells with receptive fields with ON and OFF subfields (Waitzman and Stryker, unpublished observation). The simple cells of cats and monkeys appear to receive convergent

excitation from ON and OFF geniculate cells (Tanaka, 1983, 1986; Malpeli et. al, 1981; Schiller, 1982; Sherk and Horton, 1984), as discussed below. However, cortical units with a single excitatory "subfield", either ON or OFF, are encountered more frequently in ferrets than in cats (Waitzman and Stryker, unpublished observation), suggesting that some cortical cells do receive input from only one type of geniculate axon. 3) Consideration of the likely patch sizes suggests that many single neurons within layer IV should be in a position to receive input from both ON and OFF geniculate afferents. Estimates of the most likely width of the ON patches are between 239 and 449 μm, the width of the OFF patches is estimated to be between 147 and 277 μm, and estimates of the width of the regions of overlap range from 20 to 37 μm. In cats, the dendritic-field diameters of the of the spiny stellate cells in layer IV, believed to be the geniculate-recipient cells, are on the order of 200 to 300 μm (Kelley and Van Essen, 1974; Gilbert and Wiesel, 1979; Martin et al., 1984). These cells have not been measured in ferrets, but, for now, let us assume that they are about the same size in ferrets as in cats. If the width of the OFF patches is at the upper end of the estimated range, only those cortical neurons located in the center of a patch of OFF afferents will be accessible to OFF afferents exclusively; if the actual width of the OFF patches is at the lower end of this range, no geniculate-recipient neurons should be accessible to only OFF afferents. There is a greater chance that a geniculate-recipient cell will be accessible only to ON afferents, but, in this case as well, if the patch sizes are at the lower end of the estimated range, only those cortical neurons located in the middle of a patch of ON afferents should receive input from ON afferents exclusively. This situation is analogous to that of the ocular dominance columns: although the geniculocortical afferents serving the two eyes terminate in separate patches, most neurons in area 17 are binocular (Law et al., in preparation).

The contributions of ON and OFF geniculate input to the responses of cortical neurons has been studied directly in cats and macaques, neither of which has anatomically distinct ON

and OFF geniculocortical projections. The results obtained in these species indicate that both ON and OFF geniculate cells contribute to the responses of single cortical neurons. Conversely, the results of psychophysical experiments in humans and monkeys imply that there are separate channels for processing light and dark stimuli. Experiments of both types will be reviewed below.

Electrophysiology. Convergent excitation from ON and OFF LGN cells onto single cortical neurons in cat striate cortex has been demonstrated using a cross-correlation analysis applied to responses recorded simultaneously in area 17 and the LGN (Tanaka 1983, 1986). Of the five simple cells studied in striate cortex, Tanaka was able to demonstrate convergence of both on-center and off-center LGN cells onto one cortical neuron; the receptive fields of the ON and OFF geniculate cells did not overlap. Input from only one center-type of LGN cell was demonstrable for the remaining four simple cells; since he was only able to demonstrate correlated activity for 2 - 5 geniculate cells for each cortical cell, Tanaka believed that the finding of only one type of geniculate input was due to "technical limitations" of the experiment. However, on-center and off-center geniculate cells were found to converge onto 5 of 8 standard-complex cells studies; in this case, the geniculate cells had overlapping receptive fields. The delay times between the geniculate and cortical cell responses were not reported for these particular geniculate cell-striate cell pairs, so it is not clear whether these convergent inputs represented monosynaptic excitation from LGN to cortex. However, Tanaka did report that, of 82 geniculate cell-striate cell pairs that exhibited positive correlations in their responses to light stimuli, most (80%) pairs had delay times that were consistent with a monosynaptic connection. The laminar distribution of the cortical cells was not reported for these particular cells, but for Tanaka's larger sample , 9/10 simple cells were found in layers IV and VI, 1/10 was found in layer II+III; 7 standard-complex cells were found in layers II+III, V, and VI; 7

special-complex (no length summation) in layer V; 3 E_{on} (exclusively ON response to flashing stimuli in the receptive field) or E_{off} cells were all in layer IV.

In several other experiments, ON or OFF geniculate cells were selectively inactivated, and the effects on cortical responses were studied. Intraocular injections of 2-amino-4-phosphonobutyric acid (APB), a glutamate analog that eliminates the responses of ON-bipolar cells (Slaughter and Miller, 1981), were used to deactivate the ON channels in monkeys (Schiller, 1982) and cats (Horton and Sherk, 1984). Single-unit recordings in the LGN revealed that ON-center geniculate cells lost both their ON-center and OFF-surround responses after such treatment in both species. Single-unit recordings of neurons in the striate cortex also yielded similar results in the two species: light edge responses were reduced or eliminated in most cortical cells while dark edge responses persisted (monkeys, Schiller, 1982; cats, Sherk and Horton, 1984). The results of these studies do not require convergent monosynaptic excitation from ON and OFF channels through the LGN; they could also be accounted for by convergence of the ON and OFF geniculate input via cortical neurons. These results confirmed the results of an earlier study in which microinjections of a local anesthetic were used to selectively block the activity of specific LGN laminae in monkeys: injections of lidocaine into the dorsal parvocellular layers of the LGN drastically reduced the light-edge responses of cortical neurons, while inactivation of the ventral parvocellular layers reduced the dark-edge responses (Malpeli et al., 1981).

Psychophysics. The electrophysiological experiments discussed above demonstrate that many single neurons in striate cortex receive convergent excitation from the ON and OFF channels through the LGN. However, there is evidence from human and animal psychophysical studies that channels for processing light-incremental and light-decremental stimuli remain at least partially independent.

Studies of the "frequency shift effect" in humans have lead to the conclusion that adaptation to the light bars of grating stimuli proceeds independently of adaptation to the dark bars (DeValois, 1977; Burton et al., 1977). After viewing a grating of black and white bars, human subjects were presented with another grating and asked to adjust the widths of the bars to match the frequency of the adaptation stimulus. When square wave gratings were used, the perceived spatial frequency of the test grating was higher than its actual spatial frequency following exposure to an adaptation grating of a lower spatial frequency (Blakemore et al., 1970). If rectangular wave gratings were used, and subjects were asked to independently adjust the black and white bars of the test grating (Burton et al.,1977) or to match the widths of test bars rather than gratings (DeValois, 1977), black bars and white bars were shifted in apparent width independently of each other. These results do not depend on the segregation of ON and OFF inputs to the cortex; they can also be explained by proposing that cortical neurons with receptive fields composed of different arrangements of subfields feed separate channels through the cortex.

Schiller, et al. (1986) have provided more compelling evidence that there are at least partially separate channels through cortex that originate from the on-center and off-center retinal ganglion cells. These authors found that intraocular injection of APB impairs the ability of monkeys to detect light-incremental, but not light-decremental, stimuli.

There are few published reports of how the ON and OFF geniculocortical projections interact in the cortex in species in which there is anatomical separation of these pathways. In tree shrews, single cortical neurons in layers III and V give both ON and OFF responses to flashing stimuli, implying that the ON and OFF channels converge in these layers (Kretz et al., 1986). Most cortical neurons in ferrets and mink respond to both light onset and light offset, suggesting that the ON and OFF pathways through the LGN also converge in the cortex in these species. It is possible that the surround responses of their geniculate inputs underly the cortical

responses to one polarity of stimulation; recordings of cortical responses after intraocular injections of APB should answer this question. As mentioned above, segregation of the ON and OFF geniculocortical projections could have subtle effects on cortical organization; such effects might have consequences for visual processing that are not detectable with electrophysiological recordings of single- or multi-unit responses. An investigation of the organization of ON and OFF channels in more species might reveal some correlation between the animals' visually-guided behavior and the pattern of the ON and OFF projections from retina to LGN and/or LGN to striate cortex.

Development.

It is also possible that the segregation of on-center and off-center cells into separate geniculate laminae and/or the segregation of the geniculocortical axons in the cortex are functionally neutral consequences of developmental mechanisms that exist for other purposes. For example, a mechanism that strengthens simultaneously active afferent inputs to a common post-synaptic cell may have been selected for because it refines topographic maps. This mechanism could also cause ON/OFF segregation, which might have no adaptive significance or particular importance for visual processing. Alternatively, it might not matter functionally precisely how things are segregated, but economy of connections may make it advantageous for segregation to take place, as suggested by Hubel and Wiesel (1962).

The similar organization of the eye-specific and center-type-specific channels of the ferret's retinogeniculocortical projection tempts us to propose that the same developmental mechanisms could give rise to both types of segregation.

Ferrets are born relatively early during the development of the retinogeniculate projection, at a time when the axons from the two eyes almost completely overlap in the LGN. The axons segregate into eye-specific laminae during the first two postnatal weeks. Leaflet formation is first detectable anatomically late in the second postnatal week, when denser autoradiographic labelling is seen in the inner portions of each geniculate lamina after intraocular injections of ^{3}H-proline (Linden et al., 1981).

Leaflet formation thus begins before the time of natural eye-opening in ferrets (around postnatal day 28), implying that patterned visual activity is not required for the initiation of this process. It is not known when center-type patches or ocular dominance patches are first evident among the geniculate terminals within layer IV of the cortex, so it is not possible to speculate about the role of pattern vision in organizing these aspects of the geniculocortical projection.

It is, however, possible that spontaneous electrical activity has a role in organizing or refining the retinogeniculate and/or geniculocortical ON and OFF projections. The formation of ocular dominance columns in cat visual cortex appears to require spontaneous, but not light-evoked, activity in the retinogeniculocortical pathway (Stryker and Harris, 1986). It also appears that differences in the timing of the impulses from the two eyes are critical for ocular dominance column formation in cats (Stryker and Strickland, 1984; Stryker, 1986). The fact that maintained discharges of neighboring retinal ganglion cells of like center-type are correlated in adult cats, while discharges of cells of opposite center-types are anti-correlated (Mastronarde, 1983), makes it likely that the activity-dependent mechanisms that produce ocular dominance segregation could also cause ON and OFF afferents to segregate.

It is also possible that the timing of fiber ingrowth from the retina may play a role in organizing the ON and OFF geniculate layers. A common feature of the LGNs of the species in which on-center and off-center cells are found in separate laminae is that OFF parvocellular layers are found nearer the optic tract than the corresponding ON layers. (See Figure 34.)

Earlier-arriving retinogeniculate axons might terminate in the inner (farther from the optic tract) regions of the nucleus; an axon's time of arrival in the optic tract might then determine its time of arrival in the LGN. Fiber order in the optic tracts of ferrets (Walsh and Guillery, 1985) and cats (Torrealba et al, 1982; Walsh et al., 1983) has been reported to be related to the time the fibres grew into the tract: in both species, fibres already in the tract are displaced dorsally as later-arriving fibres are added to the pial (ventral) margin of the tract. Recordings from axons of retinal ganglion cells within the cat's optic tract revealed that, in general, X-ON fibres are located more dorsally within the tract than are X-OFF fibres; Y axons are displaced ventrally relative to the X axons, but there is no apparent layering of Y-ON and Y-OFF axons in the optic tract (Mastronarde, 1984). Thus, in cats, there appears to be a difference in the time of arrival in the optic tract of the axons of the ON and OFF populations of one class (X) of retinal ganglion cells that terminates exclusively in the parvocellular geniculate layers. It is also likely that ON afferents arrive in the LGN before the OFFs. Such differences may be present, perhaps to a greater degree, in those species with center-type lamination in the LGN, and an earlier arrival of ON afferents may explain the consistency among species in the positions of the laminae when they are stratified. A similar mechanism depending on relative timing might account for the difference between the pattern in LGNs of ferret, mink, and macaque on the one hand, and tree shrew on the other. Perhaps in the former species, both ON and OFF contralateral geniculate afferents arrive before any ipsilateral afferents, but within each eye ON proceeds OFF. The prediction of this mechanism for the tree shrew would be that ON contralateral afferents arrive first, followed by ON ipsilateral, OFF contralateral, and OFF ipsilateral. Such an order might be experimentally testable, using the sublaminar stratification of retrogradely labelled retinal ganglion cell dendrites to identify the center-type.

Activity-dependent mechanisms and differences in the timing of fibre ingrowth might have roles in organizing the ON and OFF retinogeniculate and geniculocortical projections.

Identical mechanisms might give rise to different final patterns in different species if certain critical parameters vary among the species. For example, attempts at modelling the development of ocular dominance patches have revealed that patch width depends on several factors, including the arbor-widths of the geniculocortical axons, the distances over which activity is correlated among geniculate cells, and the effective ranges of lateral excitatory and inhibitory interactions among cortical neurons (Miller et al., 1986). Ferrets should provide a useful model system for studying such mechanisms.

References

Anderson, P. A., J. Olavarria, and R. C. Van Sluyters (in preparation) The overall pattern of ocular dominance bands in cat visual cortex.

Bishop, P. O., W. Burke, and R. Davis (1962) The identification of single units in central visual pathways. *J. Physiol. 162*: 409-431.

Bishop, P. O., W. Kozak, and G. J. Vakkur (1962) Some quantitative aspects of the cat's eye: Axis and plane of references, visual field co-ordinates and optics. *J. Physiol. (Lond.) 163*: 466-502.

Blakemore, C., J. Nachmias, and P. Sutton (1970) The perceived spatial frequency shift: evidence for frequency-selective neurones in the human brain. *J. Physiol. (Lond.) 210*: 727-750.

Blasdel, G. G., and G. Salama (1986) Voltage-sensitive dyes reveal a modular organization in monkey striate cortex. *Nature 321*: 579-585.

Bowling, D. (1983) Responses to light at different depths in the A layers of the cat's lateral geniculate nucleus. *Invest. Ophthalmol. Suppl. 24*: 265.

Bowling, D., and C. Michael (1984) Terminal patterns of single, physiologically characterized optic tract fibers in the cat's lateral geniculate nucleus. *J. Neurosci. 4*: 198-216.

Bowling, D. B., and W. M. Schoel (1983) Functional organization across single layers of the lateral geniculate nucleus in the cat. *Soc. Neurosci. Abst. 9*: 1046.

Brunso-Bechtold, J. K., and V. A. Casagrande (1981) Effect of bilateral enucleation on the development of layers in the dorsal lateral geniculate nucleus. *Neuroscience 6*: 2579-86.

Brunso-Bechtold, J. K., and V. A. Casagrande (1982) Early postnatal development of laminar characteristics in the dorsal lateral geniculate nucleus of the tree shrew. *J. Neurosci. 2*: 589-597.

Burton, G. J., S. Nagshineh, and K. H. Ruddock (1977) Processing by the human visual system of the light and dark contrast components of the retinal image. *Biol. Cyber. 27*: 189-197.

Cleland, B. G., M. W. Dubin, and W. R. Levick (1971) Simultaneous recording of input and output of lateral geniculate neurons. *Nature New Biology 231*: 191-192.

Conley, M., D. Fitzpatrick, and I. T. Diamond (1984) The laminar organization of the lateral geniculate body and the striate cortex in the tree shrew (*Tupaia glis*). *J. Neurosci. 4*: 171-197.

Conway, J., P. H. Schiller, and L. Mistler (1980) Functional organization of the tree shrew lateral geniculate nucleus. *Soc. Neurosci. Abst. 6*: 583.

Conway, J. L., and P. H. Schiller (1983) Laminar organization of tree shrew dorsal lateral geniculate nucleus. *J. Neurophysiol. 50*: 1330-1342.

Cucchiaro, J., and R. W. Guillery (1982) The structure and development of the dorsal lateral geniculate nucleus and its retinal afferents in the albino ferret. *Soc. Neurosci. Abst. 8*: 814.

Daniel, P. M., and D. Whitteridge (1961) The representation of the visual field on the cerebral cortex in monkeys. *J. Physiol. 159*: 203-221.

De Valois, K. K. (1977) Independence of black and white: phase-specific adaption. *Br. Res. 17*: 209-215.

Gilbert, C. D., and T. N. Wiesel (1979) Morphology and intracortical projections of functionally characterized neurons in the cat visual cortex. *Nature 280*: 120-125.

Guillery, R. W. (1969) An abnormal retinogeniculate projection in Siamese cats. *Br. Res. 14*: 739-741.

Guillery, R. W. (1971) An abnormal retinogeniculate projection in the albino ferret (*Mustela furo*). *Br Res. 33*: 482-485.

Guillery, R. W., and J. H. Kaas (1971) A study of normal and congenitally abnormal retinogeniculate projections in cats. *J. Comp. Neurol. 143*: 73-100.

Guillery, R. W., A. S. LaMantia, J. A. Robson, and K. Huang (1985) The influence of retinal afferents upon the development of layers in the dorsal lateral geniculate nucleus of mustelids. *J.Neurosci. 5*: 1370-1379.

Hall, W. C., J. H. Kaas, H. Killackey, and I. T. Diamond (1971) Cortical visual areas in the grey squirrel (*Sciurus carolinesis*): a correlation between cortical evoked potential maps and architectonic subdivisions. *J. Neurophys. 34*: 437-457.

Hickey, T. L., and R. W. Guillery (1979) Variability of laminar patterns in the human lateral geniculate nucleus. *J. Comp. Neurol. 183*: 221-246.

Horton, J. C., and H. Sherk (1984) Receptive field properties in the cat's lateral geniculate nucleus in the absence of on-center retinal input. *J. Neurosci. 4*: 374-380.

Hubel, D. H. (1957) Tungsten microelectrode for recording from single units. *Science 125*: 549-550.

Hubel, D. H., and T. N. Wiesel (1961) Integrative activity in the cat's lateral geniculate body. *J. Physiol. (Lond.) 155*: 385-398.

Hubel, D. H., and T. N. Wiesel (1962) Receptive fields, binocular interaction and functional architecture in the cat's visual cortex. *J. Physiol. 160*: 106-154.

Hubel, D. H., and T. N. Wiesel (1968) Receptive fields and functional architecture of monkey striate cortex. *J. Physiol. 195*: 215-243.

Hubel, D. H., and T. N. Wiesel (1974) Laminar and columnar distribution of geniculo-cortical fibers in the macaque monkey. *J. Comp. Neurol. 146*: 421-450.

Hubel, D. H., T. N. Wiesel, and S. LeVay (1974) Visual field representation in layer IV C of monkey striate cortex. *Soc. Neurosci. Abst. 4*: 264.

Hubel, D. H., T. N. Wiesel, and M. P. Stryker (1978) Anatomical demonstration of orientation columns in macaque monkey. *J. Comp. Neurol. 177*: 361-380.

Humphrey, A. L., J. E. Albano, and T. T. Norton (1977) Organization of ocular dominance in tree shrew striate cortex. *Br. Res. 134*: 225-236.

Kaas, J. H., M. F. Huerta, J. T. Weber, and J. K. Harting (1978) Patterns of retinal terminations and laminar organization of the lateral geniculate nucleus of primates. *J. Comp. Neurol. 182*: 517-554.

Kalia, M., and D. Whitteridge (1973) The visual areas in the splenial sulcus of the cat. *J. Physiol. 232*: 275-283.

Kaufmann, P. G., and G. G. Somjen (1979) Receptive fields of neurons in areas 17 and 18 of tree shrews (*Tupaia Glis*). *Br. Res. Bull. 4*: 319-325.

Kelly, J. P., and D. C. Van Essen (1974) Cell structure and function in the visual cortex of the cat. *J. Physiol. 238*: 515-547.

Kretz, G., G. Rager, and T. T. Norton (1986) Laminar organization of on and off regions and ocular dominance in the striate cortex of the tree shrew (*Tupaia belangeri*). *J. Comp. Neurol. 251*: 135-145.

Kuffler, S. W. (1953) Discharge patterns and functional organization of mammalian retina. *J. Neurophysiol. 16*: 37-68.

Law, M. I., K. R. Zahs, and M. P. Stryker (in preparation) The projection of the visual field onto primary visual cortex (area 17) of the ferret.

LeVay, S., and C. D. Gilbert (1976) Laminar pattern of geniculocortical projection in the cat. *Br. Res. 113*: 1-19.

LeVay, S., and S. K. McConnell (1982) On and off layers in the lateral geniculate nucleus of the mink. *Nature 300*: 350-351.

LeVay, S., S. K. McConnell, and M. B. Luskin (1987) Functional organization of primary visual cortex in the mink (*Mustela vison*), and a comparison with the cat. *J. Comp. Neurol. 257*: 422-441.

LeVay, S., M. P. Stryker, and C. J. Shatz (1978) Ocular dominance columns and their development in layer IV of the cat's visual cortex: A quantitative study. *179: 223-244.*

Linden, D. C., R. W. Guillery, and J. Cucchiaro (1981) The dorsal lateral geniculate nucleus of the normal ferret and its postnatal development. *J. Comp. Neurol. 203*: 189-211.

Lockard, B. I. (1982) Telencephalon of the ferret (*Mustela furo*). In *Comparative Correlative Neuroanatomy of the Vertebrate Telencephalon*, E.C. Crosby and H.N. Schnitzlein, eds., pp. 484-500. New York: Macmillan Publishing Co.

Malpeli, J. G., and F. H. Baker (1975) The representation of the visual field in the lateral geniculate nucleus of *Macaca mulatta. J. Comp. Neurol. 161*: 569-594.

Malpeli, J. G., P. H. Schiller, and C. L. Colby (1981) Response properties of single cells in monkey striate cortex during reversible inactivation of individual lateral geniculate laminae. *J. Neurophysiol. 46*: 1102-1119.

Martin, A. R., A. C. Kevan, and D. Whitteridge (1984) Form, function, and intracortical projections of spiny neurons in the striate visual cortex of the cat. *J. Physiol. 353*: 463-504.

Mason, C. A., and J. A. Robson (1979) Morhphology of reinto-geniculate axons in the cat. *Neuroscience 4*: 79-97.

Mastronarde, D. N. (1983) Correlated firing of cat retinal ganglion cells. I. Spontaneously active inputs to X- and Y-cells. *J. Neurophysiol. 49*: 303-324.

Mastronarde, D. N. (1984) Organization of the cat's optic tract as assessed by single-axon recordings. *J. Comp. Neurol. 227*: 14-22.

McConnell, S. K., and S. LeVay (1984) Segregation of on and off center afferents in mink visual cortex. *Proc. Nat. Acad. Sci. 81*: 1590-1593.

McGeer, E. G., J. W. Olney, and P. L. McGeer (1978) *Kainic acid as a tool in neurobiology.* New York: Raven Press.

Mesulam, M.-M. (1978) Tetramethyl benzidine for horseradish peroxidase neurochemistry: A non-carcinogenic blue reaction-product with superior sensitivity for visualizing neural afferents and efferents. *J. Histochem. Cytochem. 26*: 106-117.

Miller, K. D., J. B. Keller, and M. P. Stryker (1986) Models for the formation of ocular dominance columns solved by linear stability analysis. *Soc. Neurosci. Abst. 12*: 1373.

Naporn, A., N. Berman, and B. R. Payne (1985) Segregation of "ON" and "OFF" units in cat dorsal lateral geniculate nucleus. *Soc. Neurosci. Abst. 11*: 232.

Nelson, R., E. V. Famiglietti, and H. Kolb (1978) Intracellular staining reveals different levels of stratification for on and off center ganglion cells in cat retina. *J. Neurophysiol. 41*: 472-483.

Norton, T. T., G. Rager, and R. Kretz (1985) On and off regions in region lV of striate cortex. *Br. Res. 327*: 319-323.

Peters, A., and J. Regidor (1981) A reassessment of the forms of nonpyramidal neurons in area 17 of cat visual cortex. *J. Comp. Neurol. 203*: 685-716.

Polley, E. H., and R. W. Guillery (1980) An anomalous uncrossed retinal input to lamina A of the cat's dorsal lateral geniculate nucleus. *Neurosci. 5*: 1603-1608.

Rakic, P. (1976) Prenatal genesis of connections subserving ocular dominance in the rhesus monkey. *Nature 261*: 467-471.

Ralston, H. J. III, and K. L. Chow (1973) Synaptic reorganization in the degenerating lateral geniculate nucleus of the rabbit. *J. Comp. Neurol. 147*: 321-350.

Sanderson, K. J. (1971) The projection of the visual field to the lateral geniculate and medial interlaminar nuclei in the cat. *J. Comp. Neurol. 143*: 101-117.

Sanderson, K. J. (1974) Lamination of the dorsal lateral geniculate nucleus in carnivores of the weasel (*Mustelidae*), raccoon (*Procyonidae*) and fox (*Canidae*) families. *J. Comp. Neurol. 153*: 239-266.

Sanderson, K. J., and S. M. Sherman (1971) Nasotemporal overlap in the visual field projected to the lateral geniculate nucleus in the cat. *J. Neurophysiol. 34*: 453-466.

Schiller, P. H. (1982) Central conections of the retinal on and off pathways. *Nature 297*: 580-583.

Schiller, P. H., and J. G. Malpeli (1978) Functional specificity of lateral geniculate nucleus laminae of the rhesus monkey. *J. Neurophysiol. 41*: 788-797.

Schiller, P. H., J. H. Sandell, and J. H. R. Maunsell (1986) Functions of the on and off channels of the visual system. *Nature 322*: 824-825.

Shatz, C. J. (1977) A comparison of visual pathways in Boston and Midwestern Siamese cats. *J. Comp. Neurol. 171*: 205-228.

Shatz, C. J. (1983) The prenatal development of the cat's retinogeniculate pathway. *J. Neurosci. 3*: 482-499.

Shatz, C. J., S. Lindstrom, and T. N. Wiesel (1977) The distribution of afferents representing the right and left eyes in the cat's visual cortex. *Br. Res. 131*: 103-116.

Shatz, C. J., and D. W. Sretevan (1986) Interactions between retinal ganglion cells during development of the mammalian visual system. *Ann. Rev. Neurosci. 9*: 171-207.

Shatz, C. J., and M. P. Stryker (1978) Ocular dominance in layer IV of the cat's visual cortex and the effects of monocular deprivation. *J. Physiol. (Lond.) 281*: 267-283.

Sherk, H., and J. C. Horton (1984) Receptive field properties in the cat's area 17 in the absence of on-center geniculate input. *J.Neurosci. 4*: 381-393.

Siegel, S. (1956) *Nonparametric statistics for the behavioral sciences.* New York: McGraw Hill.

Sretevan, D. W., and C. J. Shatz (1987) Axon trajectories and pattern of terminal arborization during prenatal development of the cat's retinogeniculate pathway. *J. Comp. Neurol. 255*: 386-400.

Stone, J. (1978) The number and distribution of ganglion cells in the cat's retina. *J. Comp. Neurol. 180*: 753-772.

Stone, J. (1981) *The Whole Mount Handbook: A guide to the preparation and analysis of retinal whole mounts.* Sydney: Maitland Publications Pty. Ltd.

Stryker, M. P. (1986) The role of neural activity in rearranging connections in the central visual system. In *The Biology of Change in Otolaryngology*, R.W. Ruben et al., eds., pp. 211-224. Amsterdam: Elsevier.

Stryker, M. P., and W. A. Harris (1986) Binocular impulse blockade prevents the formation of ocular dominance columns in cat visual cortex. *J. Neurosci. 6*: 2117-2133.

Stryker, M. P., and S. L. Strickland (1984) Physiological segregation of ocular dominance columns depends on the pattern of afferent electrical activity. *Invest. Ophthalmol. Suppl. 25*: 278.

Stryker, M. P., and K. R. Zahs (1983) ON and OFF sublaminae in the lateral geniculate nucleus of the ferret. *J. Neurosci. 3*: 1943-1951.

Tanaka, K. (1983) Cross-correlation analysis of geniculostriate neuronal relationships in cats. *J. Neurophysiol. 49*: 1303-1318.

Tanaka, K. (1986) Organization of geniculate inputs to visual cortical cells in the cat. *Selected Papers of Basic Researches 20*: 36-43.

Torrealba, F., R. W. Guillery, E. H. Polley, and C. A. Mason (1981) A demonstration of several independent, partially overlapping, retinotopic maps in the optic tract of the cat. *Br. Res. 219*: 428-432.

Tusa, R. J., L. A. Palmer, and A. C. Rosenquist (1978) The retinotopic organization of area 17 (striate cortex) in the cat. *J. Comp. Neurol. 177*: 213-236.

Vitek, D. J., J. D. Schall, and A. G. Leventhal (1985) Morphology, central projections, and dendritic field orientation of retinal ganglion cells in the ferret. *J. Comp. Neurol. 241*: 1-11.

Waitzman, D., and M. P. Stryker (in preparation) Orientation columns in area 17 of the ferret.

Walsh, C., and R. W. Guillery (1985) Age-related fiber order in the optic tract of the ferret. *J. Neurosci. 5*: 3061-3069.

Walsh, C., E. H. Polley, T. L. Hickey, and R. W. Guillery (1983) Generation of cat retinal ganglion cells in relation to central pathways. *Nature 302*: 611-614.

Wassle, H., L. Peichl, and B. B. Boycott (1981) Morphology and topography of on and off alpha cells in the cat retina. *Proc. Roy. Soc. B 212*: 157-175.

Wiesel, T. N., D. H. Hubel, and D. M. K. Lam (1974) Autoradiographic demonstration of ocular-dominance columns in the monkey striate cortex by means of transneuronal transport. *Br. Res. 79*: 273-279.

Zahs, K. R., and M. P. Stryker (1985) The projection of the visual field onto the lateral geniculate nucleus of the ferret. *J. Comp. Neurol. 241*: 210-224.